Final

Technical Report

ECCC Project GCXE18S024

Measurement-Based Emission Factors Using BHGE Advanced Methane Sensing Technologies and Analytics

Prepared for:
Environment and Climate Change Canada-ECCC

March 31, 2019
Revised May 23, 2019

CONFIDENTIAL

Purpose:	Measurement-Based Emission Factors in Selected Sample of Oil & Gas Industry in Canada
Project Number:	GCXE18S024
Key words:	Emission Factors - BHGE LUMEN - Big Data Analytics - GHGI - Sustainability

Project sponsor:	Environment and Climate Change Canada (ECCC)	
Authors:	Valeria Di Filippo Ammar Abdilghanie Mohammed, PhD Jianmin (Jimmy) Zhang, PhD	Ashraf El-Messidi Pejman Kazempoor, PhD Nasr Alkadi, PI, PhD
Reviewers:	Jeanne-Mey Sun - Paul Doucette - Jon Chow - Ashraf El-Messidi	

Rev	Date	Description	By	Approved
1	3/25/2019	First Draft	Valeria Di Filippo	Nasr Alkadi
2	4/05/2019	Draft Final	Nasr Alkadi	Nasr Alkadi
3	5/16/2019	Final	Valeria Di Filippo	Nasr Alkadi

Table of Contents

1. Executive Summary 5
2. List of Acronyms, Figures, and Tables 10
3. Acknowledgement 17
4. Background 18
5. Problem Statement 18
6. Existing Methodologies and Current Approaches 19
    6.1 EPA 19
    6.2 ECCC / Clearstone 19
7. Research Objectives 20
8. Test Methodologies, Tools, and Technology 21
    8.1 BHGE- LUMEN Methane Sensing Technology 21
    8.2 Test Locations 23
    8.3 Equipment Component Characterization 25
        1. Fugitive Sources and Vented Sources 25
    8.4 Test Approach 30
    8.5 Data Acquisition 33
    8.6 Data Processing Work Flow 36
    8.7 Near-Field Plume Dispersion Model 38
    8.8 Analytics Tools Used 42
    8.9 BHGE Emission Rate Method to Estimate Emission Factors 45
    8.10 Uncertainty Analysis 46
9. Results 47
    9.1 Total Site Emissions 47
    9.2 Site-Specific Behavior 48
        1. Compressor Site 622, 06-22-041-05W5 (AER F41995) 48
        2. Wellsite Station, 13-23-043-05W5 (AER F46141) 49
        3. Westerose Compressor Station, 11-09-044-02W5 (AER F20724) 50
        4. Willesden Green 16-12 Compressor Station, 16-12-042-06W5 (AER F34318) 51
        5. Willesden Green 12-04 SWB, 100/12-04-041-06W5 SWB 52
        6. South Elkton 02-03 Compressor Station, 02-03-031-04W5 (AER F23119) 53
        7. Harmattan 12-29-031-03W5 Battery, 12-29-031-03 W5 (AER F43230) 54
    9.3 Measured-Based Emission Factors per Equipment Component 55

9.4 Emission Rate per Component Category 57
  9.4.1 Node Timeseries per Component Category 58
  9.4.2 Comparison of Newly Developed Emission Factors with Current Emission Factors 64
9.5 Key Findings 66
  1. Hi-Bleed to Low-Bleed Operation Transition 66
  2. Economic Impact of High to Low-Bleed Transition 69
  3. Methanol Pump 70
  4. Distance Piece 71
  5. Level Controller Operations – Separator vs. Compressor 72
  6. From Operations 73
10. Conclusions 74
11. Next Steps 74
12. References 76
13. Appendices 77
  13.1 Regulatory Agency Emission Rate Charts 77
14. Supplemental Material *(will be sent separately due to volume)* 79
  14.1 Detailed Statistical Analysis of Component Level Emission Rates 79
  14.2 ECCC / Bonavista Meetings (July, 2017 to March, 2019) 79
  14.3 Communications with Bonavista for validation of findings 79

1. Executive Summary

This report presents the pioneering work performed by the BHGE team for the Environment and Climate Change Canada (ECCC) to develop a continuous measurement-and-model based component-level emission monitoring solution using BHGE methane sensing and analytics platform LUMEN™ for selected oil and gas sites. The main objectives of the research program are as follows:

1. To demonstrate the quality and validity of the technology with measurement-and-model based methane leak rate data from components on oil & gas sites equipment.
2. To generate time-bound, real-time operation related emission factors in comparison with the EPA/EC O&G industrial methane emission factors for the emitting equipment components in the seven selected oil and gas production sites of Bonavista Energy Corporation in Alberta, Canada.
3. To develop a robust workflow and protocols for future larger scale methane emission studies to cover more representative oil and gas facilities and equipment/component diversities.
4. Ultimately, to establish an alternative solution for O&G Industry with robust data-driven emission monitoring so operators could source insights faster checking their emission dashboard, a win-win situation when the Industry could opt for use of smart asset management tool and the EPA/EC regulators could offer incentives encouraging methane emission-footprint reduction to the oil & gas sector in Canada with informed policy and decision making for potential GHGI mitigation opportunities.

The BHGE approach for the time-bound, real-time operation related Emission Factor determination is a departure from the industry status-quo over the past decades. Utilizing the power of the digital age technologies, i.e., *edge/cloud computing, state of the arts methane continuous monitoring/sensing as well as big data analytics*, the LUMEN™ platform solution produces preliminary unbiased emission factors which reflect, among other, different equipment operating modes, maintenance conditions, age, location and site production levels. The method considers all-encompassing sets of field conditions in estimating statistical mean emission levels for a given equipment component. This robust technique is envisioned to bridge the existing gap in understanding real equipment operational performance as it relates to frequency and intensity of methane leaks over time.

It should be noted that the emission factors developed in this study represent a limited sample size and may be insufficient for a statistically significant emission factor trend. However, the method is well applicable to broader and extended deployment to produce statistically significant emissions factors for defined sets of equipment components.

This project started in August 2017 when the BHGE research labs worked on development of the LUMEN sensor technology used in this field studies. It was funded jointly by the ECCC and Petroleum Technology Alliance Canada (PTAC) with in-kind support from the Bonavista Energy Corporation which coordinated with the BHGE team all project activities including the site selection as well as purview of daily activities during field preparation, deployment, and post deployment measurements and data analytics campaigns.

The Table 1.1 shows the overall project milestones from inception to completion. Equipment component leaks and vents that are subject to EPA/EC emission factor reviews were identified during boots on the ground visit on April 2018. Among the seven selected Bonavista production sites, a total of 78 components were screened using portable methane detector. Out of the 78 components screened the team qualified 54 as the representative components for this study. From July to November 2018, the project team deployed a total of 56 LUMEN methane sensors in the seven Bonavista sites, all located in Rimbey, Alberta, Canada. The sensors continuously sampled 54 component level methane emissions over a total period of 8 months for the first 3 sites and 4 months for the rest (the site numbering details in the Figure 1-1).

Sampling frequency was determined at two hertz (or one sampling every 2 seconds). This fast sampling pace by the BHGE patented technology enabled the LUMEN sensor network to capture the dynamics of emissions data resulting from various operating conditions and site events on a continuous basis. The sensor data were constantly transmitted via cloud to EIC servers for further modeling and analysis.

Table 1-1 Overall Project Milestones

Task #	Task Description	2017						2018												2019		
		July	Aug	Sep	Oct	Nov	Dec	Jan	Feb	March	Apr	May	June	July	Aug	Sep	Oct	Nov	Dec	Jan	Feb	March
Task 1	Resume Development/De-Risking/Building Ruggadized 40 Sensor Nodes		8 Months	■	■	■	■	■	■	■												
Decision Point 1	*GO/NO GO Decision*			X			X			X												
Task 2	Documentation for CSA International Certification					3 Months	■	■	■	■												
Decision Point 2	*GO/NO GO Decision*								X													
Task 3	Identification of Pilots & Methodology Assessment						3 Months	■	■													
Task 4	Sensor Deployments & Field Measurment Campaign 1													6 Months	■	■	■	■	■			
Decision Point 3	*GO/NO GO Decision*												X									
Task 5	Sensor Deployments & Field Measurment Campaign 2																3 Months	■	■	■		
Task 6	Data Analysis Campaign														6 Months	■	■	■	■	■		
Task 7	Report/Presentations/Meetings with the ECCC Teams																				2 months	■

The collection of sensor node data (191 million data points) were carefully processed and thoroughly filtered before going through a series of format transformation and eventually being fed into the *"Near-Field Plume Dispersion Model"* where the measured methane concentration (ppm) data were converted to leak rate (scfm).

After obtaining a full timeseries of concentration and corresponding leak rates for each node, bootstrap resampling was performed to quantify the random errors and provide a confidence range for the statistics reported. The mean leak rate for each node was calculated and compared with the like-component as well as other types of components in the same facility. Working closely with the operator Bonavista, the team was able to link several key reported events to the revealing timeseries trending, which corroborated the LUMEN data and validated the assumptions that operators could use the sensor platform as an asset management tool to assess equipment conditions for maintenance scheduling purposes.

Although Hi-Flow Sampler measurements may provide true emission behavior of a component during testing time, operators relying on such short-duration checking may grossly over-generalize their component emission characteristics.

Towards the end of LUMEN work flow, time-bound and component-specific emission factors were calculated and compared with the EPA/EC corresponding Emission Factor values which are the industry-wise average.

Key Findings and Results

Key learning discussions

Based on extensive data processing and repeated verifications and feedbacks from the field operator Bonavista, the BHGE team has concluded the following key findings that greatly enhance our confidence in LUMEN's capabilities to track site operational activities and to reveal their impact on methane emissions:

1. A show case of LUMEN's sensitivity in detecting a quick emission reduction after the operator switching over from high-bleed mode to low bleed mode.
2. In another instance of LUMEN sensitivity that after a distance piece rod packing upgrade its emission levels revealed a significant improvement, an excellent demonstration that the platform can be deployed for tracking service records on components levels as an asset management tool.
3. The third illustrative example is that how operators could leverage the data availability to show case the financial impact of emission reduction on component level. They can make decisions to comply with regulations and quantify ROI using condition-based maintenance as opposed to time-based schedules. Monitoring and measuring leak rates is the first step to minimize emissions and maximize profit.

Emission Factor Comparisons

The BHGE emission factors were compared with the data from the 1996 GRI and EPA study and 2014 Canadian-EC Clearstone study as shown in the Table 1-2. The regulatory agencies adopted methodologies (see more details in the Section 6) in emission data collections including one-time measurement, and/or an average of reported emissions, and/or an approximation based on models and correlations. The BHGE approach was based on continuous measurements methodology.

The ranges of BHGE emission factor statistical means for each component category were calculated and listed in the Table 1-2. We found that the continuous measurement approach over an extended period generated numerous insightful understandings on leak source characteristics and signatures over a wide range of operating and environmental conditions. The time-bound, site-specific emission factors add an important dimension to current the EPA and EC emission regulatory methodologies.

Table 1-2 BHGE Emission Factors vs. Regulatory Averages per Component Categories

Equipment Component Category 7 Bonavista Sites		**Fugitive vs. Vented Emission**	**BHGE Emission Factors* Range (scfm) Using 56 LUMEN Sensors**	**Leak Rate Range (scfm) Using Hi-Flow Sampler****	**EC Emission Factors*** (scfm) Clearstone Study March, 2014**	**EPA Emission Factors*** (scfm) EPA/GRI Study, 1990 Published on June 1996**
1	Distance Piece (n =3)	Vented	0.006 - 0.469	0.07 - 0.39	0.050	0.860
2	Dump Valve (n =4)	Vented	0.016 - 1.923	0 - 0.28	0.002	0.002
3	Level Controller (n=18)	Vented	0.002 - 1.381	0 - 0.91	0.041	0.002
4	Main Flange (n=1, 3 sensors)	Fugitive	0.001	-	-	0.000
5	Methanol Pump (n=3)	Vented	0.017 -1.411	0 - 0.43	0.003	0.002
6	Pre-Lube Pump Column (n=1)	Vented	0.229	-	0.003	0.002
7	Pressure Controller (n=13)	Vented	0.003 -0.635	0 - 0.3	0.041	0.003
8	Start Gas (n=2)	Vented	0 - 0.379	-	-	-
9	Thief Hatch (n=3)	Vented	0.004 - 0.082	-	-	-
10	Vent Header (n=6)	Vented	0.002 -0.731	0.03 - 2.15	0.050	0.860

* *Assuming unity activity value*
** *Hi-Flow Bonavista Sites Testing Campaign: November 19th, 20th, 2018*
*** *Average value*

Due to limited sample size (54 components) the BHGE emission factors developed in this study may not be very good representations to the entire component population. However, it sheds light on the needs of developing continuous-measurement-based emission factors that are appropriately scaled to target super emitters, i.e., the top 5% of leaks at compression facilities which contribute to 68% of the total emissions. This illustrates the importance of adequately characterizing "super-emitters" while counting emission inventories and trying to apply the emission factors obtained in the studies to various regions or for whole industry-wide estimates.

Site to Site Emission Rates Variability

Figure 1-1 shows the emission footprints of the seven Bonavista sites that can be categorized into three types, i.e., compressor stations (4 sites), wellsites (2 sites), and a battery site. Understandably the site functionality correlates their total emissions. In most of the cases, compressor station sites emit more gas than the wellsites due to the distance piece vent emission together with other sources as indicated by individual "grouping" of emission rates. It should be noted that the sample size of leaking components may be insufficient for identifying statistically significant trends among sites.

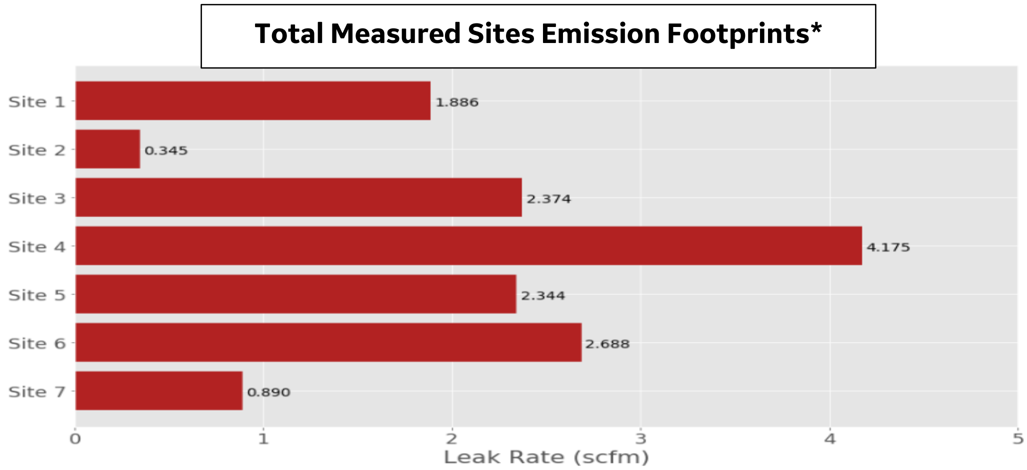

Figure 1-1 Site-Level Comparison of Emission Rates [$ER_{BHGE,t}$]

**Each site has a different number of leak sources; therefore, these rates may not be fully representing the total emissions on a given site.*

Site#	**1**	**2**	**3**	**4**	**5**	**6**	**7**
Site Type	Compressor Station	Wellsite	Compressor Station	Compressor Station	Wellsite	Compressor Station	Battery
Emission Rates (scfm)	1.886	0.345	2.374	4.175	2.344	2.688	0.890

Emission Reduction Quantification due to Transition from Hi-Bleed to Low-Bleed

The emission reductions resulted from replacement of Hi-Bleed controllers to the Low-Bleed were captured and quantified by the LUMEN monitoring system as shown in the Figure 1-2. During the testing period, Bonavista replaced 5 high-bleed controllers with the low-bleed models on two separate occasions. At the sites 1 and 2, the maintenance event occurred on October 10, 2018. The controllers (all categorized as separator pressure controllers) were monitored by the LUMEN sensor nodes 10, 23, 25 and 92. The second event occurred on November 30, 2018 at site 6 where the controller was monitored by LUMEN sensor Node 63. As expected, the controller upgrade at the site dramatically affected the emission behavior. The LUMEN sensors clearly recorded the two distinct emission levels before and after the equipment upgrade (delineated by the vertical dash line plotted on the date of controller replacement). The mean of realtime leak rate from the high-bleed controllers were about 2 to 3 times higher than that from the low bleed controllers, a very responsive emission trending to show the emission reduction.

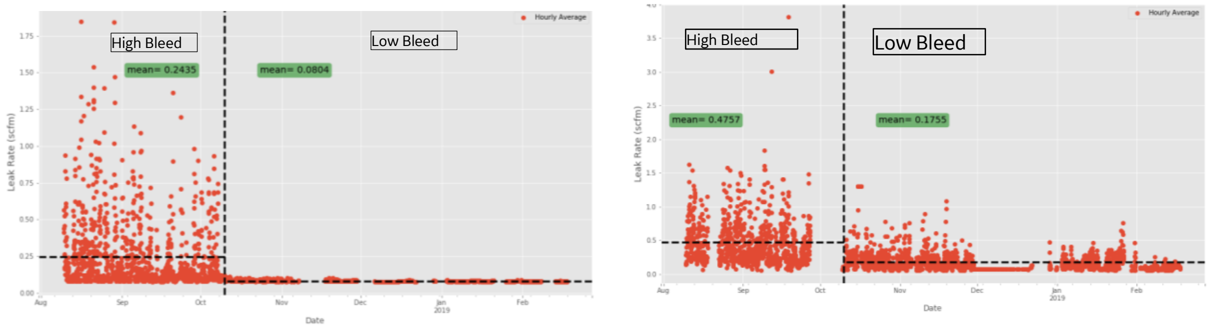

Figure 1-2 Effect of High to Low-Bleed Operation Transition on Leak Rate Reduction

Correlation of Operational Parameters and Emission Rates

A strong correlation was observed between emission rates at compressor rod packing vents (distance piece) with increased site inlet pressure. Other operational parameters such as replacement of rod packing were strongly correlated with lower emissions rates. There were also evidences of a correlation between higher emissions and compressor age. By comparing the LUMEN measurements to the sites service records, we notice that newer packing lead to emission reductions based on the distance pieces data. Bonavista service records indicate that Site 4 (LUMEN Sensor Node 46) had new packing installed recently in May 2018. Site 6 (LUMEN Sensor Node 69) had the 1st stage repacking completed recently in November 2018, while the last service for Site 3 (LUMEN Sensor Node 31) compressor packing was completed back in August 2017. Referencing **Figure 1-3**, it is evident that distance piece emission rates from sites 4 and 6 were one order lower than that of site 3.

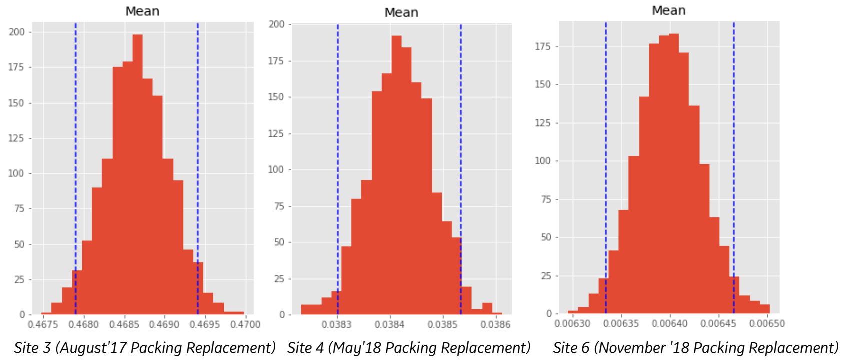

Site 3 (August'17 Packing Replacement) *Site 4 (May'18 Packing Replacement)* *Site 6 (November '18 Packing Replacement)*

Figure 1-3 Mean Emission Rates Sampling Distribution for 3 Distance Pieces at the Sites 3, 4 and 6

Distinct Emission Footprint Level Controller Operations – Separator vs. Compressor

Figure 1-4 shows two distinct emission footprints for level controllers attached to a compressor and a separator, respectively. The emission signature of the separator level controllers had an intermittent behavior that was attributed to snap action (on/off) mode. The release of gas was intermittent and short lived, the dynamic component of the reading, this is the second "baseline" that can be observed in the figure, leveling at around 2 scfm. The bottom baseline belongs to the static component of the reading. The frequency of the gas release is dependent on the frequency the liquid needs to be dumped to lower the level of the liquid.

In stark contrast the compressor level controllers showed more continuous, unimodal emissions, mostly in low levels with occasional spikes, a behavior attributed to the throttle action mode of the level controller.

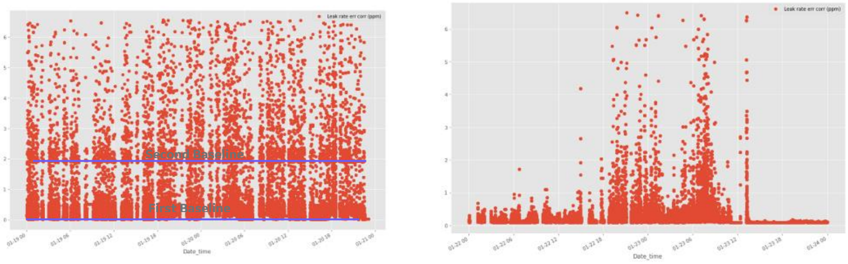

(a) Separator (b) Compressor

Figures 1-4 48-hour window of the Level Controller Emission Footprint

Finally, with the official LUMEN product launch, BHGE is positioned to scale up this type of research programs that could help customers to understand their emissions footprint as well as the regulatory agencies to develop new measured-based emission factors for the whole industry sector. By design, this study was limited to seven sites and ten different types of components categories (Distance Piece, Dump Valve, Level Controller, Main flange, Methanol Pump, Pre-Lube Pump Column, Pressure Controller, Start Gas, Thief Hatch, and Vent Header). The BHGE team is ready to expand scale of the field monitoring services such that more diversified sites and equipment components are covered to enable ECCC to promulgate a high-fidelity emission factor database based on factual measurements considering of parameters such as the age of equipment, rated capacities, materials, volumetric throughputs, geographic regions, operation modes, and potentially other factors.

2. List of Acronyms, Figures, and Tables

Acronym	Definition
BHGE	Baker Hughes, a GE Company
BS	Base Station
CFD	Computational Fluid Dynamics
DP	Distance Piece
DV	Dump Valve
ECCC	Environment and Climate Change Canada
EF_{BHGE}	Measured based Emission Factor using BHGE method
EIC	Energy Innovation Center
EPA	Environmental Protection Agency (USA)
$ER_{BHGE,t}$	Measured based Emission Rate using BHGE method for a period of time, t
ETL	Extraction, Transformation, Loading
GHG	Greenhouse Gas
GHGI	United States Inventory of Greenhouse Gas Inventory
GHGRP	Greenhouse Gas Reporting Program
GRI	Gas Research Institute
LR_{Inst}	Instantaneous leak rate (scfm)
LC	Level Controller
LMm	Laser Methane mini
M&S	Measurement and Sensing
MF	Main Flange
MP	Methanol Pump
NPRI	National Pollutant Release Inventory
PC	Pressure Controller
PP	Pre-Lube Pump
PPM	Parts per Million

PRV	Pressure Relief Valve
PTAC	Petroleum Technology Alliance Canada
SCFH	Standard Cubic Feet per Hour
SCFM	Standard Cubic Feet per Minute
SG	Start Gas
SWB	Separator, Well, Battery
TF	Transfer Function
TH	Thief Hatch
UNFCCC	United Nations Framework Convention on Climate Change
VH	Vent Header
WS	Weather Station
WSN	Wireless Sensor Network

Figure	Description
1.1	Site-Level Comparison of Emission Rates [$ER_{BHGE,t}$] (scfm)
1.2	Effect of High to Low-Bleed Operation Transition on Leak Rate Reduction
1.3	Mean Emission Rates Sampling Distribution for 3 Distance Pieces at Sites 3,4,6
1.4	48-hour window Level Controller Emission Footprint
8.2-1	Geographic Location of Bonavista Sites
8.2-2	Geographic Location of Bonavista Sites - Close-Up
8.3-1	Reciprocating Compressor Distance Piece Schematic
8.3-2	Liquid Dump Valve Schematics
8.3-3	Level Controller Schematics
8.3-4	Main Flange/Wellhead Schematics
8.3-5	Methanol Pump Schematics
8.3-6	Pressure Controller Schematics

8.3-7	Air/Gas Starter Schematics
8.3-8	Storage Tank Thief Hatch Emission
8.4-1	Deployment Timeline
8.4-2	Tagged Components
8.4-3	Sensor Nodes
8.4-4	Base Station
8.4-5	CSV Data Files
8.4-6	Sensor Nodes Deployed
8.4-7	Component Count
8.5-1	Data Acquisition Workflow
8.5-2	Weather Station Wind Vane
8.5-3	Raw Far-Field Wind Data Recorded by Weather Station Sensors
8.5-4	Near-Field LUMEN for General Area Monitoring of Methane Emissions
8.5-5	Near-Field Sensors near Leaking Sources of (a) a Reciprocating Compressor Vent; (b) a Pressure Controller on a Dehydration Unit
8.6-1	End to End BHGE Big Data Analytics Platform for Development of Measurement Based Emission Factor
8.6-2	Weekly Minima of Raw Sensor Output for Sensor 26
8.7-1	Near-Field Model Workflow (converting ppm to scfm)
8.7-2	Schematic of the Flow Field near a Cubical Building
8.7-3	Comparisons of data-driven model predictions versus CFD results in the space of input (far-field wind) and output (near-field wind) states
8.7-4	CFD Model Developed to Investigate the Flow Field around Various Objects
8.7-5	Example of Open-Field and Near-Field velocity profile (V=10 m/sec and leak rate= 0.5 gram/sec)
8.7-6	Example of Open-Field and Near-Field methane concentration (V=10 m/sec and leak rate= 0.5 gram/sec)
8.8-1	2-Second Timeseries for Node 31 in ppm (left) and scfm (right)
8.8-2	Hourly Averages for Node 31 in ppm (left) and scfm (right)
8.8-3	Daily Averages for Node 31 in ppm (left) and scfm (right)

8.8-4	Weekly Averages for Node 31 in ppm (left) and scfm (right)
8.8-5	Sampling Distribution of the Mean, Standard Deviation and Median for the Leak Rate for Node 31
9.1-1	Site-Level Comparison of Emission Rates [$ER_{BHGE,t}$] (scfm)
9.2-1	Site 1 Emission Rates [$ER_{BHGE,t}$] (scfm) of each Equipment Component
9.2-2	Site 2 Emission Rates [$ER_{BHGE,t}$] (scfm) of each Equipment Component
9.2-3	Site 3 Emission Rates [$ER_{BHGE,t}$] (scfm) of each Equipment Component
9.2-4	Site 4 Emission Rates [$ER_{BHGE,t}$] (scfm) of each Equipment Component
9.2-5	Site 5 Emission Rates [$ER_{BHGE,t}$] (scfm) of each Equipment Component
9.2-6	Site 6 Emission Rates [$ER_{BHGE,t}$] (scfm) of each Equipment Component
9.2-7	Site 7 Emission Rates [$ER_{BHGE,t}$] (scfm) of each Equipment Component
9.3-1	Measurement-Based Emission Factors per Component Category Compared with Regulatory Averages
9.4-1	Emission Factor [EF_{BHGE}] (scfm) per Equipment Component Category
9.4-2	Distance Piece Timeseries in relation to Hi-Flow Sampler Measurements
9.4-3	Dump Valve Timeseries in relation to Hi-Flow Sampler Measurements
9.4-4	Level Controller Timeseries in relation to Hi-Flow Sampler Measurements
9.4-5	Main Flange Timeseries in relation to Hi-Flow Sampler Measurements
9.4-6	Methanol Pump Timeseries in relation to Hi-Flow Sampler Measurements
9.4-7	Pre-Lube Pump Timeseries
9.4-8	Pressure Controller Timeseries in relation to Hi-Flow Sampler Measurements
9.4-9	Start Gas Timeseries in relation to Hi-Flow Sampler Measurements
9.4-10	Thief Hatch Timeseries in relation to Hi-Flow Sampler Measurements
9.4-11	Vent Header Timeseries in relation to Hi-Flow Sampler Measurements
9.5-1	Effect of High to Low-Bleed Operation Transition on Node 10
9.5-2	Emission Rate Trend- Node 10
9.5-3	Seasonal Component of Emission Rate - Node 10

9.5-4	Effect of High to Low-Bleed Operation Transition on Node 23
9.5-5	Emission Rate Trend - Node 23
9.5-6	Seasonal Component of Emission Rate - Node 23
9.5-7	Node 54 Methanol Pump
9.5-8	Distance Piece Timeseries: Node 31, Node 46, Node 69
9.5-9	Distance Piece Timeseries: (a) Node 31 (b) Node 46
9.5-10	48-hour window **(a)** Norriseal Separator Level Controller - Node 44 **(b)** Fisher L2 Separator Level Controller - Node 51
9.5-11	48-hour window **(a)** Fisher L2 Compressor Level Controller - Node 45 **(b)** Norriseal Compressor Level Controller-Node 18
9.5-12	Site 4 Operations
9.5-13	Site 5 Operations

Table	Description
1-1	Overall Project Milestones
1-2	BHGE Measurement-Based Emission Factors per Component Category Compared with Hi-Flow Sampler and Regulatory Averages
8.2-1	Site, Equipment Description, Node Count
8.3.1-1	Fugitive and Vented Sources by Component Category
8.8-1	Summary of Python Libraries used for the ETL, SV Pipelines
9.1-1	Site-Level Comparison
9.2-1	Site 1 Equipment Component Emission Rates [$ER_{BHGE,t}$] (scfm)
9.2-2	Site 2 Equipment Component Emission Rates [$ER_{BHGE,t}$] (scfm)
9.2-3	Site 3 Equipment Component Emission Rates [$ER_{BHGE,t}$] (scfm)
9.2-4	Site 4 Equipment Component Emission Rates [$ER_{BHGE,t}$] (scfm)
9.2-5	Site 5 Equipment Component Emission Rates [$ER_{BHGE,t}$] (scfm)
9.2-6	Site 6 Equipment Component Emission Rates [$ER_{BHGE,t}$] (scfm)
9.2-7	Site 7 Equipment Component Emission Rates [$ER_{BHGE,t}$] (scfm)
9.3-1	Emission Rates [$ER_{BHGE,t}$] (scfm) by Sensor Node and Component Type
9.4-1	Effect-Size Comparison for Distance Piece Nodes
9.4-2	Effect-Size Comparison for Level Controller Nodes
9.4-3	Effect-Size Comparison for Thief Hatch Nodes
9.4-4	Component Statistical Mean Emission Factor Compared with Regulatory Averages

3. Acknowledgement

This work was sponsored by the Ministry of Environment and Climate Change, Ottawa, Canada and the Petroleum Technology Alliance Canada (PTAC). The field-testing campaign took place at Bonavista Energy Corporation, Rimbey, Alberta, Canada.

The authors would like to acknowledge both organizations and the Bonavista Energy Corporation Team who have contributed valuable time and resources over the past two years. We are particularly indebted to the Bonavista Environment, Safety and Regulatory team (Colin Hennel and Dan Boutin) who shared their internal company practices, information, and facilitated the continued enhancement of this important work. A special thanks is also extended to Craig Andrew, CEO of CEI Control Services for successful deployment of LUMEN sensor systems in Bonavista well sites and compressor stations. Finally, the team wish to thank Joshua Anhalt, President, GreenPath Energy Ltd for successful Hi-Flow sampler surveys as part of this work.

Dominique Blain	Environment, Climate Change Canada (ECCC)
Steve Smyth	Environment, Climate Change Canada (ECCC)
Frank Neitzert	Environment, Climate Change Canada (ECCC)
Mark Godin	Petroleum Technology Alliance Canada (PTAC)
Dan Boutin	Bonavista Energy Corporation
Colin Hennel	Bonavista Energy Corporation
Craig Andrew	CEI Control Services
Joshua Anhalt	GreenPath Energy Ltd

Special thanks are also due to BHGE business and technology teams who participated on the project and/or provided review, comments, excellent support and logistics at different times throughout the duration of the project:

Glen Parkes	BHGE – Sensors Solutions
Myalee Muller	BHGE – Sensors Solutions
Jon Chow	BHGE – Sensors Solutions
John Corcoran	BHGE – Sensors Solutions
Jeanette Patel	GE Canada
Katy Howe	BHGE-EIC
Chuck Womble	BHGE-EIC
Sam Tanner	BHGE-EIC
Radislav Potyrailo	GE Research Center

4. Background

In 2011, the Canadian GHG emissions for upstream oil and gas flaring, methane venting and fugitives were 34.4 million tonnes CO_2 equivalent, 65% of which were from Alberta sources. Direct methane emissions account for 89% of this amount and are primarily composed of fugitives (33%), venting (30%), and others (26%) including a number of small releases from pneumatic equipment and other process sources[1]. To combat climate change and mitigate greenhouse gas emissions as participants in the international Paris Agreement, the Canadian government has put in place new regulations addressing methane emissions from the oil & gas industry which handles the highest amount of methane emissions in Canada[2].

These new regulations are intended to enable a 40 to 45% reduction in emissions from 2012 levels by the year 2025. Since methane (the primary component of natural gas) is 25 times more potent than Carbon Dioxide, and as natural gas continues to be an economically viable energy source, ensuring that the resource is kept within the infrastructure is key for environmental sustainability. However, there are currently knowledge gaps and accuracy concerns related to the current status of oil & gas emissions and the leak estimation and reporting methodologies employed by oil & gas operators. To achieve meaningful reductions, the current emission footprints of operators need to be understood at a granular, quantitative level. It was determined that one way to close these knowledge gaps is by utilizing and deploying leak source direct measurements techniques, and parting ways with emission rate estimates generated from high-level measurement campaigns that are widely considered as outdated and uncomprehensive. This report provides the results of the study and concludes with proposed updated emission factors for each of the monitored component leak sources.

5. Problem Statement

It is in the interest of the oil and gas industry that the information reported through both the GHGRP and the National GHG inventory are consistent and as accurate as possible. Considering this, the oil and gas industry has been working to identify improved emission estimation techniques and update emission factors. The hypothesis that this project addresses is that the use of autonomous and continuous monitoring network of sensors will reduce the uncertainties of estimating emission factors from oilfield equipment. The uncertainties associated with emissions from individual equipment component could be significant in many cases. Today's available emission factors were generated using the best available technology at the time and are based on periodic, discrete measurements coupled with component count estimation resulting in low confidence of accuracy.

To improve the accuracy in these reports, the BHGE team has undertaken this pilot study in partnership with the Environment Climate Change Canada (ECCC) and Bonavista Energy Corporation. The team used the recently developed cutting edge BHGE-LUMEN patented technology in this research. This ubiquitous sensing technology is enabled by Wireless Sensor Network (WSN) for real-time monitoring of methane emissions from each equipment component at these sites. A total of 56 sensor nodes and 7 weather stations were distributed around 7 different operational sites to continuously monitor various known leaking components – from storage tank thief hatches to pneumatic level controllers – and characterize the dynamic signature of emissions from these sources. Additionally, to study the benefits of continuous emissions measurements on reducing the standard error in the reported emission factors by discrete methods (Hi-Flow Sampler and Method 21).

6. Existing Methodologies and Current Approaches

6.1 EPA

Approach:

The average emission factor is determined by measuring the emission rate from a large number of randomly selected components from similar types of facilities. This factor is then combined with the average number of components in the facility to estimate the average facility emissions, which are then extrapolated to a national estimate by the number of facilities in the gas industry. Since regional differences were found between similar facilities that affected the emissions, separate measurement programs were conducted to account for regional differences[3].

Methods of Quantifying Emission Factors:

1. EPA Method 21. Using a portable instrument to detect total hydrocarbon leaks. The value is then converted to an emission rate by using a correlation equation (for each component type) developed from data collected using an enclosure method. (Western US, offshore, and gas processing) Uncertainty may be high. [EPA, Section 3.1]
2. Using the GRI Hi-Flow Sampler equipment which directly measures the leak rate of a component. (Atlantic and Great Lakes region, gas transmission and storage facilities, and customer meter sets). It can measure all leaking components of a facility. The GRI Hi-Flow sampler generates a flow field around the component that captures the entire leak. As the sample stream passes through the instrument, both the sample flow rate and THC concentration are measured. With accurate flow rate and concentration measurements, the mass emission rate can be calculated as the product of the flow rate and concentration. [EPA, Section 3.2]

6.2 ECCC / Clearstone

Approach:

Emission assessment uses bottom-up approach, beginning with individual facilities and their equipment, and the following primary types of primary emissions sources. For each target substance, the determined emissions have been aggregated to determine overall emissions by facility type, activity type and geographic area[4].

Methods of Quantifying Emission Factors [EC, Section 2.2]

1. Emission Monitoring Results – Based on operating facility reports. Preferred method when available. Typically, continuous emission monitoring will yield emission estimates with uncertainties in the range of ±5 percent.
2. Emission Source Simulation Results – Computer models apply empirical correlations and/or fundamental engineering principles to develop rigorous emission estimates based on the specific operating and design parameters of the source. When properly applied, simulators offer the ability to predict accurately emissions from individual sources (generally to within ±25 percent or better), but have the disadvantage of requiring more time, effort, user knowledge, and input data to apply.
3. Emission Factors –Statistical approach in which the average emission from a group of sources is related to an appropriate activity value using a simple relation in the form of:

$$ER_{i,j} = EF_i * A_i * X_{i,j} * (1 - CF_i) * OF_i * g_c$$

Where, $ER_{i,j}$ = emission rate of substance j from source i (t/y).
EF_i = emission factor for source i (kg/unit of activity).
A_i= activity value for source i (unit activity per unit of time).
$X_{i,j}$ = mass fraction of substance j in the emissions from source i (kg/kg).
CF_i = control factor for a specific control measure or device applied to source i which indicates the fraction by which the emissions are reduced (kg/kg).
OF_i= operating factor which indicates the fraction of the time the source is active (d/d).
g_c= a constant of proportionality used to convert the results to units of t/y.

Where published or default values for specific parameters are used, the references for these are stated.

7. Research Objectives

The objective of this study is to develop measured-based, component-level, statistically robust emission factors based on BHGE continuous methane monitoring technology (LUMEN patented technology). This technology combined with data analytics methods enabled the BHGE team to revise the “default” EPA/EC methane emission factors for key equipment components in a small sample (7 sites) of oil and gas sites in Alberta, Canada. This study (initial pilot phase) is envisioned as a precursor to a larger scale study to cover more representative sample sizes of sites and equipment component diversities. This initial pilot phase is intended to serve as a technology demonstration and proof of concept of the BHGE-LUMEN methodology and is not expected to result in direct or immediate changes to the published emission factors currently used by the industry. Once the proof of concept is established, this work will be reviewed along with other data sources and could provide a basis for an expanded study later. Ultimately, and upon expanding this work, the refined emission factors will replace the current estimates, thereby improving the accuracy of the GHGI. This will have positive implications on the understanding of this segment contribution to methane emissions footprint within the oil & gas sector and informing policy and industrial decision making for potential mitigation opportunities.

One of the main objectives of this study is to characterize methane emissions from reciprocating compressor components and above-ground oil and natural gas equipment to improve the quantification of methane emission factors Greenhouse Gas Reporting Program (GHGRP). A key focus of the study is to assess short-term and long-term variability of emissions from a variety of components at G&B compressor stations and well sites, using a suite of measurement and leak detection technologies. Key research questions addressed by this study include:

1. Do emissions from the same site or piece of equipment vary over time?
2. What effect does sample duration have on the measured emission rate?
3. Do operation parameters (e.g. throughput, gas composition, compressor age) correlate with higher emission rates?
4. Do emission rates vary from site to site?
5. How do measured emissions compare to estimates calculated from published emission factors?
6. Do the data support the current component categories in ECCC/EPA?

To achieve these goals, seven (7) Bonavista Energy sites were selected to demonstrate the capability of this new technology, its superiority to currently available methods, and to test this new methodology for developing measured-based statistically robust emission factors.

BHGE's methodology is founded on continuous measurements of methane leaks at the equipment component level using its newly developed innovative, multivariable, methane sensing technology and data analytics platforms (LUMEN Technology). This robust technique will bridge the existing gap in understanding equipment operational performance as it relates to frequency and intensity of methane leaks over time. BHGE EIC's sensing platform continuously measured different equipment components leak rates and leak frequencies to disaggregate and characterize leaks from these assets.

8. Test Methodologies, Tools, and Technology

8.1 BHGE- LUMEN Methane Sensing Technology

BHGE have recently developed a ground breaking digital integrated methane monitoring solution (LUMEN) to support oil and gas customers' sustainability programs. BHGE Technology focuses on solving poor gas selectivity by combining thick film catalytic combustion metal oxide semiconductor with conventional impedance analyzers. BHGE researchers disrupted the method of conventional sensing from resistive read out to impedance read out. This gave us the ability to move from measuring the sensor response using a single point measurement to resistance and impedance as a function of the frequency range 1 to 100 KHZ. This also enabled us to have high sensor stability, and rejection of interferences. To overcome the insufficient selectivity limitation of existing sensors and sensor arrays and to improve their reliability, we developed a new generation of gas sensors based on multivariable response principles.

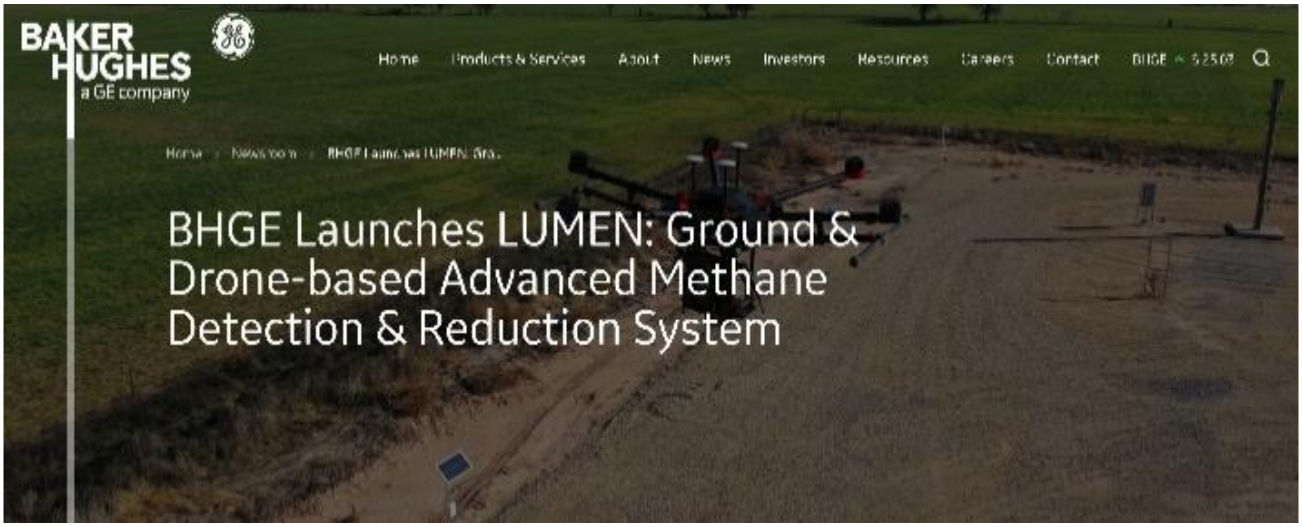

BHGE Launches LUMEN: Ground & Drone-based Advanced Methane Detection & Reduction System

LUMEN technology utilizes a multivariable algorithm to eliminate numerous limitations of existing sensors with the ability to quantify multiple individual gases, accurately detect gases in the presence of numerous chemical interferences, to have self-correction for temperature, and to reject chemical interferences at a several million-fold excess. LUMEN creates a digital mesh network and continuously and remotely ‘sniff’ for leaks, without the need for human intervention. LUMEN represents a major differentiator compared to previous batch or discrete leak measurements leading to a more comprehensive understanding of leak source characteristics and emission mitigation.

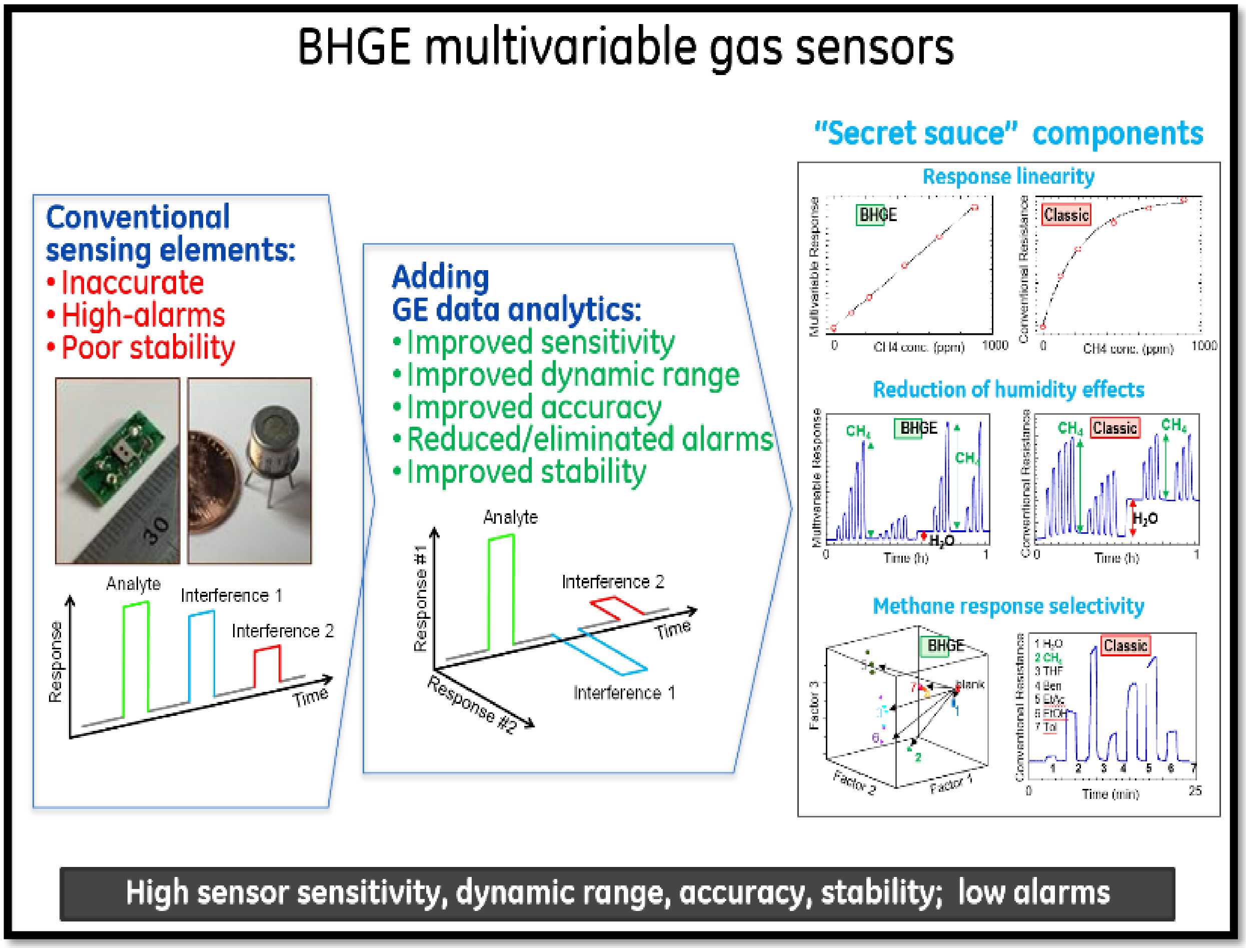

BHGE multivariable gas sensors

Conventional sensing elements:
- Inaccurate
- High-alarms
- Poor stability

Adding GE data analytics:
- Improved sensitivity
- Improved dynamic range
- Improved accuracy
- Reduced/eliminated alarms
- Improved stability

"Secret sauce" components

High sensor sensitivity, dynamic range, accuracy, stability; low alarms

The key scientific innovations of LUMEN technology that deliver sensing capabilities that are unmatched over other types of gas detectors are two-fold. First, LUMEN technology incorporates a new paradigm of gas sensing based on multivariable electromagnetic radio-frequency (RF) transducers, their detection principles, and sensor-excitation rules that provide an elegant low-power and cost-effective technological solution to boost the range of measured methane concentrations to more than six orders of magnitude and to achieve a highly desired sensor gas-selectivity. Second, it incorporates machine learning data analytics methodologies to correct performance of individual sensors against environmental effects and to collectively analyze dynamic data from the deployed sensor network to locate and quantify gas leaks over the surveillance area.

8.2 Test Locations

The 56 LUMEN sensor nodes and 7 Base stations including 7 mini computers, routers, and 7 Weather Stations were deployed in a total of 7 sites operated by Bonavista Energy Corporation in Rimbey, Alberta, Canada. These locations include 3 well sites and 4 compression stations that contain a variety of equipment and components that release some natural gas as part of the operations. This gas is then vented to atmosphere. BHGE LUMEN sensor nodes were placed within inches of the venting sources to better capture these vented emissions. It should be mentioned that these sites were selected based on two criteria a) grid power availability and b) Diversification of components. We attempted as much as possible to have a good mix between Compressor Stations, Wellsites, Battery site given the basic requirement of grid power availability.

Table 8.2-1 Site, Equipment Description, Node Count

Site No.	Site Description	No. Nodes	Main On-Site Equipment	
1	Compressor Station **"Compressor 622"**	10 + BS	Separator Compressor Dehydrator with Glycol Reboiler Storage Tank	
2	Wellsite **"Wellsite 102/03-23-043-03W5"**	7 + BS	Electric Pump Jack 2 Separators Storage Tanks Multi-well Oil Battery	
3	Compressor Station **"Westerose Compressor Site"**	7 + BS	Separator 2 Reciprocating Compressors Metering Building Pig Launcher	Dehydrator Fuel Gas Scrubber Vent Stack
4	Compressor Station **"Willesden Green 16-12 Compressor"**	10 + BS	2 Line Heaters 2 Separators Reciprocating Compressor Screw Compressor	Dehydrator Vent Stack Storage Tanks
5	Wellsite **"Willesden Green 12-04 SWB"**	6 + BS	Separator Methanol Pump Storage Tank	
6	Compressor Station **"South Elkton 02-03 Compressor Station"**	10 + BS	2 Separators Compressor Driver Condensate Skid Dehydrator	Storage Tank
7	Tank Battery **"Harmattan 12-29-031-03W5 Battery"**	6 + BS	2 Separator Storage Tanks Production from Several Wells	

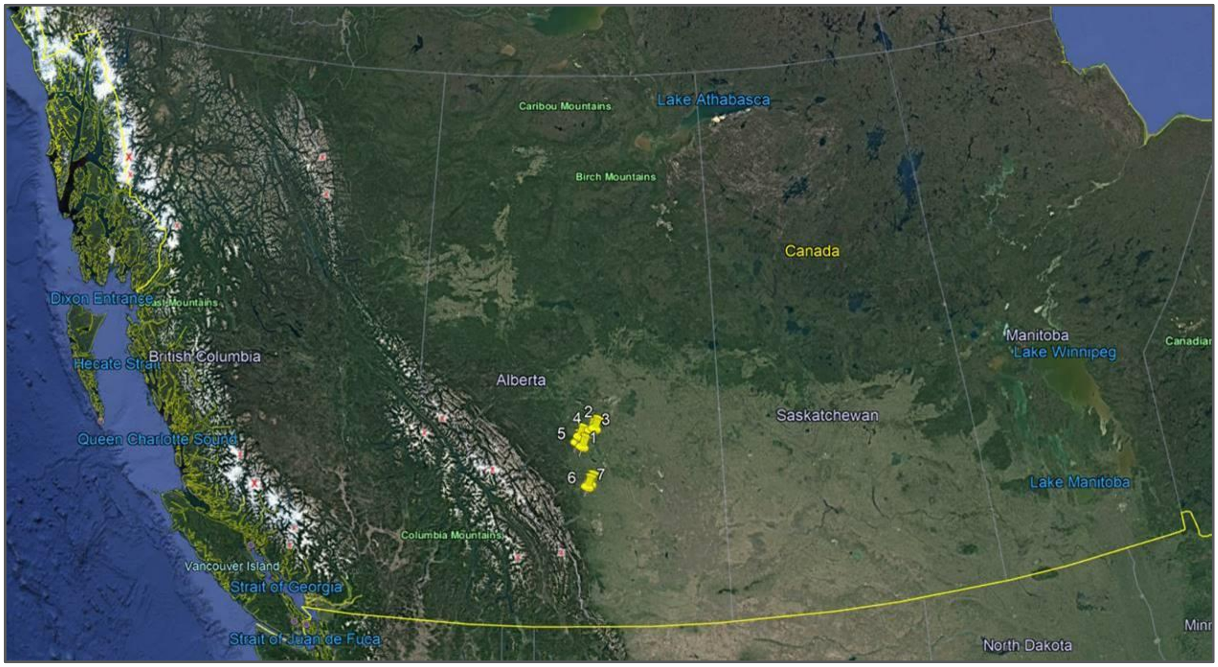

Figure 8.2-1 Geographic Location of Bonavista Sites

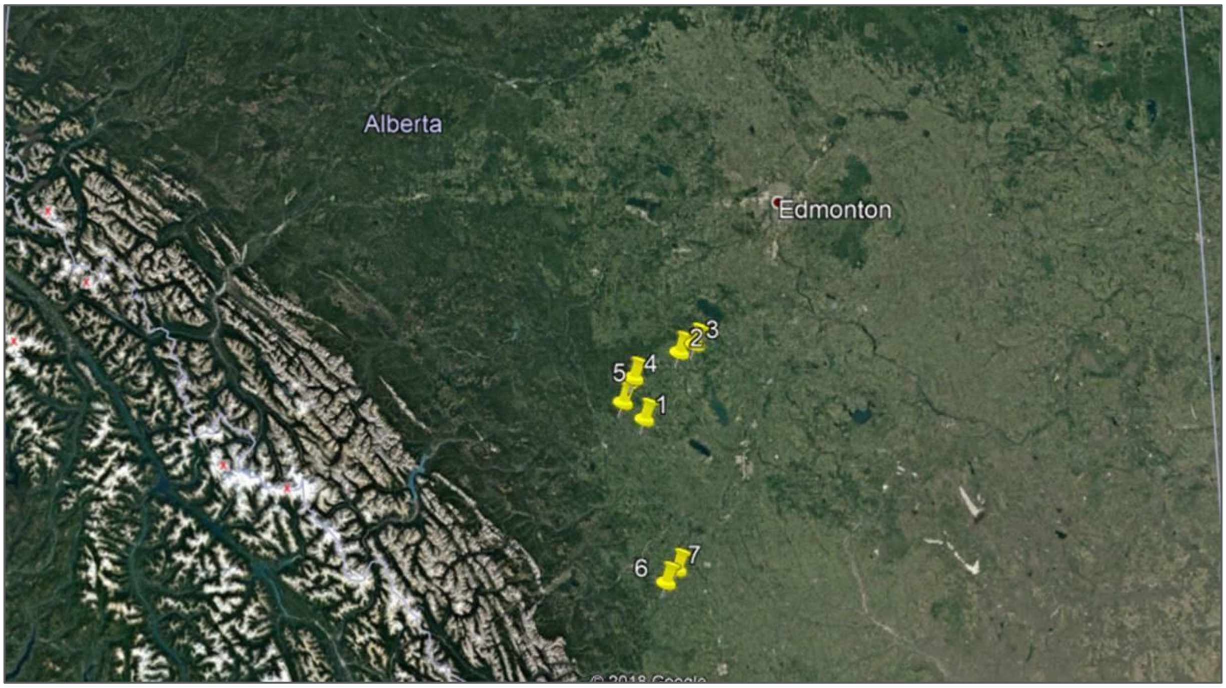

Figure 8.2-2 Geographic Location of Bonavista Sites - Close-Up

8.3 Equipment Component Characterization

The objective of this section is to deep dive into each type of equipment component monitored by LUMEN to understand and highlight the underlying operational rhythm for venting methane under normal and abnormal conditions. This step is critical in our characterization of methane emissions from these components and paves the way to pair our analytics with the equipment component performance and service records provided by Bonavista team.

1. Fugitive Sources and Vented Sources

Equipment components in this study were categorized into fugitive sources and vented sources as shown in **Table 8.3-1**. Fugitive emissions are unintentional releases from piping components and equipment leaks at sealed surfaces, as well as from underground pipeline leaks. Fugitive emissions are usually low volume leaks of process fluid (gas or liquid) from sealed surfaces, such as gaskets, resulting from the wear of mechanical joints, seals, and rotating surfaces over time. Specific fugitive emission source types include various components and fittings such as valves, flanges, PRVs, or sampling connections. In this study, the team was able to only Identify one of these leak sources, main flange (site 2) monitored by sensor nodes number 20, 21, and 22. It should be mentioned here that the team was unable to find many of these type of fugitive emissions during the boots on the ground phase of this project, credit to Bonavista team on keeping fugitive methane emissions under control.

Vented sources occur as releases resulting from normal operations, maintenance and turnaround activities, and emergency and other non-routine events. These include sources such as crude oil, condensate, oil, and gas product storage tanks; blanket fuel gas from produced water tanks; as well as equipment components that release methane as part of their operation such as chemical injection pumps, pneumatic devices, reciprocating compressor distance piece, methanol pumps, pre-lube pump columns, etc.

Table 8.3.1-1 Fugitive and Vented Sources by Component Category

	Equipment Component Category	Fugitive/Vented Emission
1	Distance Piece (n =3)	Vented
2	Dump Valve (n =4)	Vented
3	Level Controller (n=18)	Vented
4	Main Flange (n=1, 3 sensors)	Fugitive
5	Methanol Pump (n=3)	Vented
6	Pre-Lube Pump Column (n=1)	Vented
7	Pressure Controller (n=13)	Vented
8	Start Gas (n=2)	Vented
9	Thief Hatch (n=3)	Vented
10	Vent Header (n=6)	Vented

Distance Piece:

In normal operations, the distance piece, or packing system, in a reciprocating compressor acts as a barrier preventing natural gas from entering the crankcase. It is composed of a series of rings and springs that are subject to wear and tear due to shaft axial movement, vibration, and mechanical loads, causing methane to leak to the atmosphere.

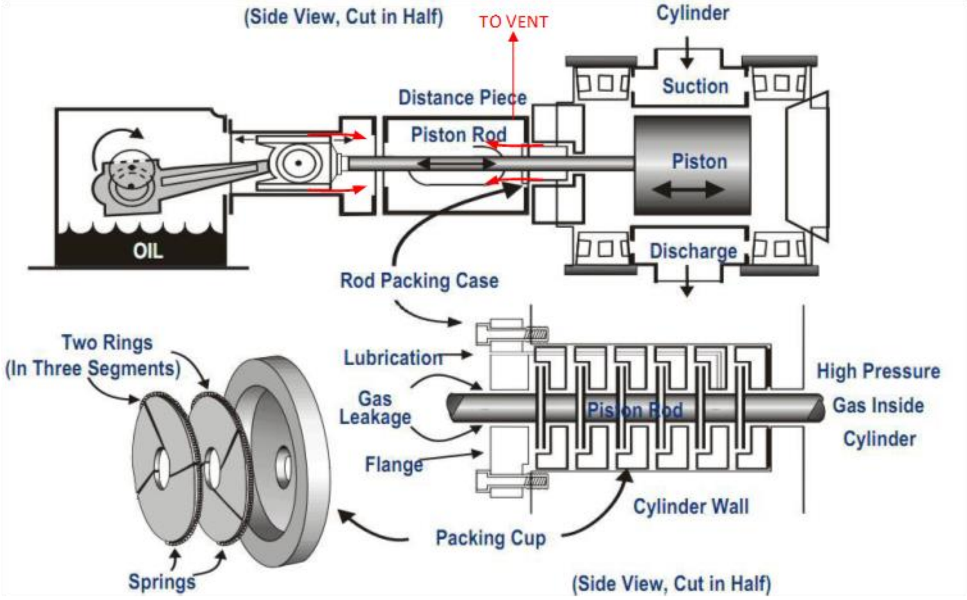

Figure 8.3-1 Reciprocating Compressor Distance Piece Schematic

Dump Valve:

The dump valve controller is a binary device that opens or closes the dump valve. When the controller calls for the dump valve to open the power gas is vented from the valve's control diaphragm. The dump valve controller can be either electrically or pneumatically operated. In both cases gas is released from the control valve until the pressure is vented and the valve has moved to its normal closed or normally open position. Vents only during the transition from closed to open.

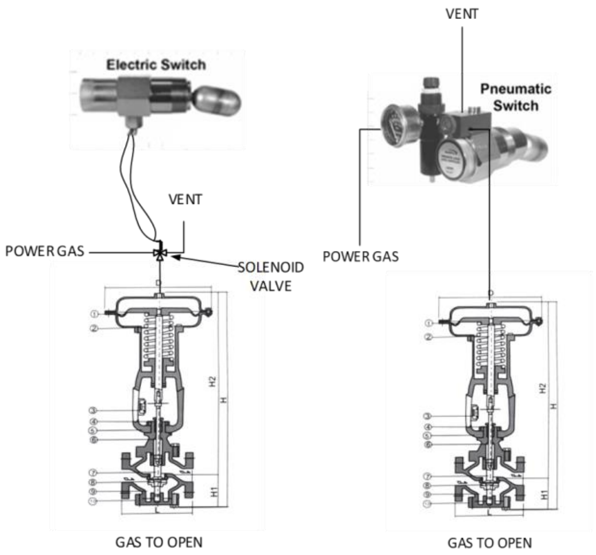

Figure 8.3-2 Liquid Dump Valve Schematics

Level Controller:

There are two types of pneumatic control devices typically used in the oil and gas industry. The level switch and the level controller. The level switch uses gas to move the valve to the open or closed position depending on the fail position of the valve. If the valve is a fail close valve the valve will remain closed until gas is applied to the valve by the switch to open the valve. If open and the switch changes to close the valve the switch will vent the gas and allow the valve spring to close the valve. The power gas, instrument air or produced gas, is released from the valve actuator. The release of gas is intermittent and short lived. The frequency of the gas release is contingent on the frequency the liquid needs to be dumped to lower the level of the liquid. The level switch can be electric or pneumatic.

Level controllers are pneumatic regulators used to control liquid levels at a more constant level than level switches. The controller Is based on the Force Balance Principle, which states that the buoyant force created by an object submerged in a liquid Is directly proportional to the weight of the liquid displaced. The regulator uses a spring to balance the weight displaced and triggers the movement of a shaft that creates a rotational movement, which opens the thrust pin and releases pressure. The controller vents power gas continuously from the controller as well as the valve when the valve is unloading towards the fail-safe condition.

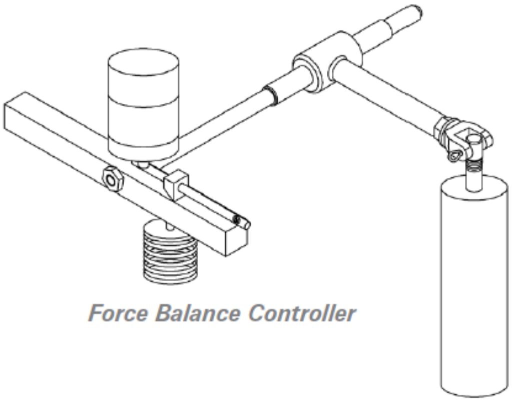

Figure 8.3-3 Level Controller Schematics

Main Flange:

The wellhead provides the structural and pressure-containing interface for the drilling and production equipment. It is the first surface component to be in contact with production fluids, and therefore the first possible occurrence for leaks. A leak would occur due to the failure or wear of seals, design capabilities exceeded in operation, presence of dirt or foreign particles from installation, problems related to vibration, not enough tightening of flange, corrosion of components, or overall faulty design of wellhead.

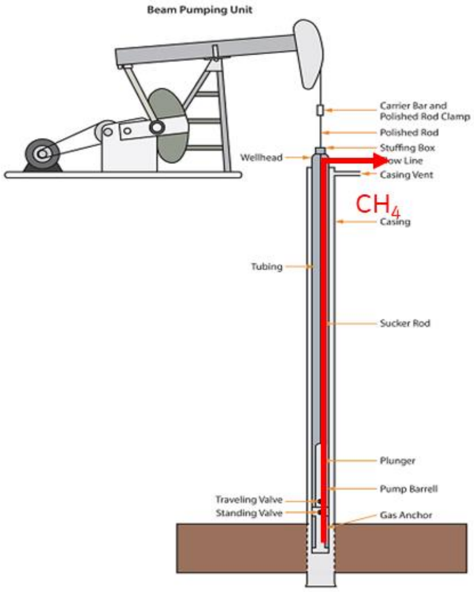

Figure 8.3-4 Main Flange/Wellhead Schematics

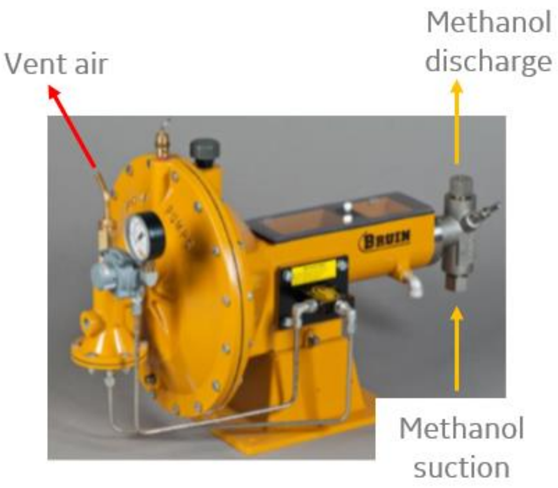

Methanol Pump:

Pneumatic pumps are typically used to inject methanol into natural gas production facilities in order to prevent hydrate formation. Most wells are not on the electric grid, and normal practice is to use natural gas driven pneumatic pumps to inject the methanol. This type of pump uses the pressure energy of the produced gas to operate the pump, and then vents the spent gas to the atmosphere. The energy that could have been derived from combustion is wasted. Furthermore, the vented gas stream is largely methane, a high impact GHG.

Figure 8.3-5 Methanol Pump Schematics

Pre-Lube Pump Column:

The engine driver for a reciprocating compressor will typically have a pre/post lube oil system. The pre-lube system is used to fill the oil cooler, oil lines and bring the lubrication system up to operating pressure before starting the engine. The post-lube pump is used for cooling turbocharger bearings, if required. The pre/post lube pump is powered by compressed air, or compressed gas when air is not available. At start up, the pre-lube pump is started either manually or automatically. At shutdown the post-lube pump is started either manually or automatically. They are run for a set amount of time before they are shut down.

The reciprocating compressor may have a pre-lube pump to perform the same service for the crankcase. Additionally, the cylinder lubricators may have a hand operated pre-lube pump that is used to initiate lubricant flow to the cylinders to ensure they are not operated dry.

Pressure Controller:

In proportional-only controllers, supply pressure enters the relay and bleeds through the fixed orifice before escaping through the nozzle. Nozzle pressure also registers on the large relay diaphragm and loading pressure (controller output pressure).

A change in the process pressure moves the beam and flapper or contracting the Bourdon tube arc. An increasing pressure with direct action produces a nozzle-flapper restriction that increases the loading on the large relay diaphragm and opens the relay valve. Additional supply pressure flows through the relay chamber to increase the loading pressure on the control valve actuator. A decreasing process pressure does the opposite.

Pressure controllers are very similar to level controller, except they employ the bourdon tube as a pressure sensing device instead of a displacement sensing device to control the signal sent to the control valve. The controller vents power gas continuously from the controller as well as from the valve when the valve is unloading towards the fail-safe condition.

Figure 8.3-6 Pressure Controller Schematics

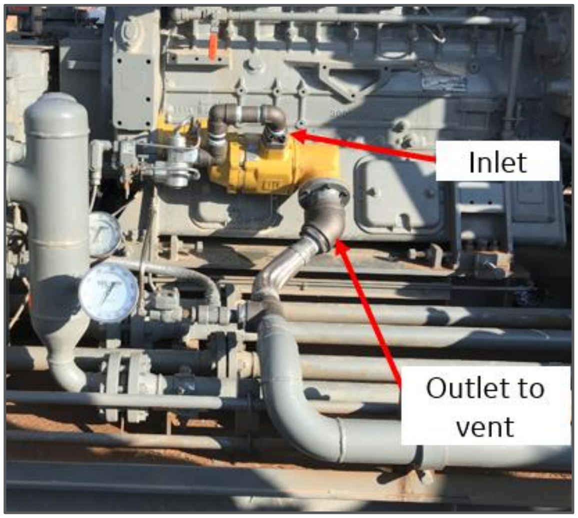

Figure 8.3-7 Air/Gas Starter Schematics

Start Gas:

The engine driving a reciprocating compressor will typically have a compressed air or compressed gas starter. This type of starter is used when starting torque requirements are high or when electric power is not available for a conventional electric drive starter. The extra torque is required due to the need to spin both the engine and compressor during startup. Larger engines can have multiple air/gas drive starters. The starter can be energized manually or automatically depending on the control system used.

The starter is engaged normally under 1 minute for startup. During maintenance it may be run for longer periods or multiple times.

Thief Hatch:

Storage tanks are the end of the road for produced liquids after going through the separation process to remove produced water and natural gas. However, due to pressure differentials and fluid properties, some gas remains in solution and travels to the storage tank along with the oil. When the thief hatch Is opened, this gas comes out of solution and is released to the atmosphere, and these are the emissions that we're measuring. These will depend on the hydrocarbon composition as well as the frequency the thief hatch is opened. An additional reason for leakage can be attributed to faulty gaskets and seals within the hatch.

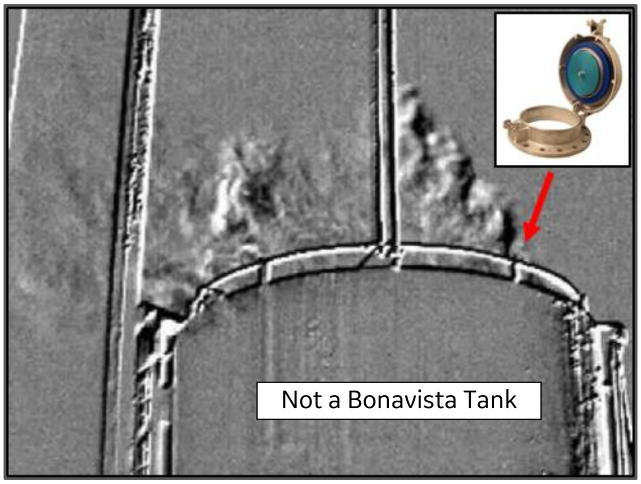

Figure 8.3-8 Storage Tank Thief Hatch Emission

Vent Header:

The vent header is a line that collects the leaks from multiple sources, distance pieces, crankcases, control valves, controllers, etc. Common header in most cases vents to the atmosphere.

Some of the causes for leaks may be dirt or foreign matter, worn rod, insufficient/too much lubrication, packing cup out of tolerance, improper break-in on start-up, incorrect packing installed.

8.4 Test Approach

Figure 8.4-1 summarizes key events and dates for this testing. Between April 2018 and February 2019, a total of 56 LUMEN Sensors were deployed in 7 Bonavista sites located in Rimbey, Alberta, Canada to continuously sample component level methane emissions. Sampling rate was determined to be every two seconds to allow for capturing dynamic behavior of each equipment component required to develop robust measured based emission factors as will be explained further in this report.

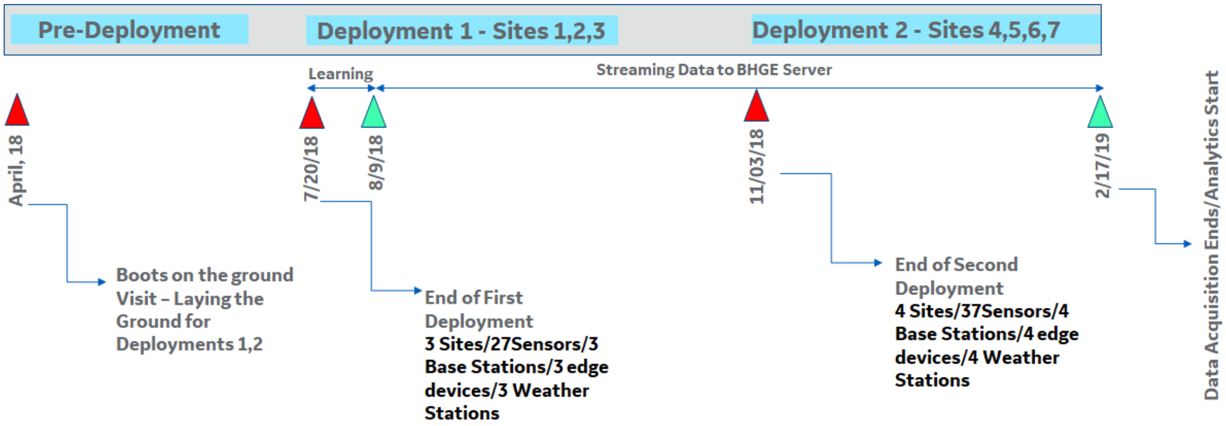

Figure 8.4-1 Deployment Timeline

Continuous sampling method is a unique approach that sets this study apart was performed at these sites to capture variability in activity data, such as sites operational modes, weather conditions, and facilities gas throughput. Equipment component leaks and vents were identified during boots on the ground visit in April 2018.

During the boots on the ground campaign, a total of 78 components were screened using an SA3C32A-BE open path Laser Methane mini (LMm) to safely and quickly measure existence of a leak in a given component remotely from a distance up to 30 meters. This method was adequate for difficult-to-reach leak sources. Out of the 78 components screened, we qualified our 57 components as our representative sample for this study. Each of the 57 components was clearly tagged as shown in **Figure 8.4-2.**

Figure 8.4-2 Tagged Components

During the field deployment campaigns 1 and 2, all LUMEN nodes were taken out of the shipping containers and moved to the field, labeled and prepared for the installation. Base Stations including all data acquisition and network Hardware /Software were installed and commissioned as shown in **Figures 3-5**.

Figure 8.4-3 Sensor Nodes

Figure 8.4-4 Base Station

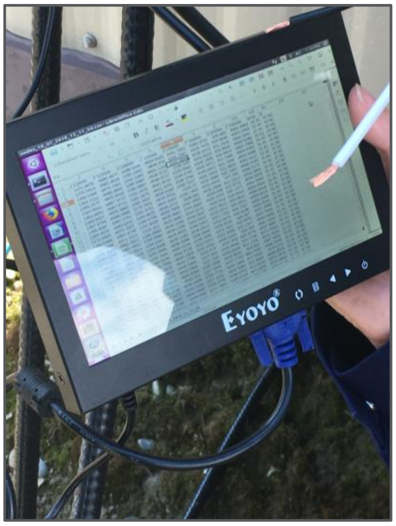

Figure 8.4-5 CSV data files

After identifying all emitting components, individual components were labeled and tagged to prepare for the LUMEN sensors deployment at appropriate locations to log emissions data continuously at the component level as shown in **Figure 8.4-6**.

Figure 8.4-6 Sensor Nodes Deployed

Figure 8.4-7 shows equipment count and classification of components at the 7 Bonavista Energy test sites. Although the count of components covered in this study is limited per the agreed SOW between ECCC and BHGE, these components match component sub-classifications listed in the USEPA and ECCC studies for emission factors. Additionally, this study is envisioned to serve as a technology demonstration and proof of concept of the **BHGE-LUMEN** methodology and is not expected to result in direct or immediate changes to the published emission factors of these components. Once the proof of concept is established, this work will be reviewed along with other data sources and could provide a basis for an expanded study later. Ultimately, and upon expanding this work, the refined emission factors will replace the current estimates, thereby improving the accuracy of the GHGI.

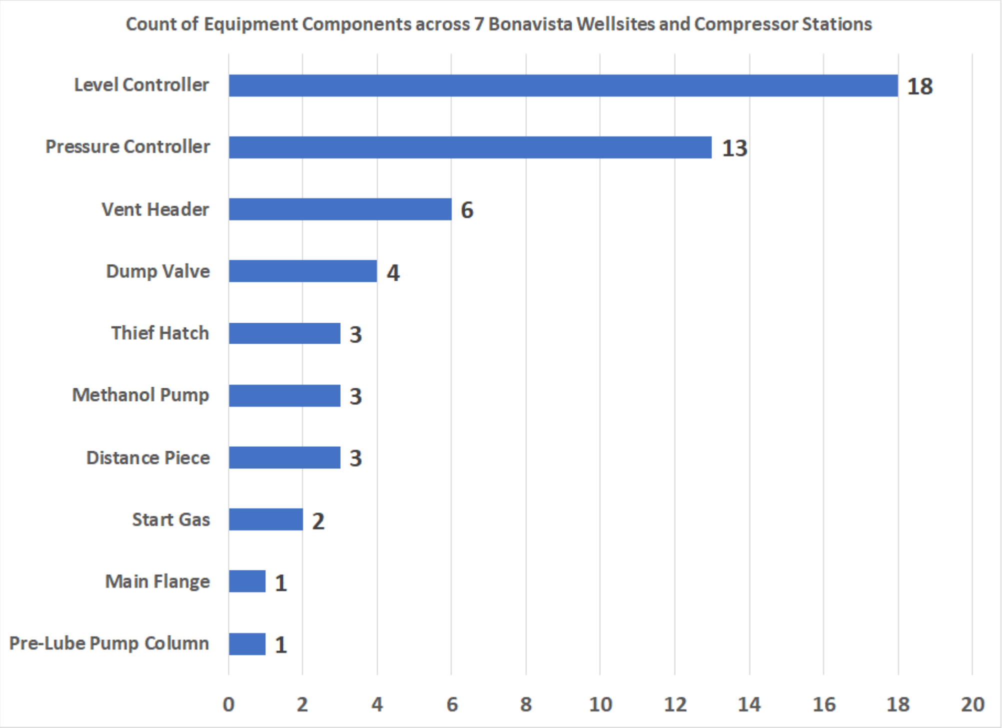

Figure 8.4-7 Component Count

Use of Hi-Flow Sampler

As part of this study, the Hi-Flow Sampler was used by an independent party (Greenpath Energy, LLC) to spot check instantaneous leak rates of each equipment component and to determine if emission rates for component categories were significantly different. The high volume (Hi-Flow) sampler is a portable, intrinsically safe, battery-powered instrument designed to determine the rate of gas leakage around various pipe fittings, valve packings, and compressor seals found in natural gas transmission, storage, and processing facilities. Three Hi-Flow sampler measurements were taken for each component and the zone of low to minimum values were added in the time series charts for the 7 components studied in this measurements campaign. The Hi-Flow sampler is used only as a reference instrument as it is widely used in industry. It is also critical is to note that the Hi-Flow Sampler technology is manually operated and has an accepted significant variability as reported in numerous studies such as "Touché Howard, Thomas W. Ferrara & Amy Townsend-Small (2015) Sensor transition failure in the high flow sampler: Implications for methane emission inventories of natural gas infrastructure, Journal of the Air & Waste Management Association, 65:7, 856-862,DOI:10.1080/10962247.2015.1025925, http://dx.doi.org/10.1080/10962247.2015.1025925"

8.5 Data Acquisition

BHGE sensor technology (LUMEN) is a system that integrates wireless sensor nodes, weather sensor, and edge device, all powered via site power. Measured data include far field wind speed and wind direction as well as gas emission concentration signals sampled at a frequency of two second interval to provide a representative sample for further statistical modeling and analytics as will be discussed in Section 8.8 in this report.

All measured data from 56 sensors nodes associated with the different equipment components (191 million data points) were pushed through cloud-based internet to a remote server equipped with user interface capable of handling, filtering and analyzing of big data rendered in various formats as shown in **Figure 8.5-1**.

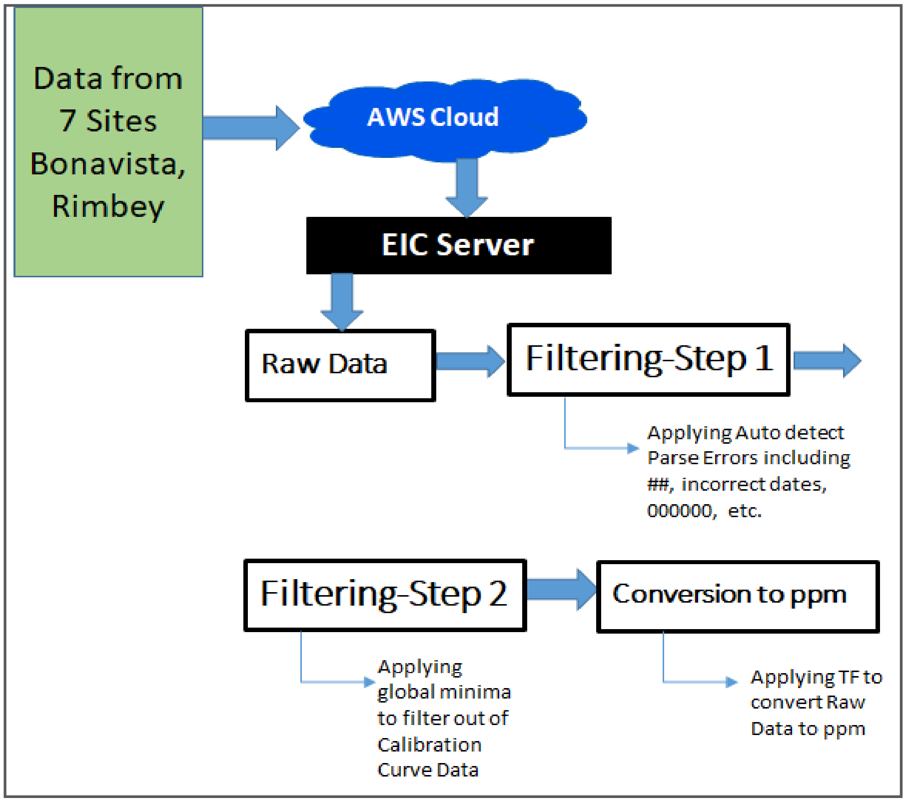

Figure 8.5-1 Data Acquisition Workflow

Wind Data Acquisition

The deployed weather station consists of an anemometer for measuring wind speed and a wind vane for measuring horizontal wind direction as shown in the **Figure 8.5-2**. The anemometer uses a three-cup and hub assembly to sense wind velocity. As the wind blows past the cups, the pressure of the wind against the insides of the cups causes them to rotate. There are three permanent magnets embedded in the hub that holds the cups. Each magnet, as it rotates past a fixed point on the sensor base, activates a magnetic reed switch mounted in the base. Three closures of the reed switch will be produced for each revolution of the cup assembly. The wind vane is mounted on top of the anemometer.

Figure 8.5-2 Weather Station Wind Vane

As the wind blows past the vane, the design of the counterweight and the tail fin align the point of the counterweight into the wind. The motion of the wind vane is translated to the potentiometer shaft causing a change in the potentiometer's resistance. Connecting the potentiometer wires to a voltage source allows easy measurement of the wind direction as a change in voltage.

The typical time series (sampling frequency is every 2 seconds) far field wind data are illustrated in **Figure 8.5-3** below.

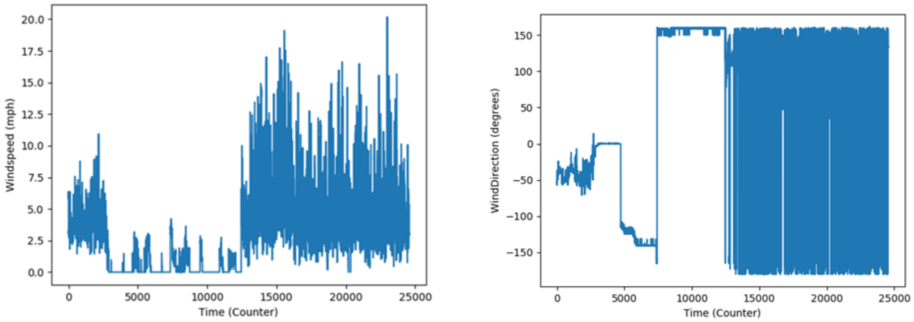

Figure 8.5-3 Raw Far-Field Wind Data Recorded by Weather Station Sensors

Methane Emissions Data Acquisition

There are two types of LUMEN sensor used in this study, one is referred as far field sensor device (also referred to as area monitor) that is positioned away from the potential gas emission sources on the periphery of a given site such that they maximize the chance of capturing potential leak plume downstream of the site seasonal prevalent winds. However, since the focus in this study is on the development of part level emission factors we have only deployed on the LUMEN far field version to help understand "albeit limited" the emissions footprint of the site at large. As such, one LUMEN far-field version per site deemed appropriate for this purpose as shown in **Figure 8.5-4**.

Figure 8.5-4 Far-Field LUMEN for General Area Monitoring of Methane Emissions

56 Near-Field LUMEN methane detection sensors (LUMEN) were installed in a proximity to potential leak sources (12 to 16 inches distance typical). **Figure 8.5-5 a and b** show how the LUMEN Near-Field sensors were installed downstream of a reciprocating compressor vent and pressure controller for a dehydration unit as an example. The gas sensors measure methane concentration in ppm every two seconds, convert the time series analog signals into digital values and then stream them to a cloud service for analytics processing.

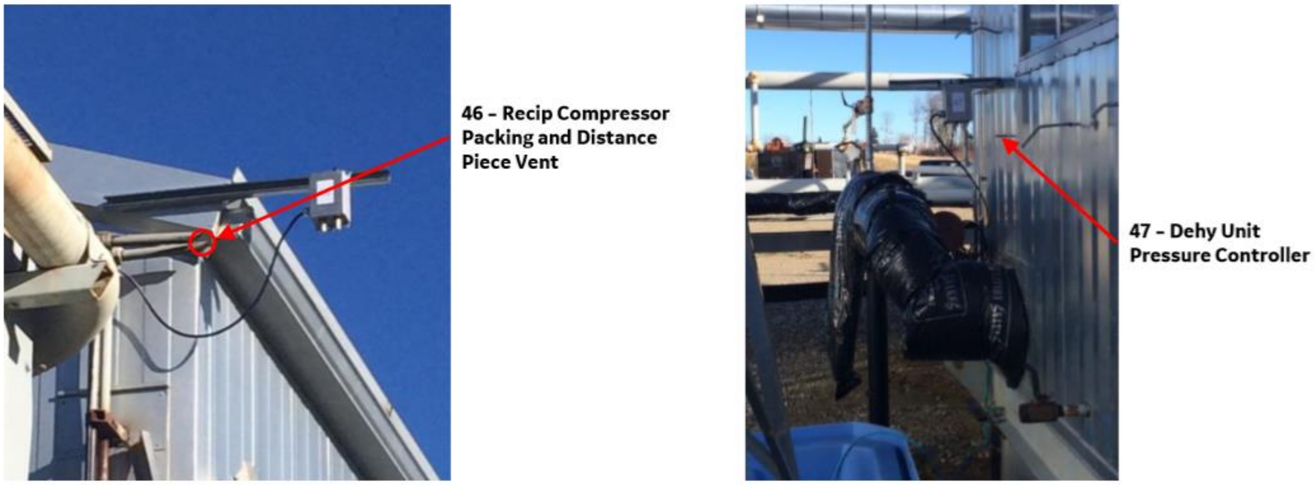

(a) **(b)**

Figure 8.5-5 Near-Field Sensors near Leaking Sources of (a) a Reciprocating Compressor Vent; (b) a Pressure Controller on a Dehydration Unit

8.6 Data Processing Work Flow

Figure **8.6-1** shows the end to end BHGE Big Data Analytics Platform for the development of measurement-based emission factors in this study. This framework was developed as a demonstration of BHGE approach for emission factor development which is a departure from traditional discrete measurements methods to estimate emission factors. Utilizing the BHGE sensor technology LUMEN, we were able to continuously sample in excess of 190 million data points representing emission rates for different equipment components in this study.

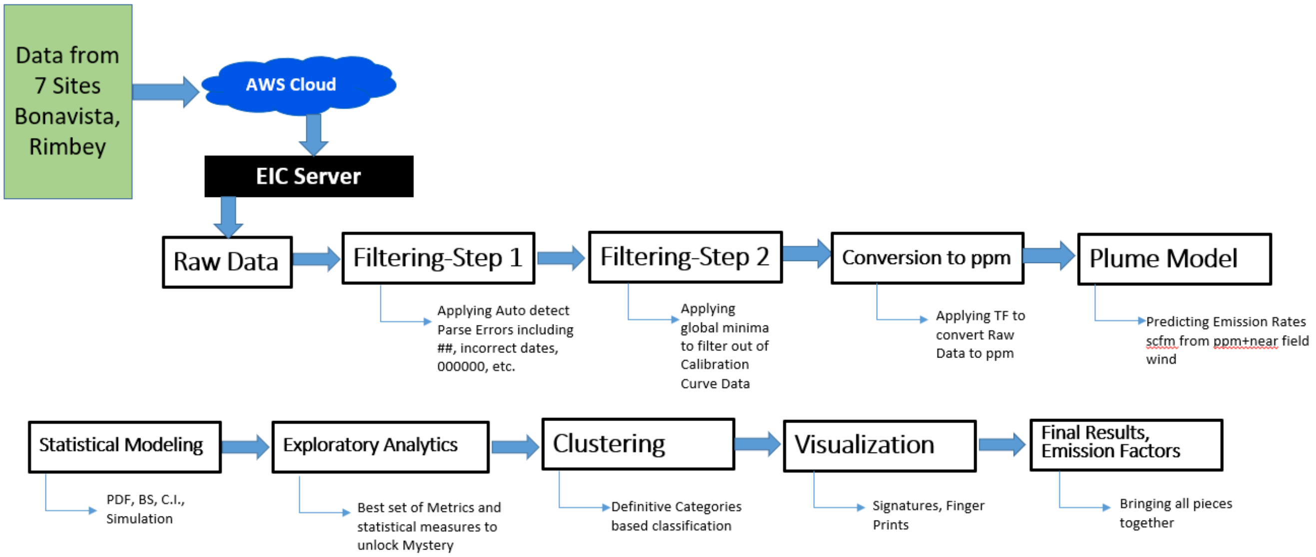

Figure 8.6-1 End to End BHGE Big Data Analytics Platform for Development of Measurement Based Emission Factor

As part of this workflow, raw sensor data is first filtered out to flag erroneous data points such as -9999 and other anomalous sensor outputs that usually resulted from exporting data over several media to AWS cloud server. For an ideal sensor, the minimum output corresponding to the background/environment should be nearly constant. However, for situations in which the sensor must operate in harsh conditions, this minimum needs to be periodically checked and the sensor output be correspondingly recalibrated. In our data extraction, transformation and loading (ETL) pipeline, we display weekly minima (referred to as Global Minima) so we can have a solid idea of what sensor minima drifts looks like for the entire dataset and to exclude outliers if any. As an example, for sensor 26, the weekly minima are shown in **Figure 8.6-2** below.

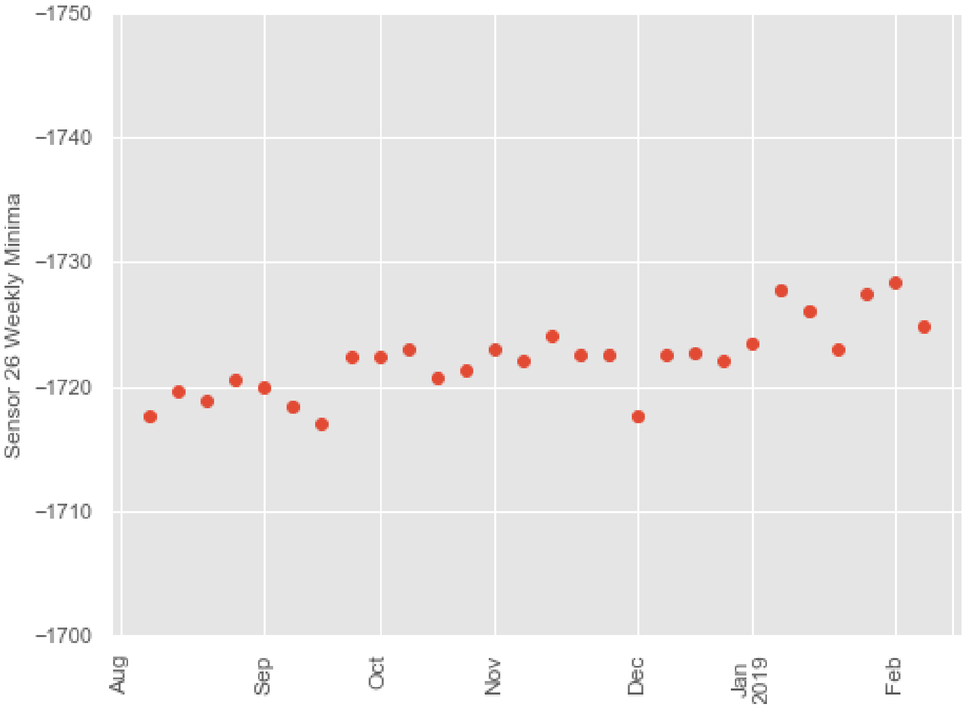

Figure 8.6-2 Weekly Minima of Raw Sensor Output for Sensor 26

For this sensor, it can be clearly seen that the minimum is quite stable. The weekly minima have a mean value of -1722.26 and a standard deviation of 2.9. For this reason, it is appropriate to use the global minimum (-1728.29) as the background signal level for the entire data set. The calibration equations and measurement error polynomials are then used to convert the raw signal to concentration in ppm units. For example:

$$C_r\ [ppm] = a_5 v^5 + a_4 v^4 + a_3 v^3 + a_5 v^2 + a_1 v + a_0 \qquad \textbf{Eq. 8.6-1}$$

Where v is the raw sensor output and C_r is the concentration in ppm. a small concentration-dependent experimental correction ΔC is then added to the baseline concentration to yield what we refer to as the corrected concentration C.

At this point, the concentration timeseries is ready for ingestion by the leak rate calculation algorithm. Finally, wind speed and wind direction data are forward-filled (i.e. missing data points are replaced by first available values from previous timestamps). In limited situations where we do not have previous historical wind data we perform backfilling where information from the future is passed backwards in time. Now that we have a complete set of concentration, wind speed and wind direction for a given node, the data is passed on to the leak rate calculation algorithm which outputs the instantaneous leak rates. Now the leak rate estimates and corresponding concentration timeseries is passed on to the computational statistics and visualization pipeline which will be elaborated on in Section 8.8.

8.7 Near-Field Plume Dispersion Model

The application of BHGE-LUMEN (near-field) in this study is a differentiator in comparison with previous studies by EPA and ECCC that used the Hi-Flow sampler as the basis for the development of today's widely used emission factors. It is our hope that this novel approach will lead to a new emission factor estimation strategy accompanied with significant cost reduction and higher measurement accuracy. **Figure 8.7-1** shows the end to end Near-Field Model Workflow (converting ppm to scfm). In this section, we discuss the methods that BHGE has developed to estimate the emission source rate from the concentration and weather data.

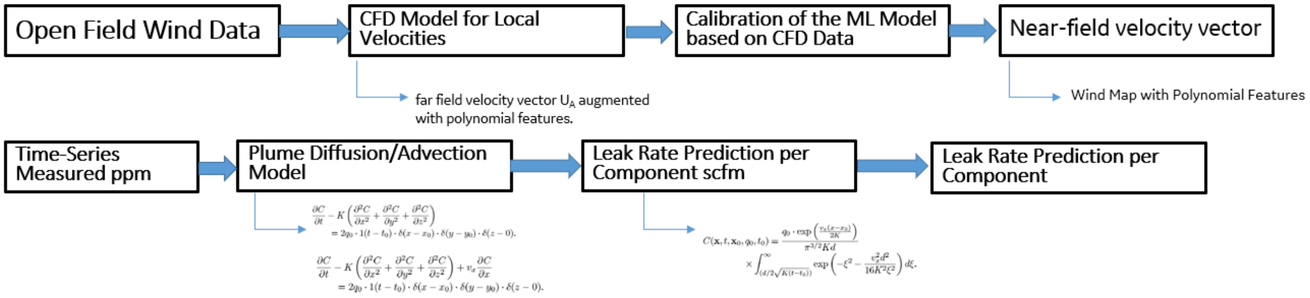

Figure 8.7-1 Near-Field Model Workflow (converting ppm to scfm)

The dispersal behavior of the plume is modeled by turbulent diffusion (eddy diffusion) and advection[5] as follows:

$$\frac{\partial C}{\partial t} - K\left(\frac{\partial^2 C}{\partial x^2} + \frac{\partial^2 C}{\partial y^2} + \frac{\partial^2 C}{\partial z^2}\right) = 2q_0 * 1(t-t_0) * \delta(x-x_0) * \delta(y-y_0) * \delta(x-0) \qquad \textbf{Eq. 8.7-1}$$

where C is the concentration, K is the diffusivity tensor, and the source position is denoted by $X_0 = (x_0, y_0)$, and the source start time is t_0.

Equation 8.7-1 describes molecular diffusion with very small diffusion coefficients. In addition to this molecular diffusion, turbulence in the air leads to so-called turbulent diffusion (eddy diffusion). The turbulence is caused by thermal effects, and wind. The turbulent diffusion is very complex and is thus hard to model mathematically. However, the diffusion equation 8.7-1 is a reasonable approximation in many cases, especially if some averaging of the measured concentrations is applied. The effect of turbulent diffusion is usually much stronger than molecular diffusion, and thus, the turbulent diffusion coefficient is much larger than for molecular diffusion (up to $K = 100\ m^2/s$). The turbulent diffusion coefficient is almost independent of the diffusing substance but depends highly on the environment[6].

In addition to diffusion, the plume dispersion is also characterized by advection when wind is present which is the case with this sensor deployment. All emission sources are located outdoors near LUMEN sensor nodes (12" to 14") and were impacted by wind speed and direction as a function of space and time. The analytical solution for the dispersal model described by the diffusion-advection equation is:

$$\frac{\partial C}{\partial t} - K\left(\frac{\partial^2 C}{\partial x^2} + \frac{\partial^2 C}{\partial y^2} + \frac{\partial^2 C}{\partial z^2}\right) + v_x \frac{\partial C}{\partial x} = 2q_0 * 1(t - t_0) * \delta(x - x_0) * \delta(y - y_0) * \delta(x - 0) \qquad \textbf{Eq. 8.7-2}$$

The analytical solution of the dispersal model results from the diffusion-advection equation in conjunction with simplified assumptions on the initial and boundary conditions is given below for large t(t→ ∞). **Equation 8.7-3** was used to determine the unknown leak rate Q (ft3/s) from the source given the measured methane concentration (ppm) and Near-Field wind speed U (ft/s) in a direction of a given LUMEN sensor at a given source-to-sensor distance d (ft).

$$C(x, \infty, x_0, q_0) = \frac{q_0 * e^{\left(-\frac{vx}{2K} * \left(d - (x - x_0)\right)\right)}}{2\pi K d} \qquad \textbf{Eq. 8.7-3}$$

Mapping Open Field Wind to Near-Field Wind

For near-field plumes, the velocity fields that transport the concentration field is strongly influenced by the infrastructure near the leak/sensor. To derive the relationship between the near-field velocity vector and the far-field sensor measurements, a data-driven modeling approach was devised. This data-driven model can estimate the near-field wind information to be used in the dispersion model based on the data measured at the far-field wind sensor locations. To build such a model that can operate over a wide range of wind conditions, we leveraged CFD models of the flow around a subset of representative infrastructures and different values of the wind vector (wind speed and directions) discretized over typically observed range of values. For example, the velocity magnitude and wind values were parameterized over a representative range of 0.5-9.5 m/s and 0-360 degrees (every 30 degrees) for a wind sensor placed at a height of five feet. Further, to build this dataset, we assumed a square infrastructure of a standard size of 15 feet. Illustrative CFD results for this case are presented in the next section.

From this ensemble of simulations, a database of input and output features corresponding to open (far) field and near-field velocity measurements are generated for training a machine learning (ML) model. The ML architecture aims to learn a linear map in a feature space using an extended basis consisting of polynomials up to order two which is similar to a shallow neural network or a single layer feed forward neural network (SLFNN). We note that learning more complex nonlinear models such as that using a deep neural network (DNN) is equally plausible but were avoided for simplicity. The data was split into training and validation datasets in a ratio of 4:1.

Figure 8.7-2 show a sample comparisons of data-driven model predictions versus CFD results in the space of input (far-field wind) and output (near-field wind) states. The subscript A corresponds to the far field measurement and the subscript B, the near-field velocity from the CFD model and U,V and W represent the east-west, north-south and vertical wind components. The model performance was assessed by comparing the predicted vs true data for both the training and validation sets combined as shown the plots which present the correlation between components of the far field and near field wind vectors (red represents true data and green the predicted data). Overall, the model shows strong qualitative accuracy and bounded quantitative accuracy with performance deteriorating at smaller values of wind components as expected. The SLFNN model is then deployed for practical estimation of the near field velocities.

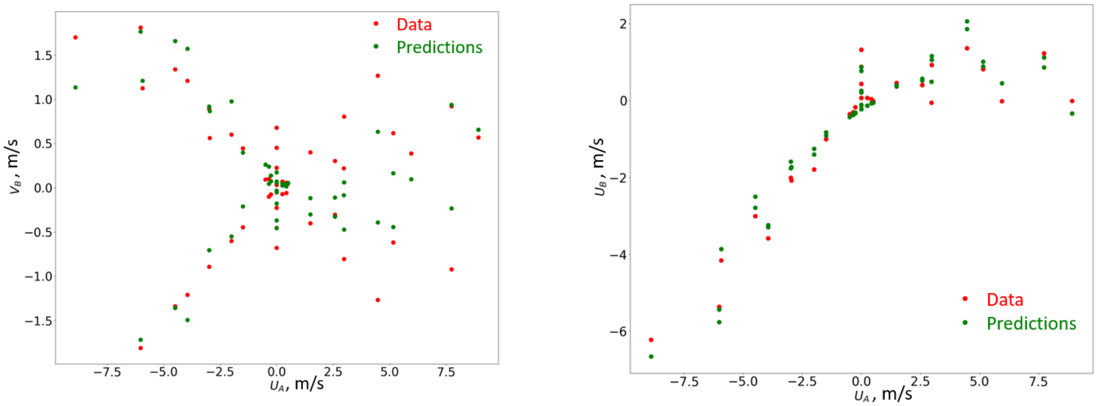

Figure 8.7-2 Comparisons of data-driven model predictions versus CFD results in the space of input (far-field wind) and output (near-field wind) states

CFD Model Description

As discussed earlier, near-field LUMEN sensors have been deployed immediately downstream of buildings or infrastructures. This configuration presents complex flow fields at the wake of these buildings. A CFD model was developed to help understand the complex flow structure and behavior in the presence of various geometrical and meteorological conditions. **Figure 8.7-3** shows an example of eddies, cavities, backwash and boundary layer effects upstream and downstream such infrastructures.

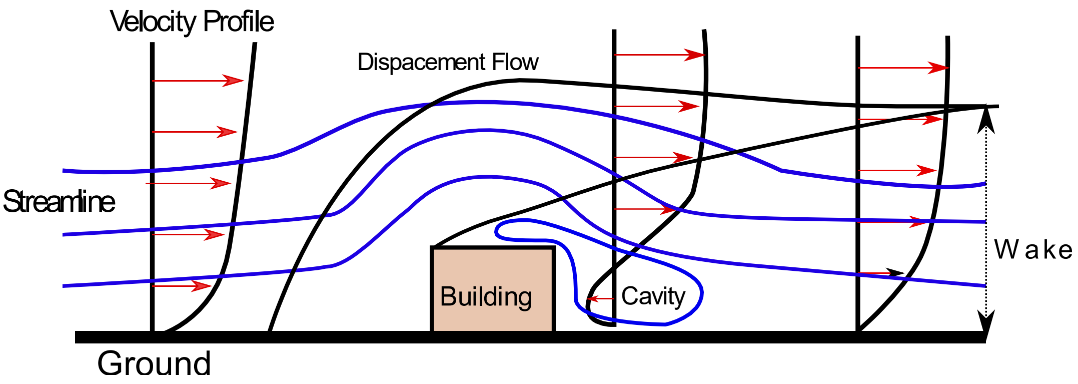

Figure 8.7-3 Schematic of the Flow Field near a Cubical Building

The developed model was used to understand the effect of geometrical and meteorological conditions and generate information needed to calibrate the data driven model that predicts the Near-Field wind profile. The CFD model was developed in ANSYS-Fluent to handle various boundary conditions. This CFD model can predict the complex flow structure behind different objects such as ones used traditionally in the O&G

industry, e.g. compressor buildings, tanks, separators, etc. The model geometry is shown in **Figure 8.7-4** and involves computational domain, sample cubical building and leak source. The leak source location and direction (X-Axis) are considered constant for all simulation cases. The cylindrical domain considered around the leak source facilitates the implementation of various wind profiles and directions. An exponential velocity profile is considered as the inlet velocity to compensate the boundary layer effect. The mesh sensitivity analysis has been performed to understand the best grid size. The k-E turbulence is selected for the analysis that also includes Enhance Wall Treatment.

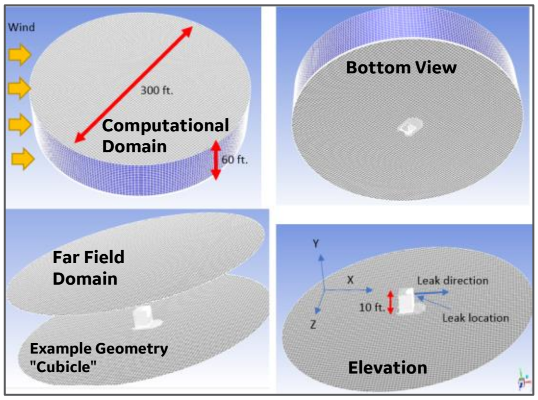

Figure 8.7-4 CFD Model Developed to investigate near flow field around objects (example cubicle object representing compressor station building)

Figure 8.7-5 and 8.7-6 show the models results for the wind speed equal to 10 m/sec blowing in the x- direction (counter-flow direction with respect to the leak). The velocity profile demonstrated in **Figure 8.7-5** shows the effect of the considered cubical building on the velocity field. As can be seen, the vortexes generated around the building and leak source creating areas with significant velocity gradients. The magnetite and size of such vortexes are connected to the wind velocity. **Figure 8.7-6** shows the methane concentration for the same case.

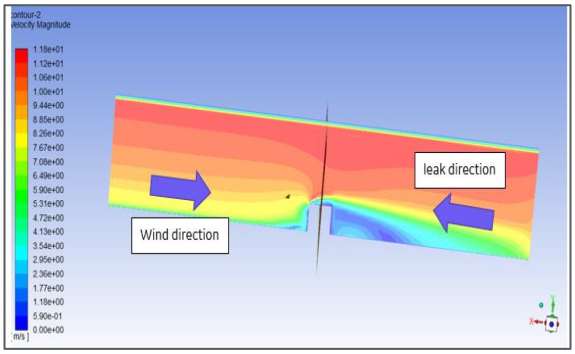

Figure 8.7-5 Example of velocity profile around a cubicle geometry (compressor building) (V=10 m/sec and leak rate= 0.5 gram/sec)

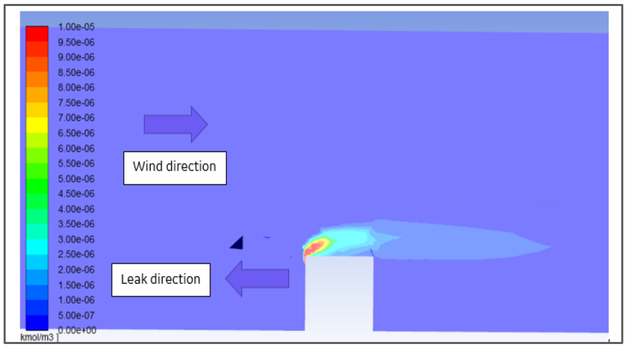

Figure 8.7-6 Example of methane concentration profile around a cubicle geometry (compressor building) (V=10 m/sec and leak rate= 0.5 gram/sec)

The above model has been executed for various cases including wind velocity from 0-9 m/sec in various directions (0-360° with 30° steps). The model and boundary conditions considered for this case reflect a real experimental test performed by the BHGE team in an open field located in the 7 Bonavista Sites in Rimbey, Alberta. In all the cases, the open field velocity field and concentration are saved and transformed for the data driven model.

8.8 Analytics Tools Used

The team used open-source python-based libraries to construct the data pre-processing (ETL) and Statistical computing and visualization (SV) pipelines. A summary of the different libraries along with short description is shown in **table 8.8-1** below:

Table 8.8-1 Summary of Python Libraries used for the ETL, SV Pipelines

Library	Description
Pandas, Numpy , Scipy	Manipulation of timeseries data, performing database like functionality (grouping, joining...etc.) and common timeseries operations (resampling, shifting, slicing, rolling means, etc.)
Matplotlib, Scipy (stats), and Seaborn	For visualization of timeseries, histograms, probability/kernel density functions
Os, shutil, pickle, json	Various utilities to move data around the operating system, read/load and save data files
numpy.random.choice	For sampling a timeseries with replacement to construct a bootstrap

We first display full instantaneous sensor timeseries datasets for concentration and corresponding leak rates and then hourly averages, daily averages and weekly averages (see **Figures 8.8-1 through 4**) of such data using pandas resampling and windowing capabilities. As explained in the data preprocessing section, we have also performed forward and backward-filling of missing wind data.

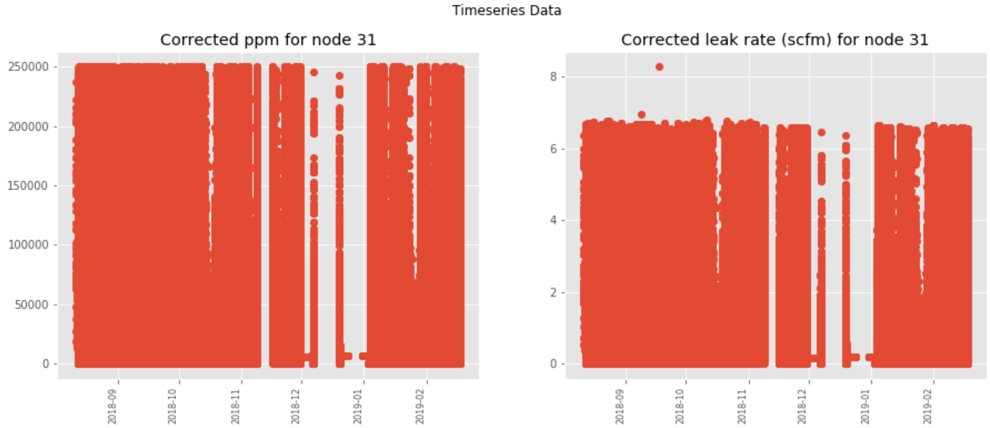

Figure 8.8-1 2-Second Timeseries for Node 31 in ppm (left) and scfm (right)

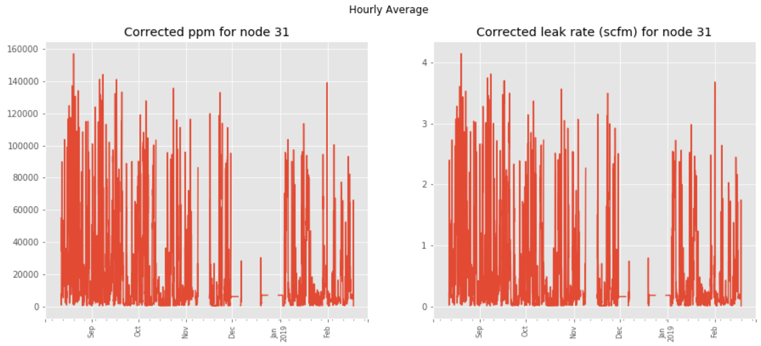

Figure 8.8-2 Hourly Averages for Node 31 in ppm (left) and scfm (right)

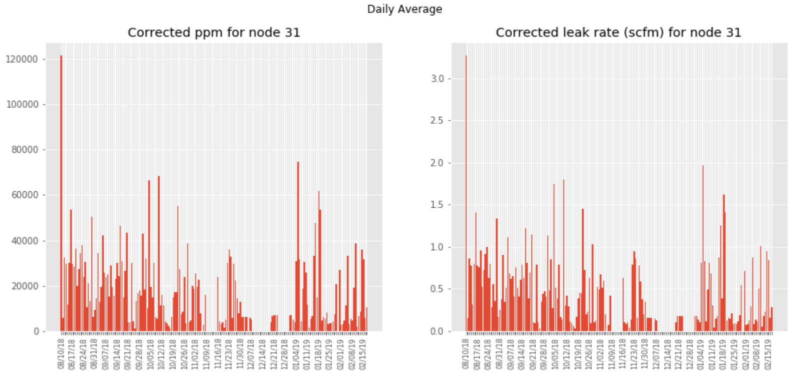

Figure 8.8-3 Daily Averages for Node 31 in ppm (left) and scfm (right)

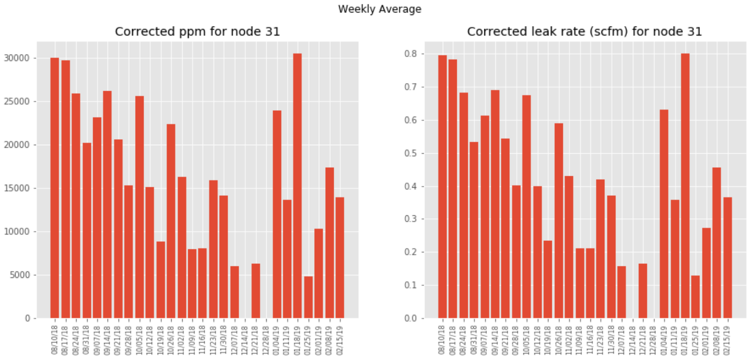

Figure 8.8-4 Weekly Averages for Node 31 in ppm (left) and scfm (right)

The inputted data is then passed on to the diffusion model (explained in Section 8.7) for leak rate estimation. We then compute summary statistics and estimate the precision of the reported statistics using bootstrap resampling. Bootstrapping is a statistical procedure involving the generation of random samples with replacement allowing us to quantify the random sampling errors and provide a confidence interval along with all statistics reported. Confidence intervals are estimated computationally[7].

On average, we found that 1500 bootstraps are required to ensure a nearly symmetric sampling distribution of all reported statistics and avoid the time-consuming procedure of bias-corrected confidence interval[8]. **Figure 8.8-5** below shows a converged sampling distribution for the mean, standard deviation of the leak rate and concentration for Node 31. The sampling distribution is nearly symmetric in all three cases and accordingly there is no need for bias-correction.

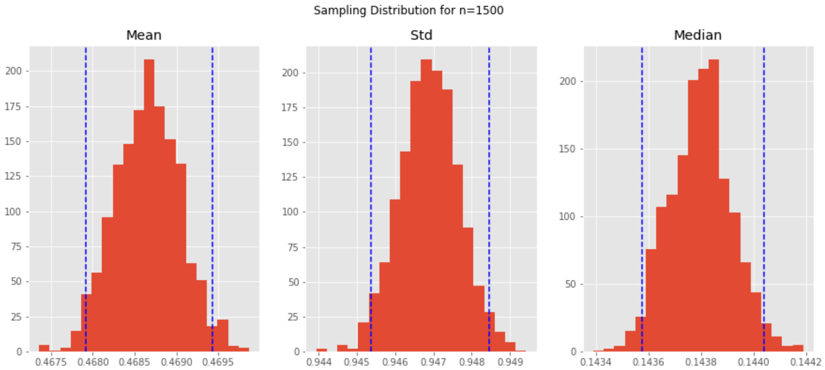

Figure 8.8-5 Sampling Distribution of the Mean, Standard Deviation and Median for the Leak Rate for Node 31

Finally, statistics comparison between nodes is based on the effect size method[9]. In medical education research studies that compare different educational interventions, effect size is the magnitude of the difference between “treatment” and “control” groups. To facilitate the comparison, we report both absolute effect size in ppm and scfm for concentration and leak rate respectively and normalized effect size that is based on the Cohen’s effect size (d):

$$d = \frac{\overline{x_1} - \overline{x_2}}{s}$$ **Eq. 8.8-1**

Where s is the pooled standard deviation defined as:

$$s = \sqrt{\frac{n_1 {s_1}^2 + n_2 {s_2}^2}{n_1 + n_2}}$$ **Eq. 8.8-2**

Where $\overline{x_1}$ and $\overline{x_2}$ are the mean and standard deviation of the two nodes. Essentially Cohen’s effect size expresses the difference in average concentration or leak rate of two nodes in terms of a standard deviation defined in terms of both nodes standard deviations. The weighted standard deviation is closer in numerical value to the higher standard deviation of two nodes (for same length timeseries i.e. n1=n2).

8.9 BHGE Emission Rate Method to Estimate Emission Factors

BHGE emission rate method ($ER_{BHGE,t}$) is a statistical approach that takes into consideration modeled instantaneous leak rates LR $_{Inst}$ (scfm) based on the measured instantaneous concentrations (ppm) over an extended period. In this work, sampling frequency was every 2 seconds using BHGE continuous sampling technology (LUMEN) and for an average time duration of 3 to 6 months to account for periodic communication drops and BHGE equipment adjustments. This is a total of 191 million measured data points that constitute the emission rate population for this study. By the virtue of this continuous sampling method, measured emission rates $ER_{BHGE,t}$ gave true representation of equipment operating modes, maintenance, age, location and site production levels since it represents an all-encompassing set of field conditions for estimating a statistically robust emission level for a given equipment component on a given site.

The mathematical formulation of the above Is given by the $ER_{BHGE,t}$

$$ER_{BHGE,t} = EF_{BHGE} * A * (1 - CF) * OF \qquad \textbf{Eq. 8.9-1}$$

where,

$ER_{BHGE,t}$ = mean of the sampling distribution of the mean of the instantaneous leak rates for a given period of time, t, scfm.
A = activity value for a given emission source
CF = control factor for a specific control measure or device applied to a given emission source which indicates the fraction by which the emissions are reduced (kg/kg)
OF = operating factor which indicates the fraction of the time the source is active (day/year)

Given the measured BHGE emission rate $ER_{BHGE,t}$ and knowing equipment specific factors (A, CF, and OF), the BHGE emission factor EF_{BHGE}, will be given by:

$$EF_{BHGE} = \frac{ER_{BHGE,t}}{A * (1 - CF) * OF} \qquad \textbf{Eq. 8.9-2}$$

If CF = 0, A and OF are equal to 1 (referred in this report as unity activity factor), EF_{BHGE} will be the same as $ER_{BHGE,t}$

8.10 Uncertainty Analysis

Experimental errors can be divided into four categories[7]:

1) **Measurement error:** This type of error is the inherent error involved in using a specific sensor that relies in its operation on some physical effect representing the response of the sensor to the quantity being measured. This error is often sizable in magnitude and could be quantified using calibration against a known reference. For BHGE sensors, we have performed experiments to estimate concentration errors at various reference concentrations. This in turn allows us to estimate an experimental error correction ΔC at a wide range of concentrations (see section 8.6).

2) **Bias error:** This error results from sampling specific regions of the underlying probability distribution, thus favoring certain times or operating conditions for the components under investigation. The only way to ensure that we are sampling all potential values for emission concentrations is to measure emissions for long enough to ensure quasi-stationary probability density functions (pdf) of the emission from a given equipment. We have estimated that in most cases the equivalent of one-month worth of complete data (i.e. every 2 seconds) is enough to ensure quasi-stationary pdf. This is not a general rule of thumb, it is just true for our datasets obtained from the three different sites.

3) **Random sampling error:** This type of error occurs because we are typically measuring a sample of a given quantity rather than the full population. In different realizations of the samples our estimates will typically be a bit different. In practice this is typically the smallest of all above three types of errors. It can be easily quantified using the bootstrapping techniques described above.

4) **ppm to leak rate conversion error:** This type of error occurs due to mapping of open field wind to near field wind in the near field model. Overall, the model shows strong qualitative accuracy and bounded quantitative accuracy with performance deteriorating at smaller values of wind components as expected. (See section 8.7)

9. Results

9.1 Total Site Emissions

This section provides the emission footprints of the seven studied Bonavista sites at a macro-level. Each site was evaluated at equipment component level for known emitters or vents, therefore these "total-site" emissions only account for the combined measured-based emissions (scfm) contributed by their components. It should be mentioned that the emission rates mentioned here represent the Sum of the "mean of the sampling distribution" for all these components, $ER_{BHGE,t}$

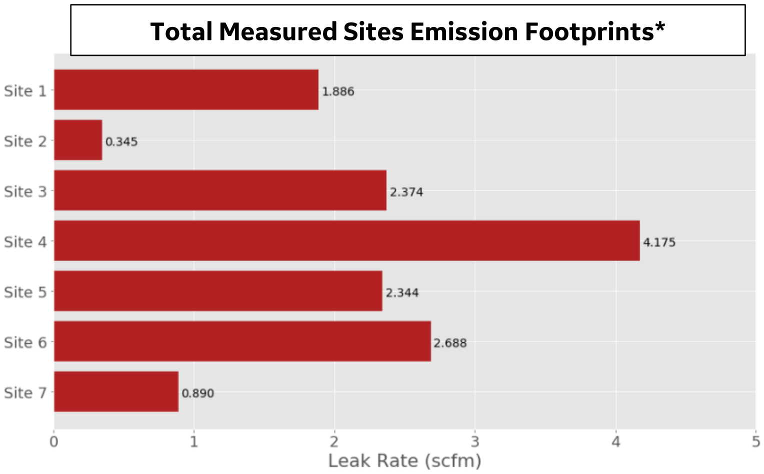

Figure 9.1-1 Site-Level Comparison of Emission Rates [$ER_{BHGE,t}$] (scfm)
Each site has a different number of leak sources; therefore, these rates may not be fully representing the total emissions on a given site

Table 9.1-1 Site-Level Comparison

Site	1	2	3	4	5	6	7
Site Type	Compressor Station	Wellsite	Compressor Station	Compressor Station	Compressor Station	Compressor Station	Battery
Number of Sensor Nodes per site	10	7	7	10	6	10	6
Site Total Emission Rates (scfm)	1.886	0.345	2.374	4.175	2.344	2.688	0.890

9.2 Site-Specific Behavior

This section explores the results at site-level, evaluating the emissions behavior of the components that make up each site. For more details on the component time series and results, please refer to the Supplemental Material.

1. Compressor Site 622, 06-22-041-05W5 (AER F41995)

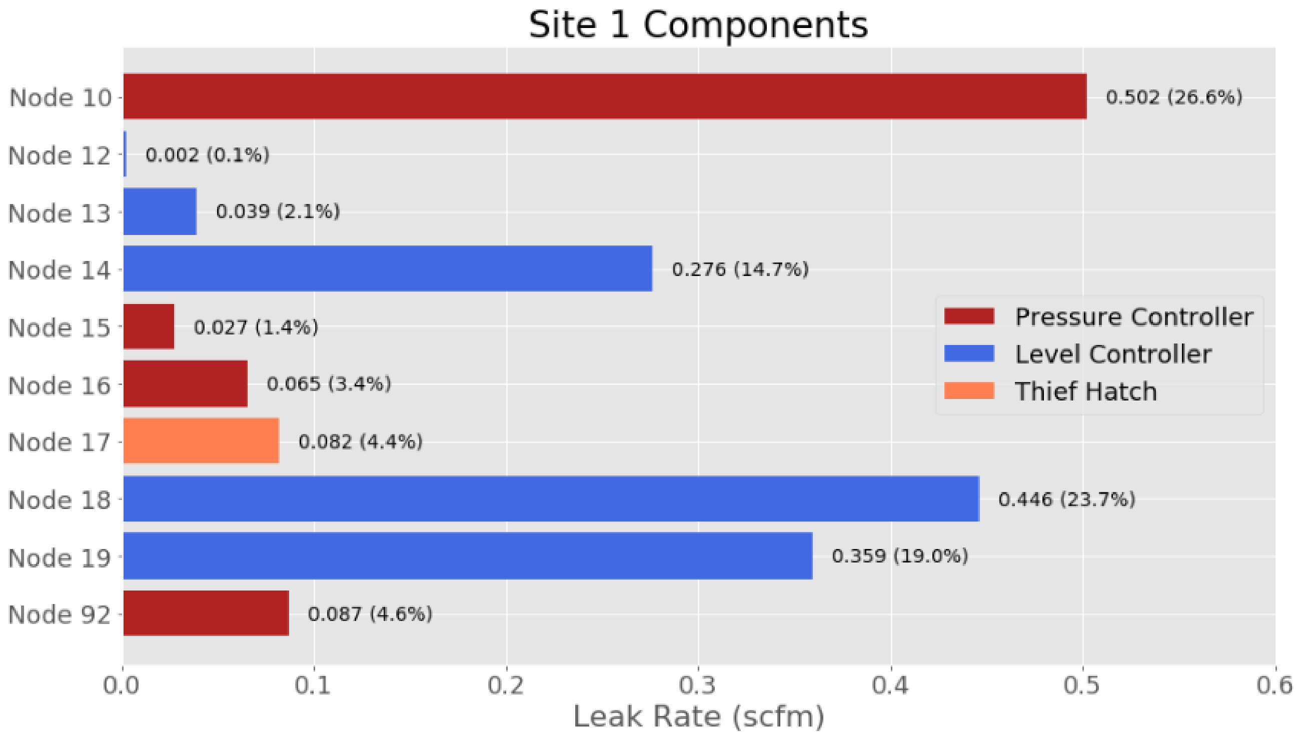

Figure 9.2-1 Site 1 Emission Rates [$ER_{BHGE,t}$] (scfm) of each Equipment Component

Table 9.2-1 Site 1 Equipment Component Emission Rates [$ER_{BHGE,t}$] (scfm)

Node	**10**	**12**	**13**	**14**	**15**	**16**	**17**	**18**	**19**	**92**
Equipment Component	PC	LC	LC	LC	PC	PC	TH	LC	LC	PC
Emission Rate (scfm)	0.502	0.027	0.065	0.082	0.002	0.039	0.087	0.446	0.359	0.276

2. Wellsite Station, 13-23-043-05W5 (AER F46141)

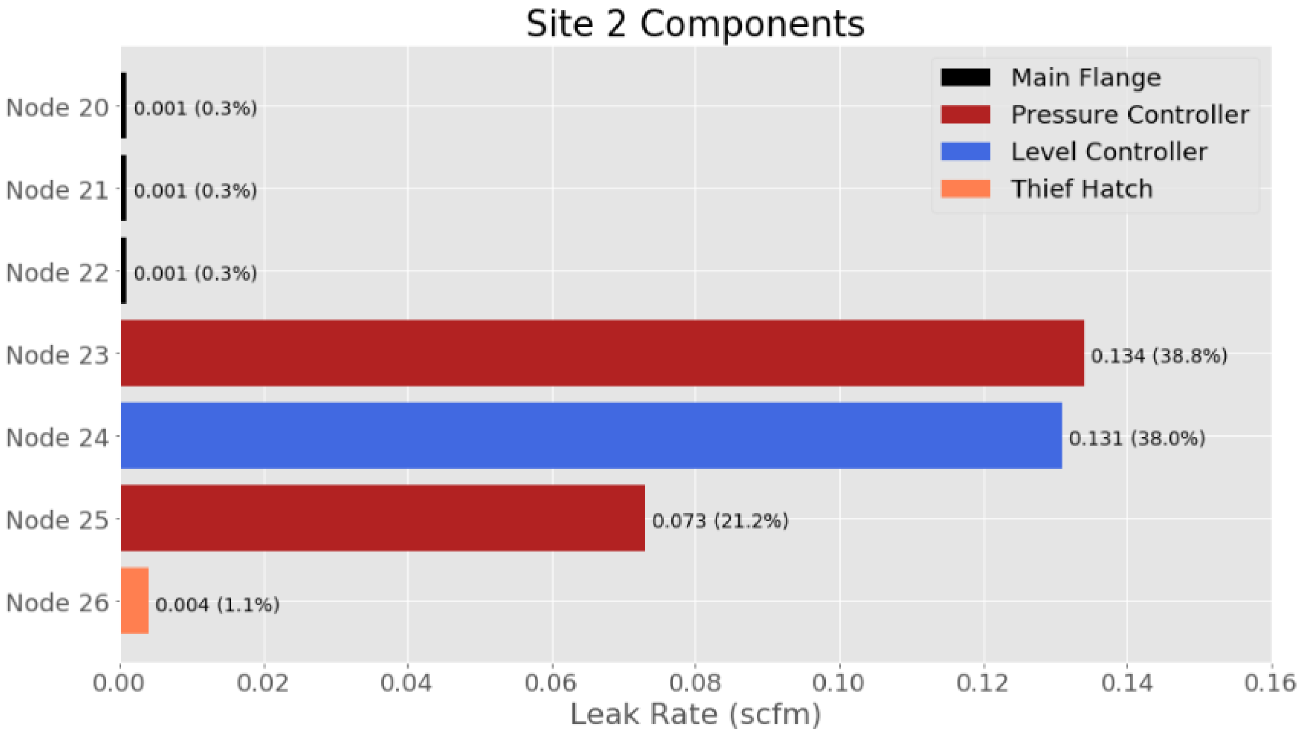

Figure 9.2-2 Site 2 Emission Rates [$ER_{BHGE,t}$] (scfm) of each Equipment Component

Table 9.2-2 Site 2 Equipment Component Emission Rates [$ER_{BHGE,t}$] (scfm)

Node	20	21	22	23	24	25	26
Equipment Component	MF	MF	MF	PC	LC	PC	TH
Emission Rate (scfm)	0.001	0.001	0.001	0.134	0.131	0.073	0.004

3. Westerose Compressor Station, 11-09-044-02W5 (AER F20724)

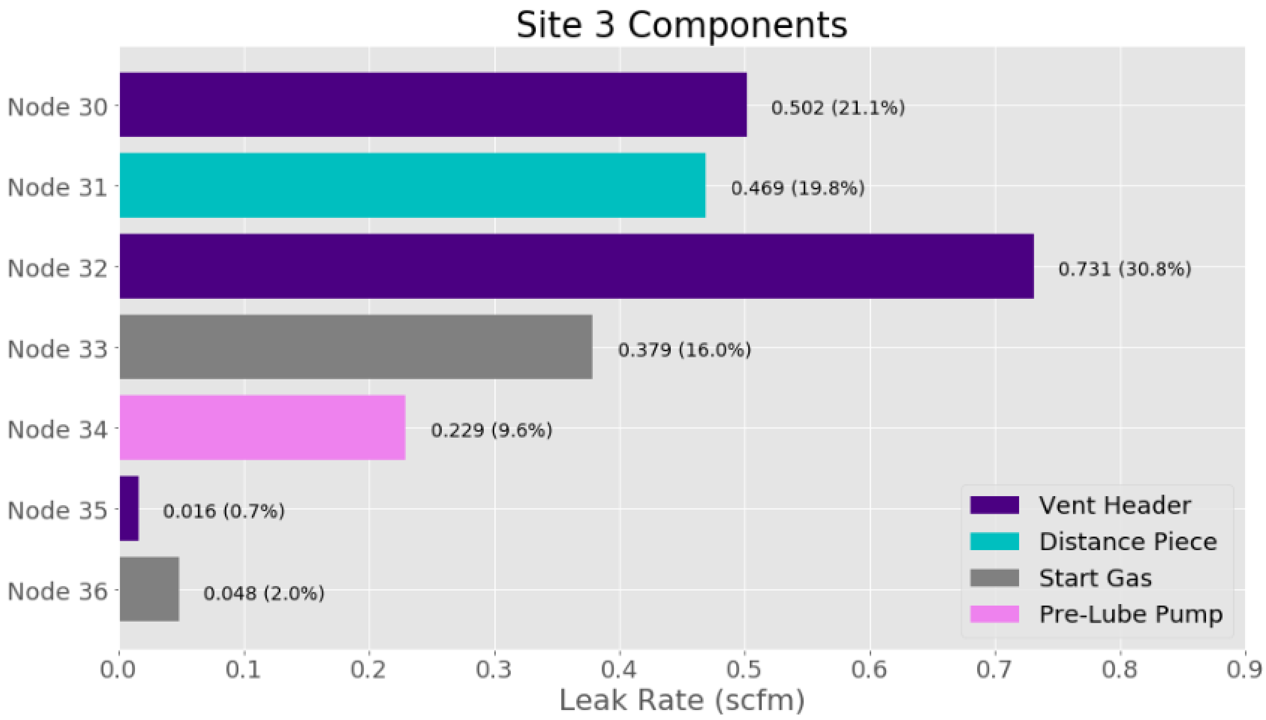

Figure 9.2-3 Site 3 Emission Rates [$ER_{BHGE,t}$] (scfm) of each Equipment Component

Table 9.2-3 Site 3 Equipment Component Emission Rates [$ER_{BHGE,t}$] (scfm)

Node	**30**	**31**	**32**	**33**	**34**	**35**	**36**
Equipment Component	VH	DP	VH	SG	PP	VH	SG
Emission Rate (scfm)	0.502	0.469	0.731	0.379	0.229	0.016	0.048

4. Willesden Green 16-12 Compressor Station, 16-12-042-06W5 (AER F34318)

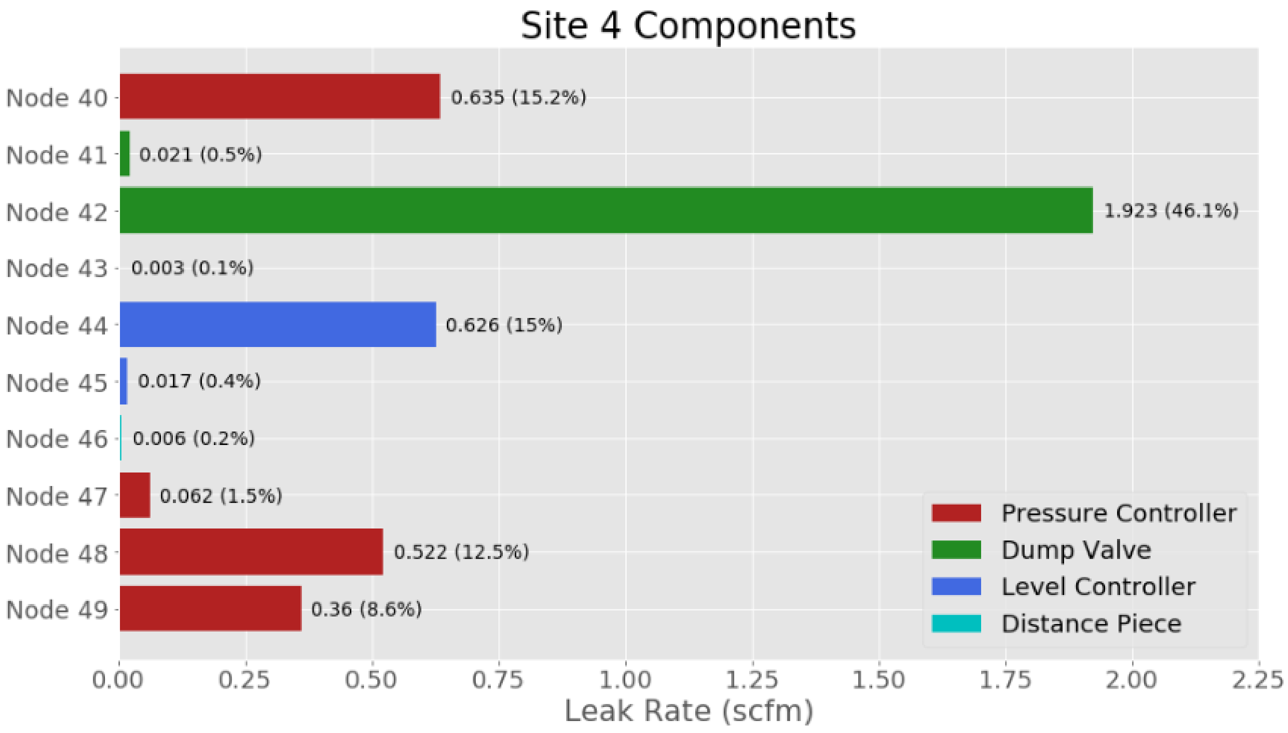

Figure 9.2-4 Site 4 Emission Rates [$ER_{BHGE,t}$] (scfm) of each Equipment Component

Table 9.2-4 Site 4 Equipment Component Emission Rates [$ER_{BHGE,t}$] (scfm)

Node	**40**	**41**	**42**	**43**	**44**	**45**	**46**	**47**	**48**	**49**
Equipment Component	PC	DV	DV	PC	LC	LC	DP	PC	PC	PC
Emission Rate (scfm)	0.635	0.021	1.923	0.003	0.626	0.017	0.006	0.062	0.522	0.36

5. Willesden Green 12-04 SWB, 100/12-04-041-06W5 SWB

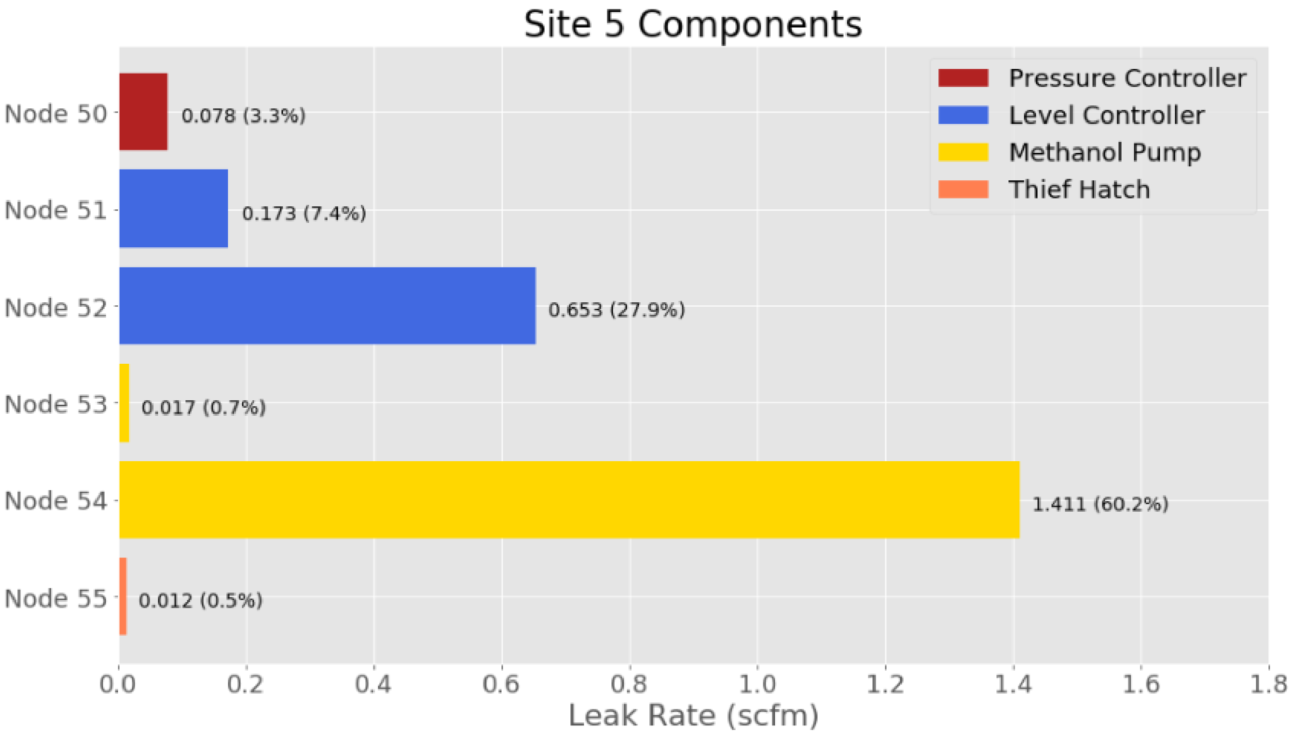

Figure 9.2-5 Site 5 Emission Rates [$ER_{BHGE,t}$] (scfm) of each Equipment Component

Table 9.2-5 Site 5 Equipment Component Emission Rates [$ER_{BHGE,t}$] (scfm)

Node	**50**	**51**	**52**	**53**	**54**	**55**
Equipment Component	PC	LC	LC	MP	MP	TH
Emission Rate (scfm)	0.078	0.173	0.653	0.017	1.411	0.012

6. South Elkton 02-03 Compressor Station, 02-03-031-04W5 (AER F23119)

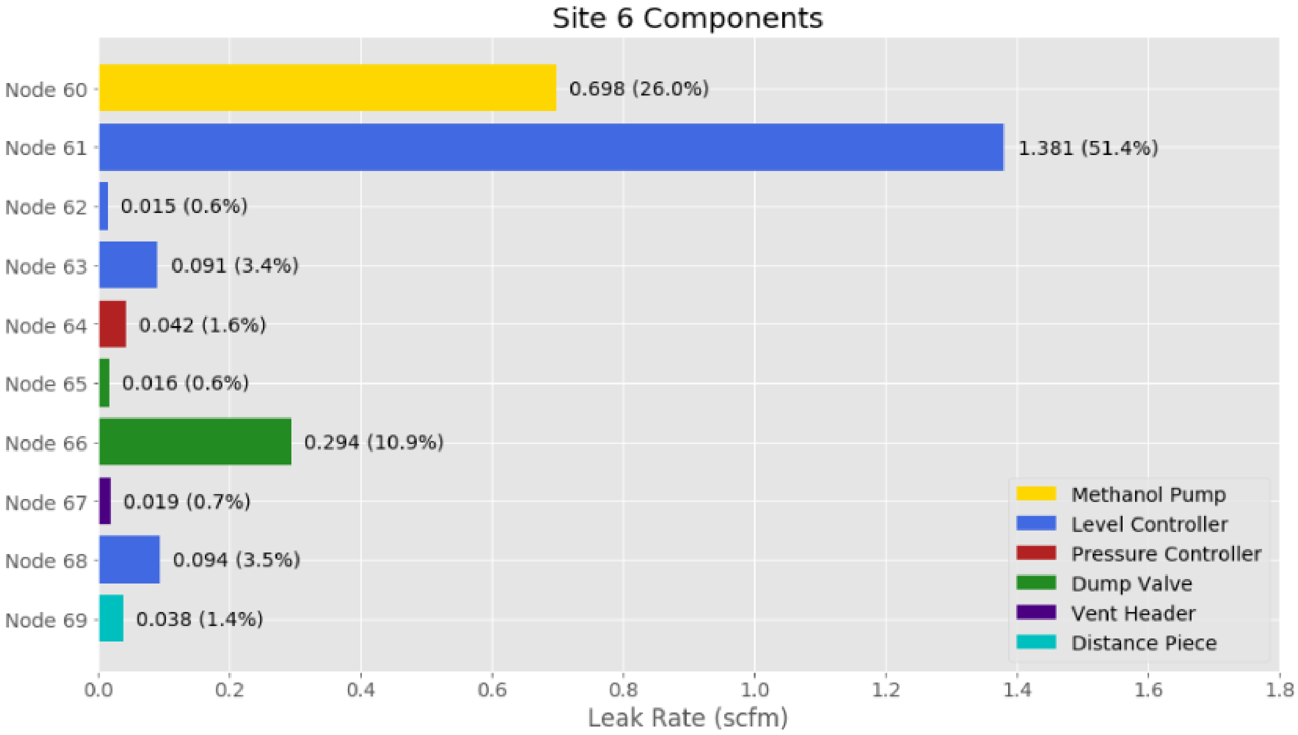

Figure 9.2-6 Site 6 Emission Rates [$ER_{BHGE,t}$] (scfm) of each Equipment Component

Table 9.2-6 Site 6 Equipment Component Emission Rates [$ER_{BHGE,t}$] (scfm)

Node	**60**	**61**	**62**	**63**	**64**	**65**	**66**	**67**	**68**	**69**
Equipment Component	MP	LC	LC	LC	PC	DV	DV	VH	LC	DP
Emission Rate (scfm)	0.698	1.381	0.015	0.091	0.042	0.016	0.294	0.019	0.094	0.038

7. Harmattan 12-29-031-03W5 Battery, 12-29-031-03 W5 (AER F43230)

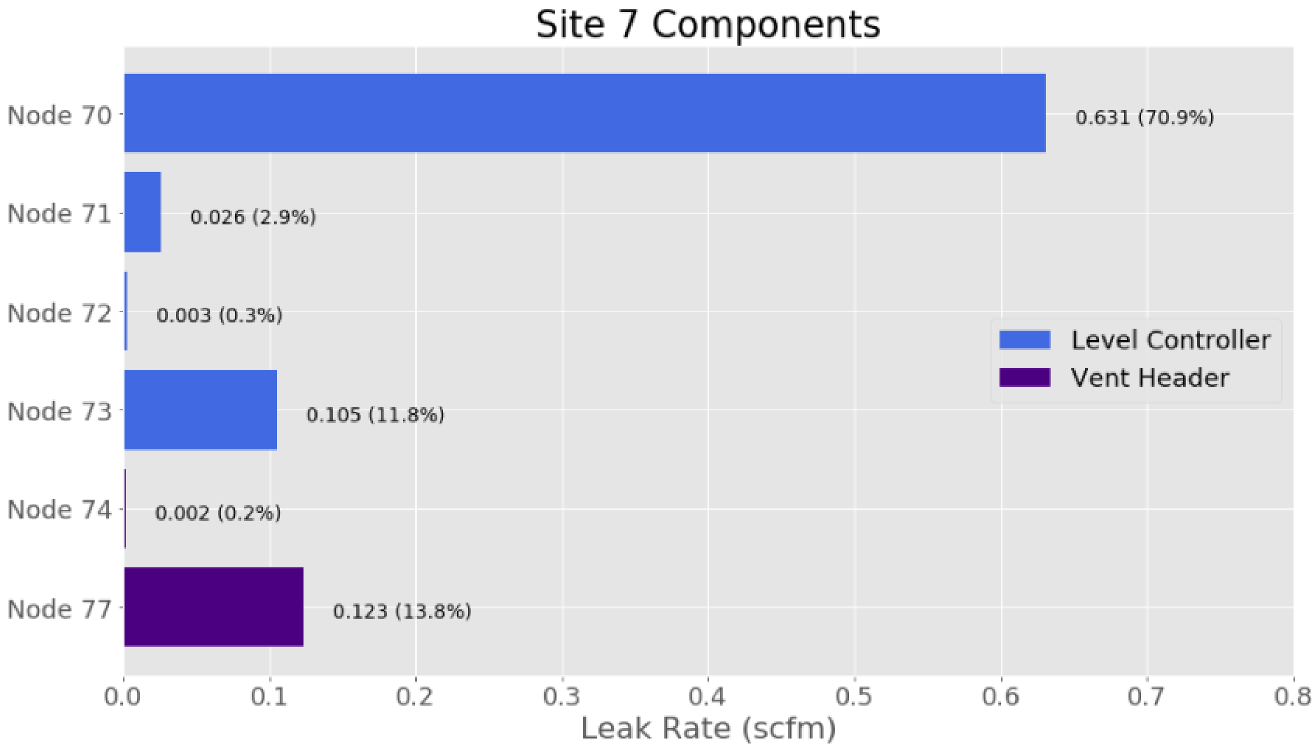

Figure 9.2-7 Site 7 Emission Rates [$ER_{BHGE,t}$] (scfm) of each Equipment Component

Table 9.2-7 Site 7 Equipment Component Emission Rates [$ER_{BHGE,t}$] (scfm)

Node	**70**	**71**	**72**	**73**	**74**	**77**
Equipment Component	LC	LC	LC	LC	VH	VH
Emission Rate (scfm)	0.631	0.026	0.003	0.105	0.002	0.123

9.3 Measured-Based Emission Factors per Equipment Component

The following figure displays the mean of bootstrap resampling distribution performed for each of the components (represented by Node#). Emission factors (scfm) are grouped by each component category to contrast their performance against similar components but at different site/equipment. The color coding represented on this chart are consistent with the color scheme followed throughout the report except for individual component charts in Section 9.4. It should be mentioned that at *unity activity factor* $ER_{BHGE,t} = EF_{BHGE}$ Please refer to section 8.9 for more details.

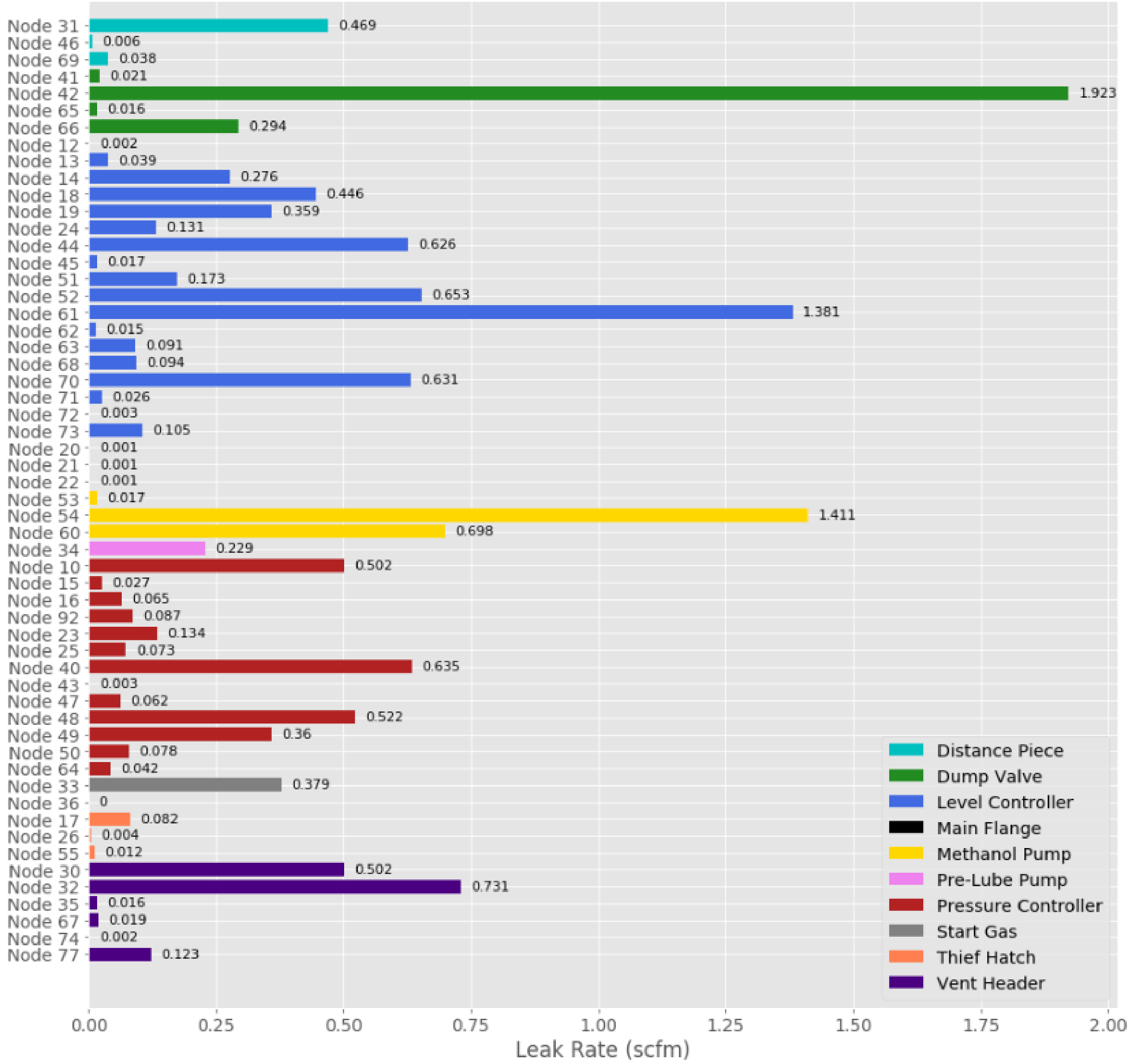

Figure 9.3-1 All Sites Equipment Component Emission Factors [EF_{BHGE}] (scfm)

Table 9.3-1 shows the same results in **Figure 9.3-1** in tabular format, purpose being to compare like components as well as components in different categories. The Hi-Flow Sampler values obtained by the team are displayed as a range, since there were multiple readings done per component.

Table 9.3-1 Measurement-Based Emission Factors per Component Category Compared with Regulatory Averages given by Sensor Node and Component Type. *Note that* $ER_{BHGE,t}$ = EF_{BHGE} *at unity activity factor* ***(section 8.9)***

No.	Node ID	Equipment Component Category	Measured-Based Emission Factors, scfm (Using 56 LUMEN Sensors)	Site-Measured Leak Rate, scfm, using Hi-Flo Sampler [min,max]	EC Emission Factors (scfm)	EPA Emission Factors (scfm)
1	Node 31	Distance Piece	0.469	[0.28,0.29]	0.0496	0.86
2	Node 46	Distance Piece	0.006	[0.38,0.39]	0.0496	0.86
3	Node 69	Distance Piece	0.038	[0.07,0.1]	0.0496	0.86
4	Node 41	Dump Valve	0.021	0	0.002	0.00159
5	Node 42	Dump Valve	1.923	0.28	0.002	0.00159
6	Node 65	Dump Valve	0.016	0.01	0.002	0.00159
7	Node 66	Dump Valve	0.294	[0.01,0.02]	0.002	0.00159
8	Node 12	Level Controller	0.002	0	0.0408	0.00159
9	Node 13	Level Controller	0.039	0	0.0408	0.00159
10	Node 14	Level Controller	0.276	0.27	0.0408	0.00159
11	Node 18	Level Controller	0.446	[0.03,0.04]	0.0408	0.00159
12	Node 19	Level Controller	0.359	[0.03,0.04]	0.0408	0.00159
13	Node 24	Level Controller	0.131	0	0.0408	0.00159
14	Node 44	Level Controller	0.626	0	0.0408	0.00159
15	Node 45	Level Controller	0.017	[0.15,0.17]	0.0408	0.00159
16	Node 51	Level Controller	0.173	[0.16,0.21]	0.0408	0.00159
17	Node 52	Level Controller	0.653	[0.18,0.19]	0.0408	0.00159
18	Node 61	Level Controller	1.381	[0.29,0.33]	0.0408	0.00159
19	Node 62	Level Controller	0.015	-	0.0408	0.00159
20	Node 63	Level Controller	0.091	0.19	0.0408	0.00159
21	Node 68	Level Controller	0.094	[0.88,0.91]	0.0408	0.00159
22	Node 70	Level Controller	0.631	[0.18,0.19]	0.0408	0.00159
23	Node 71	Level Controller	0.026	0	0.0408	0.00159
24	Node 72	Level Controller	0.003	0	0.0408	0.00159
25	Node 73	Level Controller	0.105	0.03	0.0408	0.00159
26	Node 20	Main Flange	0.001	-	-	0.00022
27	Node 21	Main Flange	0.001	-	-	0.00022
28	Node 22	Main Flange	0.001	-	-	0.00022
29	Node 53	Methanol Pump	0.017	-	0.0031	0.00159
30	Node 54	Methanol Pump	1.411	0.2	0.0031	0.00159
31	Node 60	Methanol Pump	0.698	[0.41,0.43]	0.0031	0.00159
32	Node 34	Pre-Lube Pump Colum	0.229	0	0.0031	0.00159
33	Node 10	Pressure Controller	0.502	0.05	0.0408	0.0025
34	Node 15	Pressure Controller	0.027	0.05	0.0408	0.0025
35	Node 16	Pressure Controller	0.065	-	0.0408	0.0025
36	Node 92	Pressure Controller	0.087	[0.05,0.06]	0.0408	0.0025
37	Node 23	Pressure Controller	0.134	0	0.0408	0.0025
38	Node 25	Pressure Controller	0.073	0.04	0.0408	0.0025
39	Node 40	Pressure Controller	0.635	[0.21,0.22]	0.0408	0.0025
40	Node 43	Pressure Controller	0.003	[0.27,0.3]	0.0408	0.0025
41	Node 47	Pressure Controller	0.062	[0.14,0.17]	0.0408	0.0025
42	Node 48	Pressure Controller	0.522	[0.05,0.26]	0.0408	0.0025
43	Node 49	Pressure Controller	0.36	[0.01,0.28]	0.0408	0.0025
44	Node 50	Pressure Controller	0.078	[0.09,0.12]	0.0408	0.0025
45	Node 64	Pressure Controller	0.042	[0,0.01]	0.0408	0.0025
46	Node 33	Start Gas	0.379	0	-	-
47	Node 36	Start Gas	0	0	-	-
48	Node 17	Thief Hatch	0.082	-	-	-
49	Node 26	Thief Hatch	0.004	-	-	-
50	Node 55	Thief Hatch	0.012	-	-	-
51	Node 30	Vent Header	0.502	[0.55,0.64]	0.0496	0.86
52	Node 32	Vent Header	0.731	[0.58,2.15]	0.0496	0.86
53	Node 35	Vent Header	0.016	[0.37,0.42]	0.0496	0.86
54	Node 67	Vent Header	0.019	[0.03,0.04]	0.0496	0.86
55	Node 74	Vent Header	0.002	-	0.0496	0.86
56	Node 77	Vent Header	0.123	-	0.0496	0.86

9.4 Emission Rate per Component Category

The complete list of components studied is accompanied with its emission rates calculated using the arithmetic mean of the population in each group, independent of sites or equipment. While bootstrap sampling was performed on each individual node to calculate its statistical mean, this group arithmetic mean is limited by the number of components within the group and the sample size is insufficient for a statistically significant emission factor trends among the same group. In the following figures, we will take a closer look at each component group and at the performance and behavior of each node in comparison with its counterparts, the regulatory agencies' values, and the Hi-Flow Sampler measurements we obtained.

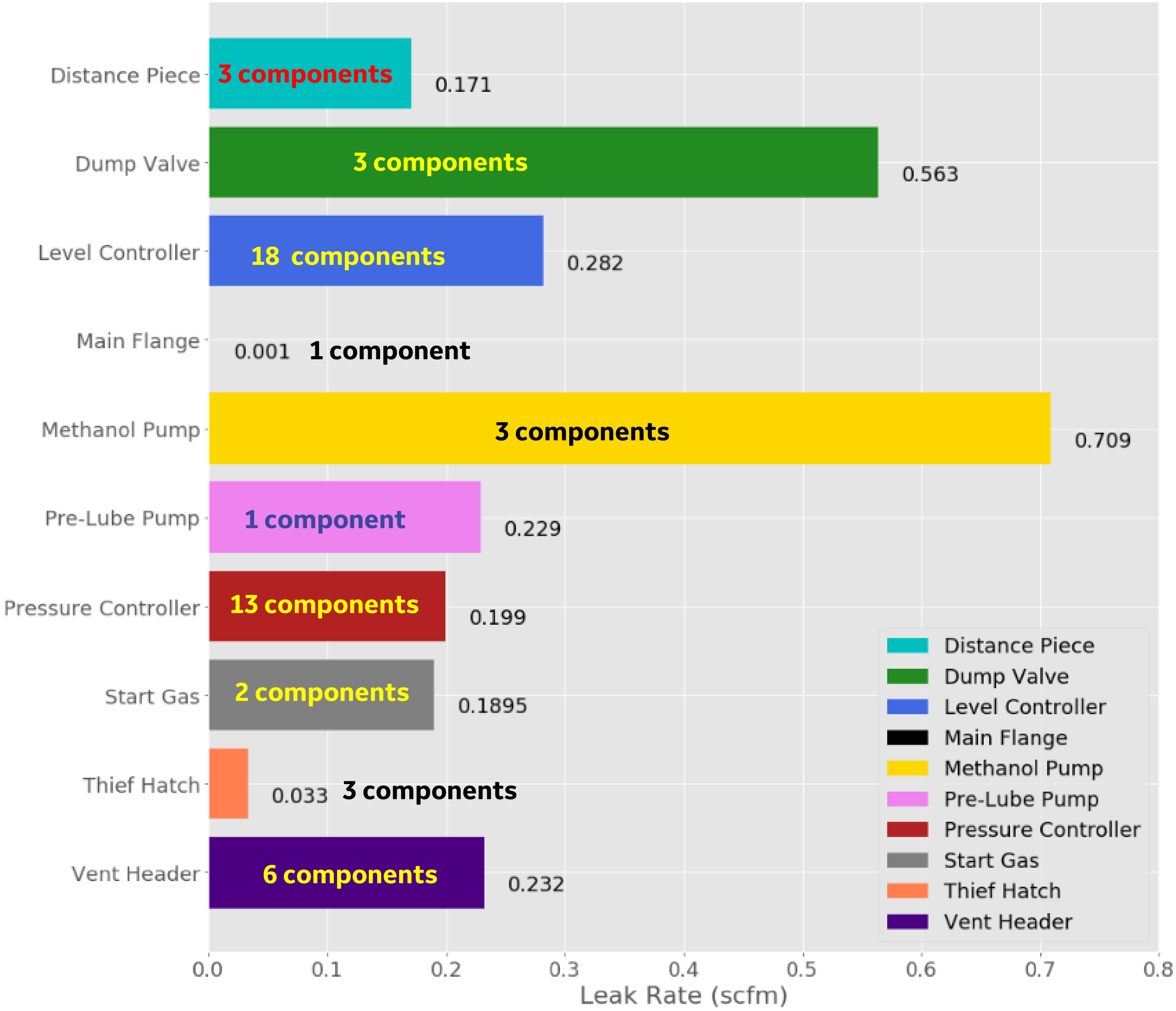

Figure 9.4-1 Emission Rate [$ER_{BHGE,t}$] (scfm) per Equipment Component Category

9.4.1 Node Timeseries per Component Category

Distance Piece

The graphic plots clearly show that #46 and #69 reciprocating compressor emissions were one order lower than that of the #31 compressor vent. The emission magnitudes from the three compressors correlate to the service records well: the prolonged repacking resulted in higher emissions. The continuous emission monitoring on distance pieces could be potentially used as a data-based asset management tool for service calls. The Hi-Flow Sampler readings are Imposed In order to visually see the effect of a one-time measurement versus the true continuous behavior of the piece and how we may be under/over estimating the rate value using this method.

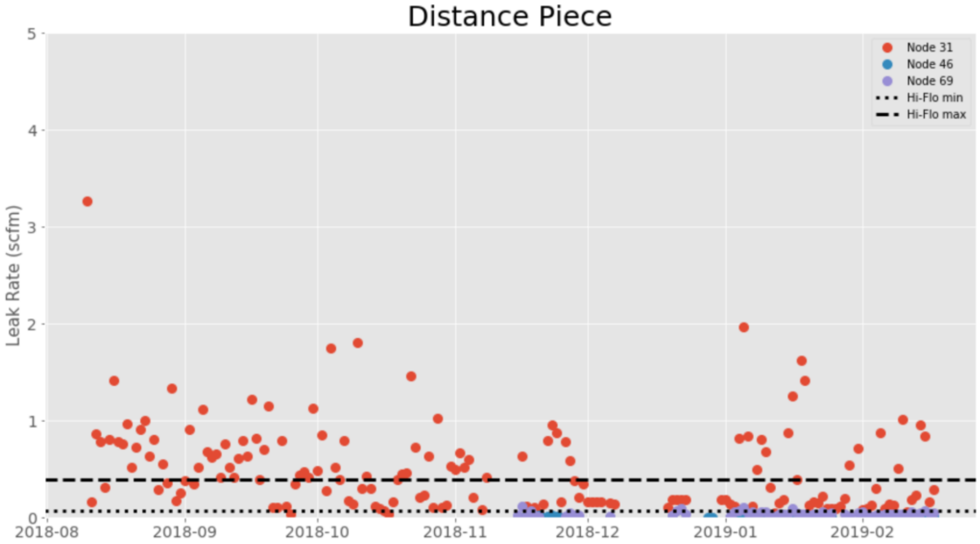

Figure 9.4-2 Distance Piece Timeseries in relation to Hi-Flow Sampler Measurements

Table 9.4-1 Effect-Size Comparison for Distance Piece Nodes

Node Pair	Mean Effect Size
(31, 46)	0.5501
(31, 69)	0.5308
(69, 46)	0.4541

There are wide variations of the mean emission rate for all three nodes with 31 being the highest leak rate. The mean of the leak rate is higher by almost 1/5 a standard deviation for 31 compared to both 46 and 69. There is a similar order of magnitude difference between the nodes with the smaller emission rates (46 and 69). The difference in the means indicates that such differences in the leak rates are statistically significant and should not be treated as coincidental.

Dump Valve

The figure below depicts the daily rolling average of the separator dump valve readings. The separator dump valve Is a pneumatic device which Is actuated when the liquid level in the separator reached a threshold. The process Is powered with natural gas thus venting during operation. There are four dump valves in the study: two In Site 4 and two In Site 6, both compressor stations. As can be observed in **Figure 9.4-3**, there are two nodes with dominating activity, Node 42 and Node 66. These two nodes are attached to the water dump vents of the separator, while the other two are on the condensate dump vents. According to the operator, water production rates are higher than condensate rates, therefore, the activity observed is consistent with operations. The black dotted lines represent the bounds of measurement by the Hi-Flow Sampler, a one-time leak rate measuring device. It can be observed that these measurements underestimate the true behavior of this component.

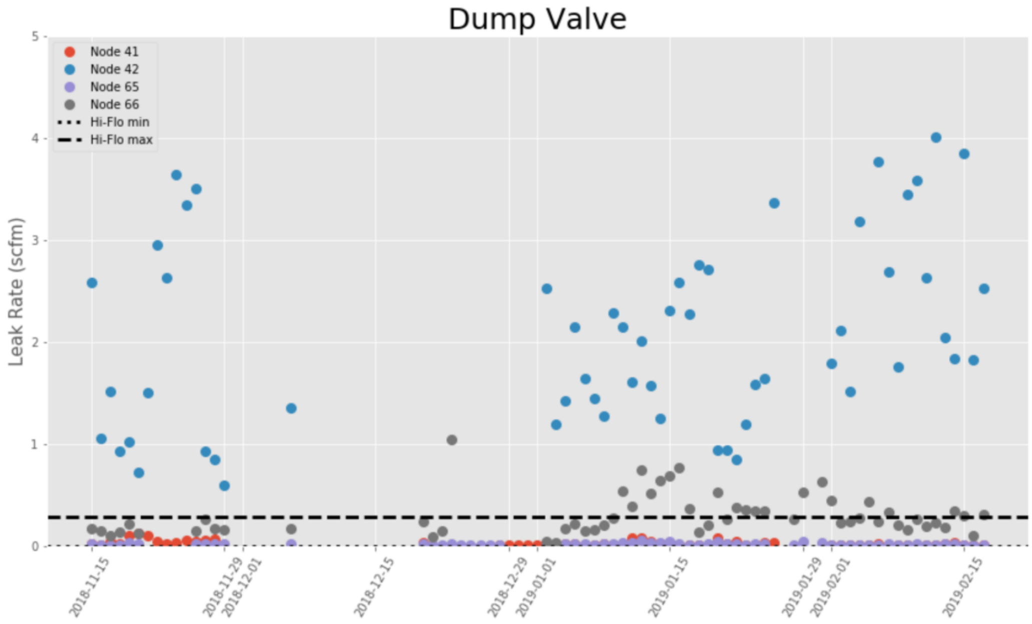

Figure 9.4-3 Dump Valve Timeseries in relation to Hi-Flow Sampler Measurements

Level Controller

Like the operations of a dump valve, level controllers are actuated as the separators fill up with fluids. Components associated with water will have a higher activity than those associated with condensate, as they are dealing with higher flowrates. The black lines determine the bounds set by the highest and lowest one-time readings of the Hi-Flow Sampler.

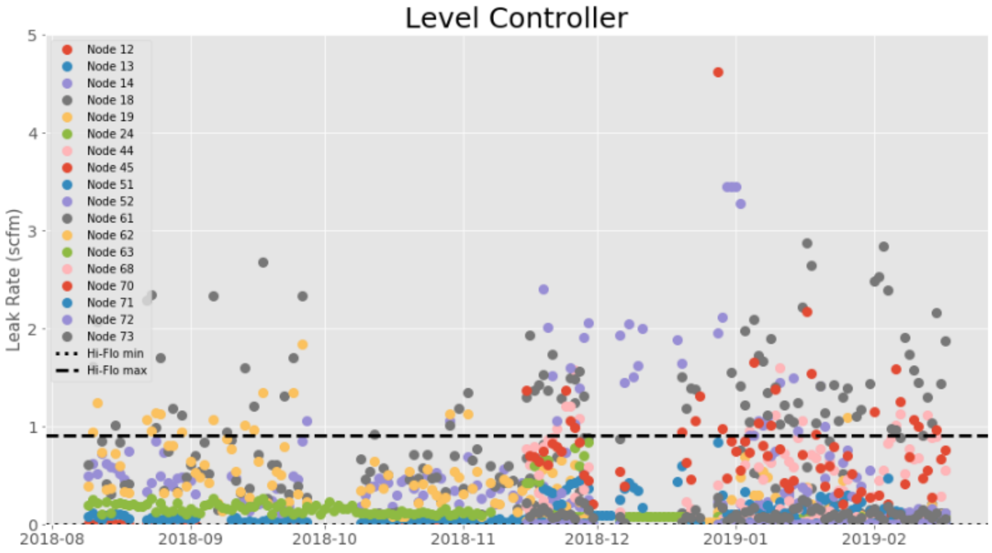

Figure 9.4-4 Level Controller Timeseries in relation to Hi-Flow Sampler Measurements

The table below shows the effect size metric as a measure of the difference in the mean leak rates of two node pairs for select level controllers.

Table 9.4-2 Effect-Size Comparison for Level Controller Nodes

Node Pair	Mean Effect Size
(13, 14)	-0.5219
(13, 12)	0.8314
(14, 12)	0.6061

It is obvious that there is a significant difference between the means of node with the highest leak rate (14) and both node 13 and 12. Such a difference in the means is normalized by the pooled standard deviation (introduced in section 8.8) of the individual nodes. The difference in the means is between half to nearly 1 standard deviation which indicates that such differences in the leak rates are statistically significant and should not be treated as coincidental.

Main Flange

The figure below depicts the daily rolling average of the wellhead methane rates. Nodes 20, 21, and 22 were set up around the wellhead on Site 2, consisting of an oil well operated by an electric pump jack. The purpose of these sensors Is not to measure known vents from the wellhead, but rather any presence of methane during operations. The sensors are picking up close-to negligible readings. The Hi-Flow Sampler readings are not available for these nodes.

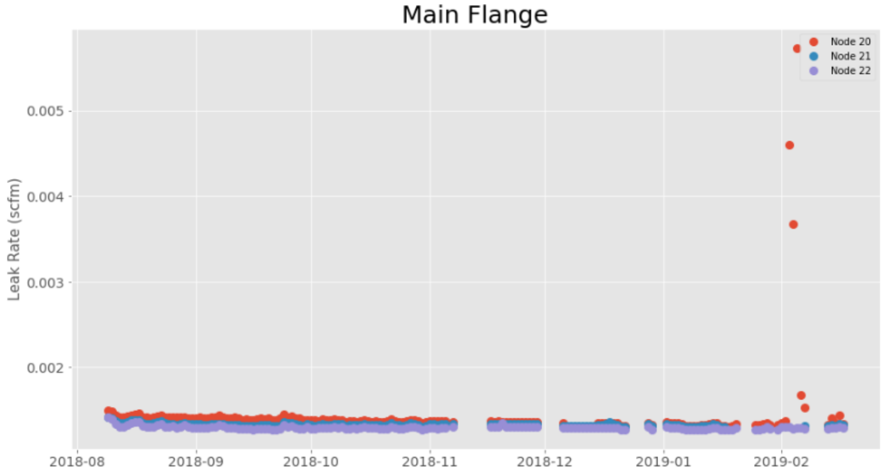

Figure 9.4-5 Main Flange Timeseries

Methanol Pump

A rolling daily average is represented in **Figure 9.4-6** over the life of the experiment. According to the operator, the methanol pump associated with Node 53 is not in use. Methanol pumps are primarily used to prevent the formation of hydrates, which occurs under high pressure and low temperature conditions. The usage of methanol pumps increases during the winter, at the operator's discretion. Additionally, the operator indicated that, on Site 5, the pump associated with Node 54 is set at a higher operation rate, while Node 60 operates normally. Two horizontal bounds were set as a window, corresponding to the absolute maximum and absolute minimum methanol pump instantaneous leak rate reading from the Hi-Flow Sampler. The graphic shows that a one-time measurement may not be representative of the true behavior of this component.

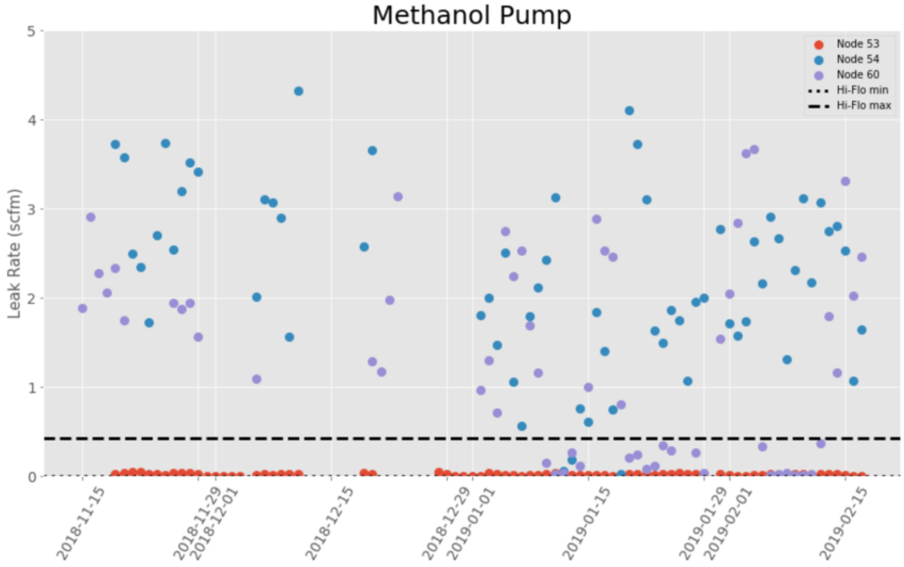

Figure 9.4-6 Methanol Pump Timeseries in relation to Hi-Flow Sampler Measurements

Pre-Lube Pump

As described in previous section, the pre-lube pump Is triggered during the start-up and shutdown of the reciprocating compressor. According to the activity log provided by the operator, the compressors on Site 3 experienced multiple shutdowns over the time of this experiment. The Hi-Flow Sampler reading was not available for this specific component.

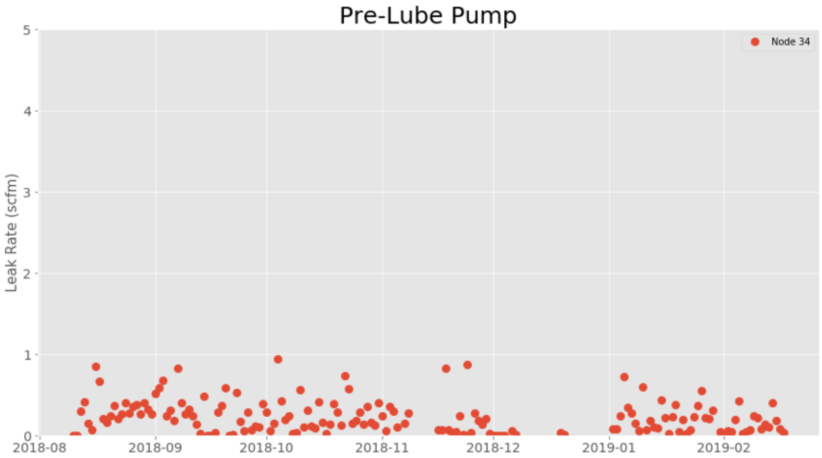

Figure 9.4-7 Pre-Lube Pump Timeseries

Pressure Controller

The pressure controller daily average time series plotted below shows the behavior of the 13 pressure controllers for the duration of this experiment. For the first half of the time-period, only the nodes for the first 3 sites had been deployed, we can see that activity picks up once the remaining 4 sites were deployed In November. Nodes 10, 92, 23, and 25 were part of a high-bleed to low-bleed operation transition Initiative on October 10th, 2018, their emissions decrease significantly. The black lines represent the high and low bounds of the Hi-Flow Sampler readings.

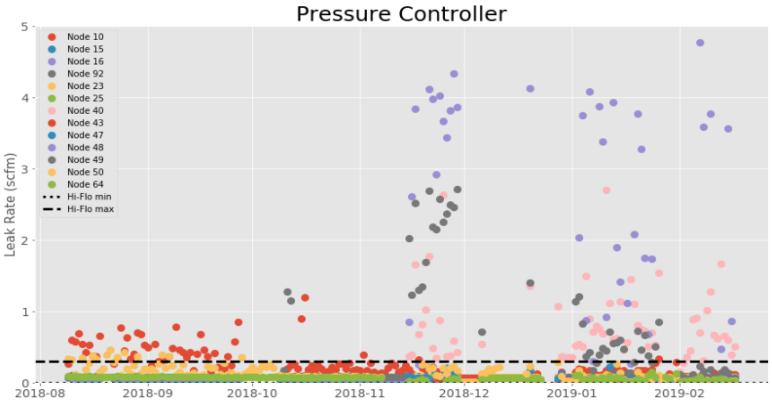

Figure 9.4-8 Pressure Controller Timeseries in relation to Hi-Flow Sampler Measurements

Start Gas

Node 33 and Node 36 are associated with the start gas vents for compressors K-101 and K-103, respectively, located on Site 3. Based on the records obtained from the operator, these two compressors sporadically go down due to pigging operations, low suction pressure, high temperature, and service. Hi-Flow Sampler readings were not available for these two nodes.

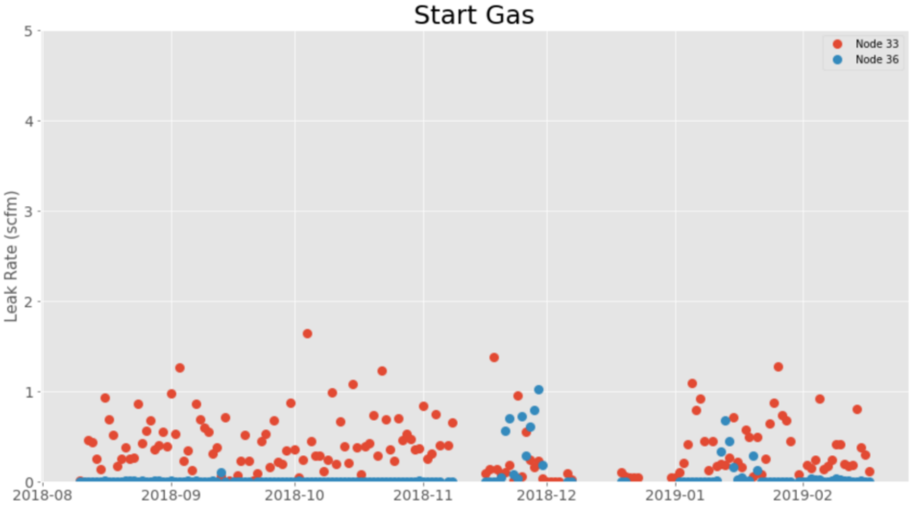

Figure 9.4-9 Start Gas Timeseries

Thief Hatch

Three thief hatches were monitored during this testing campaign. Hi-Flow Sampler readings were not available for these components. As discussed in previous sections, thief hatch emissions occur when these are opened or in the case there's a leaking seal. Emissions are expected to be low as the fluids in the tanks are at atmospheric pressure and the emitted gas comes from solution.

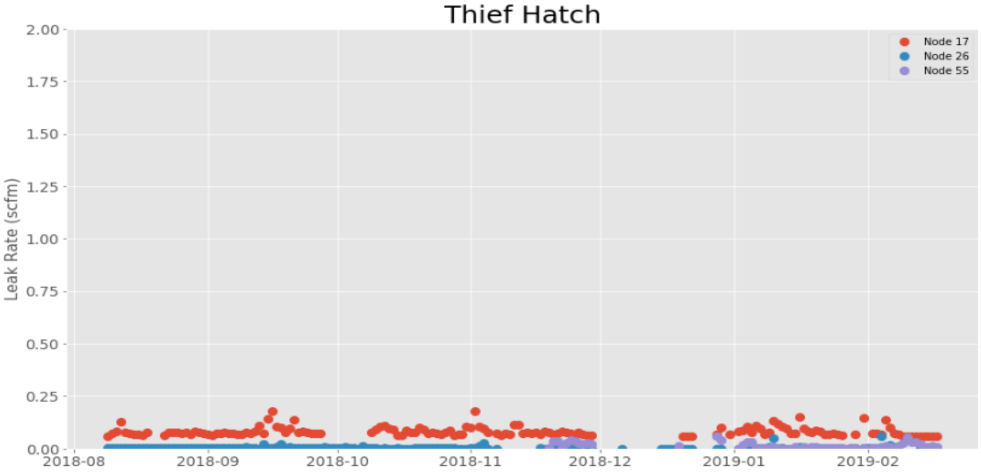

Figure 9.4-10 Thief Hatch Timeseries

Table 9.4-3 Effect-Size Comparison for Thief Hatch Nodes

Node Pair	Mean Effect Size
(26, 55)	-0.0981
(26, 17)	-0.7644
(55, 17)	-0.4973

Now, considering the leak rates for the thief hatch, node 26 and 55 are within 0.1 standard deviation while both are much less than node 17 which shows the biggest leak rate of all three. This again indicates the statistically significant differences in the measured emission rates for nodes representing the same component type. Hence it is not reasonable to use a one emission rate to represent all components of the same type.

Vent Header

As explained in previous sections, the vent header Is composed of multiple sources of leaks originating from the compressor including packing seals. The black lines mark the bounds set by our team's Hi-Flow Sampler measurements and reveal that most of the behavior of these components that was captured falls within this window. Evident by the figure, nodes 30 and 32 dominate the area, both belonging to the K-101 Caterpillar compressor in site 3. This activity points out that the status of this compressor must be assessed, since the emissions indicate less-than-efficient operations.

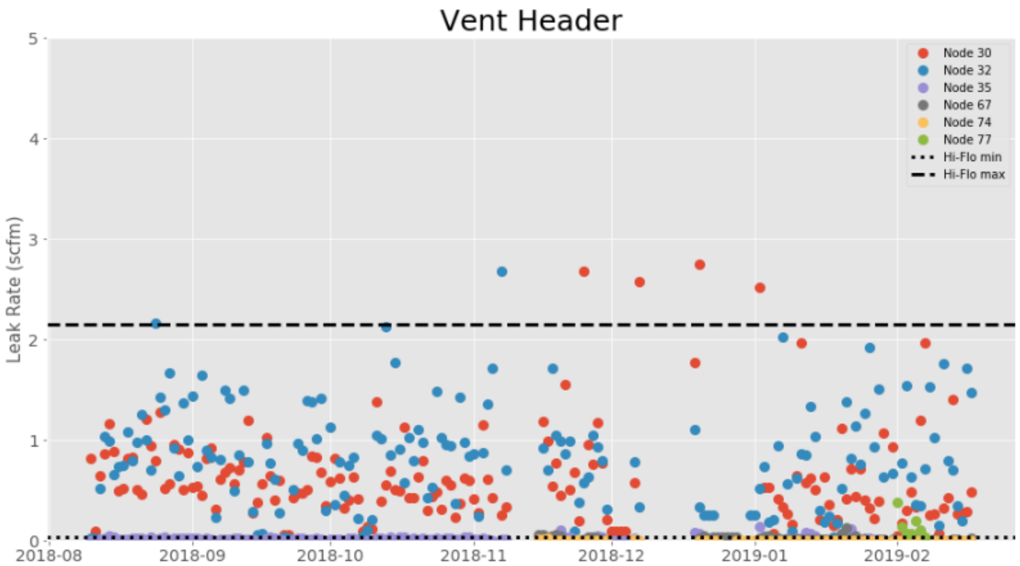

Figure 9.4-11 Vent Header Timeseries in relation to Hi-Flow Sampler Measurements

9.4.2 Comparison of Newly Developed Emission Factors with Current Emission Factors

The newly developed measured-based and statistically analyzed emission factors are compared with the current emission factors, both from the 1996 GRI and US-EPA study and from Canadian-EC, Clearstone study, March 2014. The statistical mean of the sampling distribution emission factors for each component category were calculated for the 7 Bonavista sites. The sample size was small as the number of different equipment and components is limited. Regulatory agencies, as discussed in Section 6, have different methodologies in the collection of data including one-time measurement, or an average of reported emissions, or an approximation based on models and correlations. The newly developed emissions factors were based on our patented LUMEN technology adds a new important dimension to previous methodologies. The continuous measurements methodology enables better understanding of leak source characteristics over wide range of operating and environmental conditions. Fluctuations in leak rate can only be understood over an extended period with continuous monitoring and the fusion of sites operational data. Table 9.4-4 shows newly developed emission factors compared with regulatory averages.

Table 9.4-4 Component Statistical Mean Emission Factor Compared with Regulatory Averages

Equipment Component Category 7 Bonavista Sites		Fugitive vs. Vented Emission	BHGE Emission Factors* Range (scfm) Using 56 LUMEN Sensors	Leak Rate Range (scfm) Using Hi-Flow Sampler**	EC Emission Factors*** (scfm) Clearstone Study March, 2014	EPA Emission Factors*** (scfm) EPA/GRI Study, 1990 Published on June 1996
1	Distance Piece (n =3)	Vented	0.006 - 0.469	0.07 - 0.39	0.050	0.860
2	Dump Valve (n =4)	Vented	0.016 - 1.923	0 - 0.28	0.002	0.002
3	Level Controller (n=18)	Vented	0.002 - 1.381	0 - 0.91	0.041	0.002
4	Main Flange (n=1, 3 sensors)	Fugitive	0.001	-	-	0.000
5	Methanol Pump (n=3)	Vented	0.017 -1.411	0 - 0.43	0.003	0.002
6	Pre-Lube Pump Column (n=1)	Vented	0.229	-	0.003	0.002
7	Pressure Controller (n=13)	Vented	0.003 -0.635	0 - 0.3	0.041	0.003
8	Start Gas (n=2)	Vented	0 - 0.379	-	-	-
9	Thief Hatch (n=3)	Vented	0.004 - 0.082	-	-	-
10	Vent Header (n=6)	Vented	0.002 -0.731	0.03 - 2.15	0.050	0.860

* *Assuming unity activity value*
** *Hi-Flow Bonavista Sites Testing Campaign: November 19th, 20th, 2018*
*** *Average value*

During this study, our field measuring campaign at the 7 Bonavista Sites in Rimbey, Alberta, Canada spanned over a 5-to-8-month period (see Test Approach, Section 8-4). A total sample of 191 million data points represent instantaneous methane concentration measured by 54 LUMEN sensors (at a sampling rate every 2 seconds). This represents the datasets for the 10 equipment components categories shown In Table 9.4-4. The collection of sensor data sets was carefully cleaned and thoroughly filtered before going through a series of transformations and eventually getting passed to the Near-Field Plume Dispersion Model for leak rate estimation.

After obtaining a full timeseries of concentration and associated leak rates for each node, bootstrap resampling was performed to quantify the random errors and provide a confidence Interval for the statistics reported. The mean leak rate for each node was calculated and compared both with the like-component and with other components within the same facility. Moreover, working closely with the operator, the team was able to match several key reported events that further validated our assumptions and corroborated the results. Additionally, we demonstrated that even though a one-time Hi-Flow Sampler measurement may, at times, represent the behavior of a component, relying on such instantaneous measurement may be a gross over-generalization of the population.

It should be mentioned that due to limited sample size (54 components) the new average emission factors developed in this study may not be a good representation to the entire population. However, it sheds a light on the importance of developing a measured based emission factors that are appropriately scaled to target super emitters. As an example, the largest 5% of leaks at compression facilities contribute to 68% of the total emissions. This illustrates the importance of adequately characterizing 'super-emitters' while developing inventories and while scaling emissions from studies to wider regions or whole industry estimates.

9.5 Key Findings

1. Hi-Bleed to Low-Bleed Operation Transition

As part of operations, Bonavista replaced 5 high-bleed controllers with low-bleed controller in two separate occasions. In sites 1 and 2, this change occurred on October 10, 2018, and the controllers affected were Nodes 10, 92, 23, and 25, all of which are separator pressure controllers. The second event occurred on November 30, 2018 at site 6, replacing the controller connected with Node 63.

As expected, this change in operations affected the rate at which these components release gas. The rapid drop in emission rate seen in Figure 9.5-1 is closely followed by leak sensors resulting in two distinct zones before and after the transition to low-bleed operation (clearly delineated by the dashed vertical line plotted at the date of controller replacement). The chart below shows the mean of leak rate in the high-bleed controller's zone to be nearly 3 times higher than the low bleed controller's zone mean. As a result, significant reduction in emissions is realized by replacing the controller.

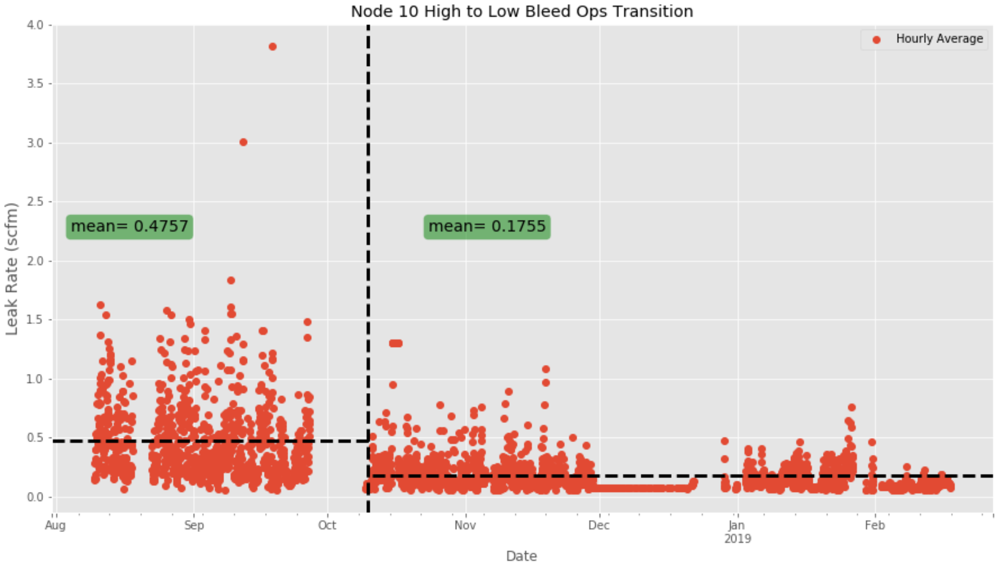

Figure 9.5-1 Effect of High to Low-Bleed Operation Transition on Node 10

To carefully analyze the emission timeseries and identify patterns, it is insightful to break it down into three components; a trend, a seasonal component and a remainder/noise component. For simplicity we will focus on the first two components. The trend can be computed by a rolling window of size that is big enough to remove local seasonality but short enough not to smooth out global trends. Looking at the trend makes it easier for us to judge the overall variation in total emission levels.

For example, Figure 9.5-2 shows that there is an overall decrease in emission levels over time with a marked reduction beyond the controller replacement date (the vertical dashed line) and eventually trending to near-constant low emission level operation.

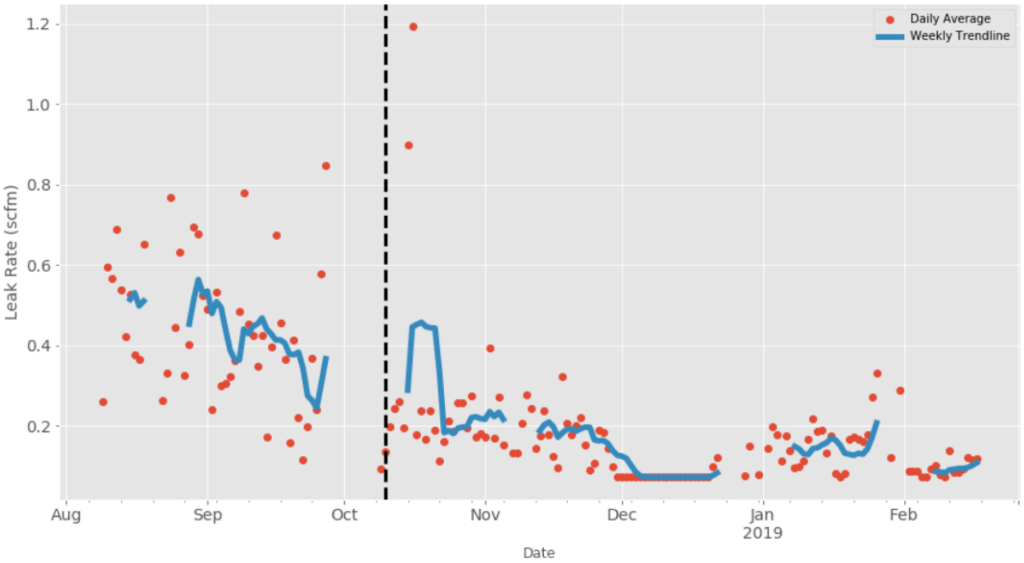

Figure 9.5-2 Emission Rate Trend - Node 10

The seasonal components on the other hand captures the variability of emission intrinsic to the day to day operation of the controller. For example, Figure 9.5-3 shows the seasonal component for node 10. There is cyclic variability in emission levels. The cycle can be estimated by measuring the number of data points/days between two consecutive peaks or troughs. The cycle is about 3-5 days in duration. One can also see a noticeable decrease in the amplitude (the height of the emission rate peak) associated with the low-bleed controller.

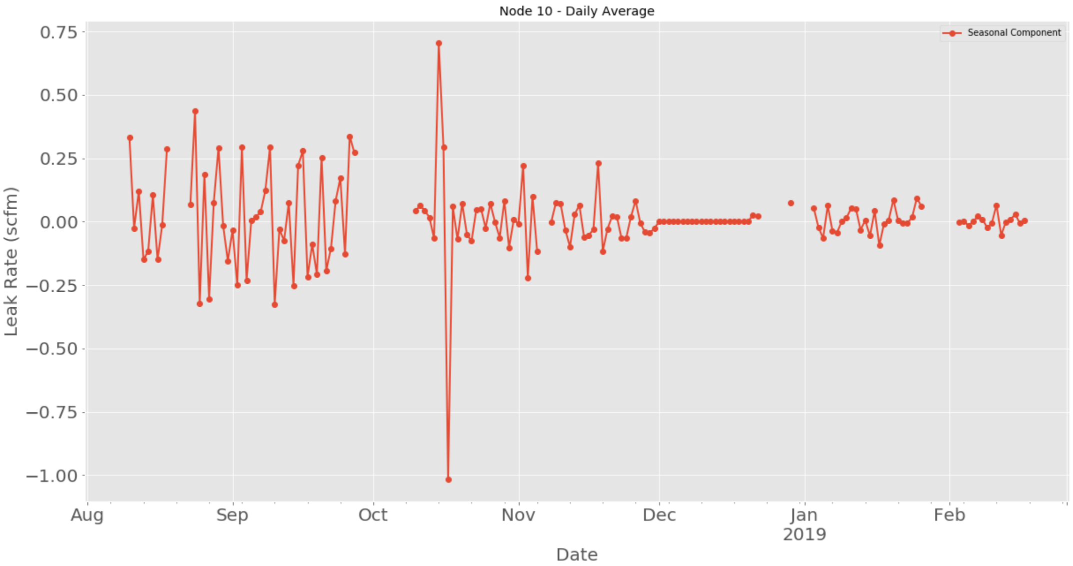

Figure 9.5-3 Seasonal Component of Emission Rate - Node 10

Similar remarks can be made about the transition to a low bleed controller for node 23. It can be seen (see Figure 9.5-4) that the mean of the emission rate for the high-bleed zone is 3 times higher than the mean beyond the transition date (marked by the vertical dashed-line).

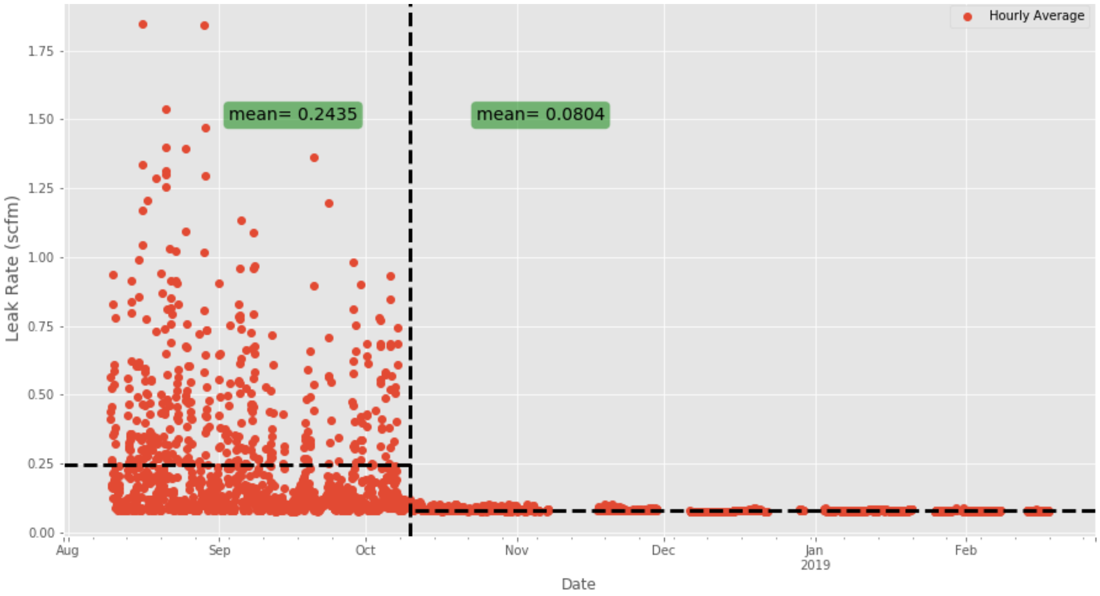

Figure 9.5-4 Effect of High to Low-Bleed Operation Transition on Node 23

A striking reduction in the trend is seen in figure 9.5-5 where there is a clear drop around the transition date (the black vertical dashed line) that turns into a near constant trend at very low levels. Hence there is a clear advantage of replacing the high-bleed controller.

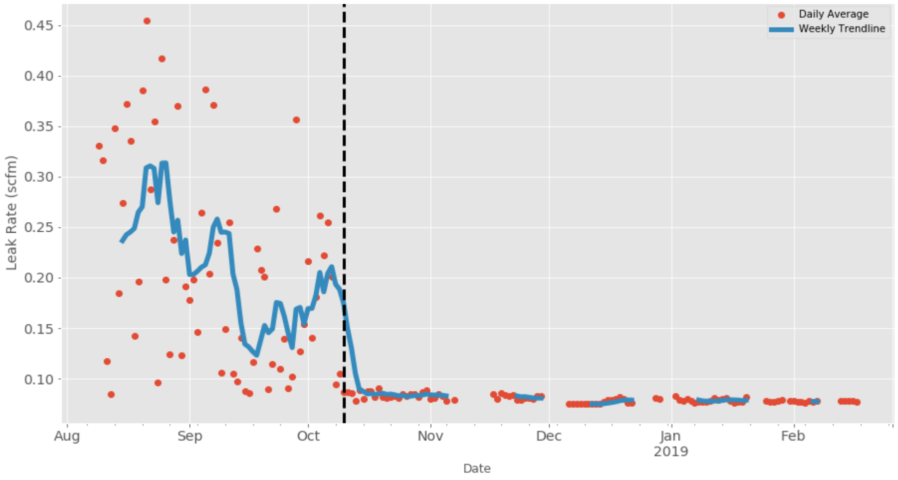

Figure 9.5-5 Emission Rate Trend - Node 23

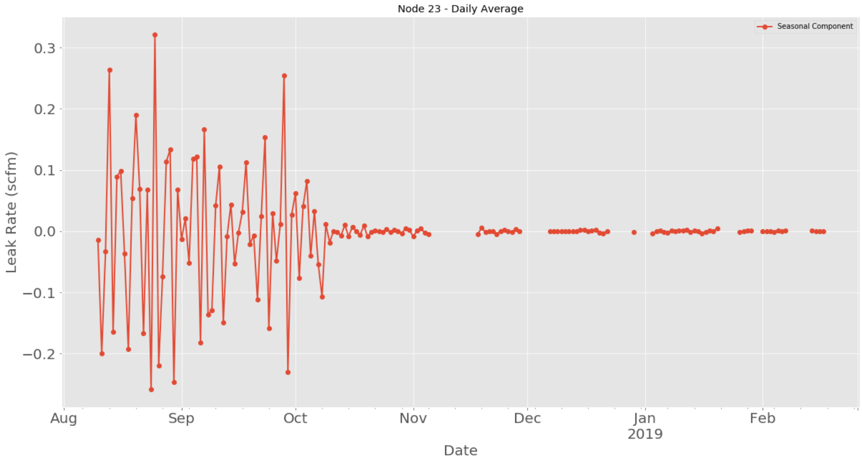

Figure 9.5-6 Seasonal Component of Emission Rate - Node 23

The seasonal component (figure 9.5-6) is showing a cycle of about 3 days with a significant reduction in amplitude after replacing the high bleed controller consistent with the significant reduction in the trend line seen in figure 9.5-5.

2. Economic Impact of High to Low-Bleed Transition

One of the many advantages of counting with continuous monitoring is the capability of calculating the potential losses/gains caused by operations, production, and maintenance.

For instance, if we consider the previous Node 63, the high to low-bleed transition occurred on November 30, 2018. The statistical mean of the emission rate for the period before the change was 0.6132 scfm, the statistical mean of the rate is now 0.0325 scfm. By Implementing this change in operations, the operator not only reduced the total emissions of that component, but this also resulted in $850/year worth of savings for just one component, an amount recovered from the gas that would have, otherwise, been lost to the atmosphere, meaning that this is an investment that will pay for itself over time.

This effect can be observed not only in the high to low-bleed operation transition but also in small changes throughout the sites like upgrading compressor packing seals and replacing worn gaskets. One great advantage the LUMEN system introduces is the identification of abnormal behavior or less-than-optimal operations. Monitoring and measuring leak rates is the first step to minimize emissions and maximize profit.

3. Methanol Pump

Methanol pumps are actuated at the discretion of the operator and are highly dependent on production and operating conditions. Methanol pumps are used to reduce the risk of hydrate formations which occur at high pressure and low temperatures, and they are expected to be more utilized in the winter rather than in the summer. Unfortunately, the testing campaign for these components did not start until the winter time, but it is evident that they are being used. On Site 5, the pump associated with Node 54 has been operating at a higher rate than normal due to the inactivity of the pump corresponding to Node 53. **Figure 9.5-7** shows process of using the rolling average over a period (2 seconds, 10 minutes, 1 day, one week) to obtain a cleaner picture that will enable us to better see the behavior of these components and draw conclusions. The daily running average chart is of greatest significance as the pump operating conditions are determined daily, with higher rates indicating favorable conditions for hydrate formation and low rates indicating the opposite.

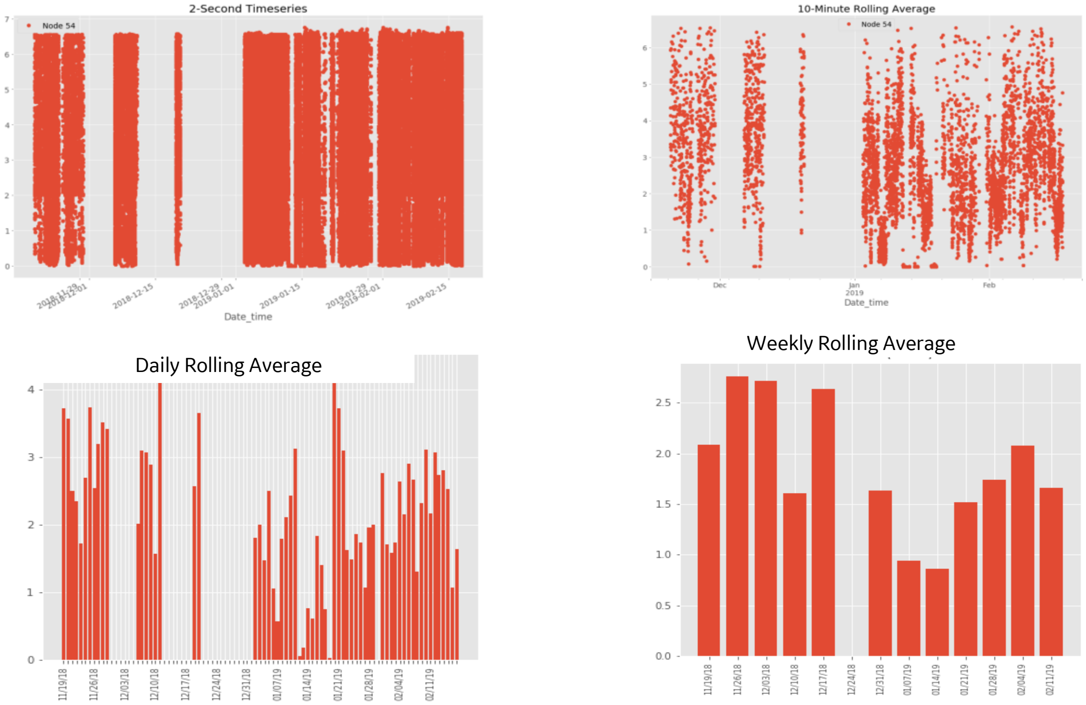

Figure 9.5-7 Node 54 Methanol Pump

4. Distance Piece

By comparing the LUMEN measurements to the sites service records, we notice that newer packing services was showing positive impacts on emission reductions from the distance pieces. Bonavista service records indicate that Node 46 compressor had new packing installed in May 2018 and Node 69 compressor got the 1st stage repacking done in November 2018, while the last service for Node 31 compressor packing was in August 2017. Referencing **Figure 9.5-8**, it is evident that Node 46 and 69 reciprocating compressor emissions were one order lower than that of Node 31 compressor vent. The density of high emission rate data is evident in 31. Such higher leak rates are only encountered rarely in the other two timeseries which are much sparser at the high emission levels. The Hi-Flow Sampler data are sporadic and could be misleading, e.g., Node 46 Hi-Flow leak rate was 0.385 scfm comparing to 0.285 scfm at Node 31, which may lead people think that Node 64 reciprocating compressor emission is worse than Node 31 emission. Apparently, it is contradictory to the long-term monitoring data. Although node 31 is the healthiest in terms of available data, there is enough data within 46 and 69 to render the statistics of both stationary. The density of high emission rate data is evident in 31. Such higher leak rates are only encountered rarely in the other two timeseries which are much sparser at the high emission levels. Because there are no measurements before and after maintenance of a specific rod-packing, these results give a suggestion that maintenance schedules impact emissions, but not proof.

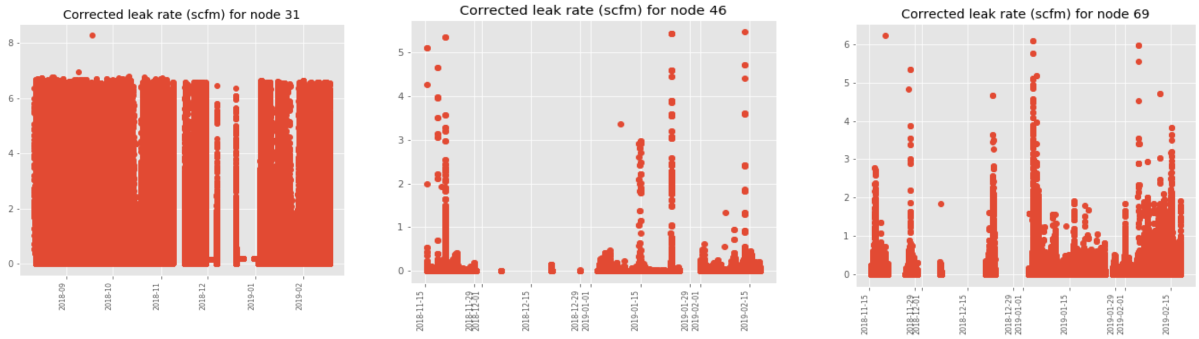

Figure 9.5-8 Distance Piece Timeseries: Node 31, Node 46, Node 69

This behavior is consistent with the probability density function (pdf) obtained from the individual timeseries shown in **Figure 9.5-9**. It is seen that the probability density of Node (31) has a much wider tail towards the right side (the higher emission rates) compared to the narrow distribution seen in Node 46 timeseries.

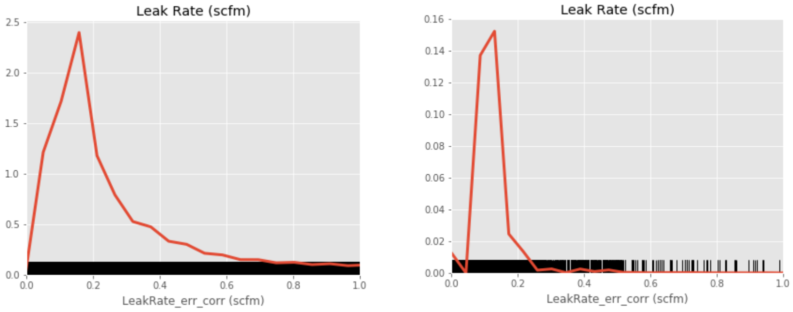

(a) **(b)**

Figure 9.5-9 Distance Piece Timeseries: (a) Node 31 (b) Node 46

5. Level Controller Operations – Separator vs. Compressor

The figure below shows two distinct modes of operation for level controllers attached to a compressor and a separator irrespective of the manufacturer/model. The signature of separator level controllers, **Figure 9.5-10**, has an intermittent behavior that is attributed to snap action (on/off) mode. The release of gas is intermittent and short lived, the dynamic component of the reading, this is the second "baseline" that can be observed in the figure, leveling at around 2 scfm. The bottom baseline belongs to the static component of the reading. The frequency of the gas release is dependent on the frequency the liquid needs to be dumped to lower the level of the liquid.

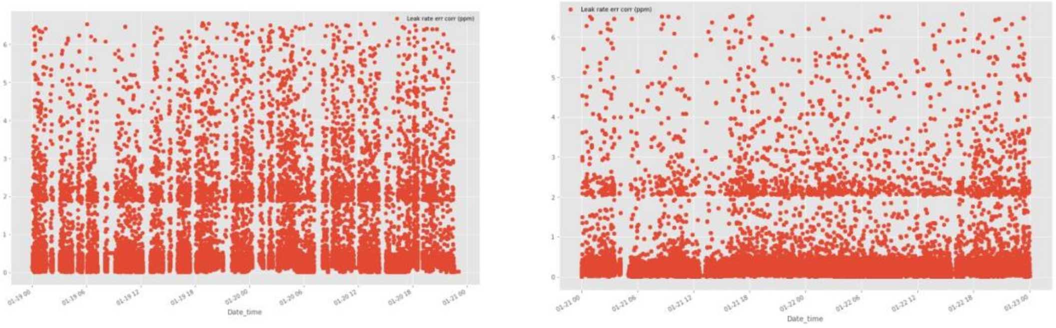

(a) (b)

Figures 9.5-10 48-hour window **(a)** Norriseal Separator Level Controller - Node 44 **(b)** Fisher L2 Separator Level Controller - Node 51

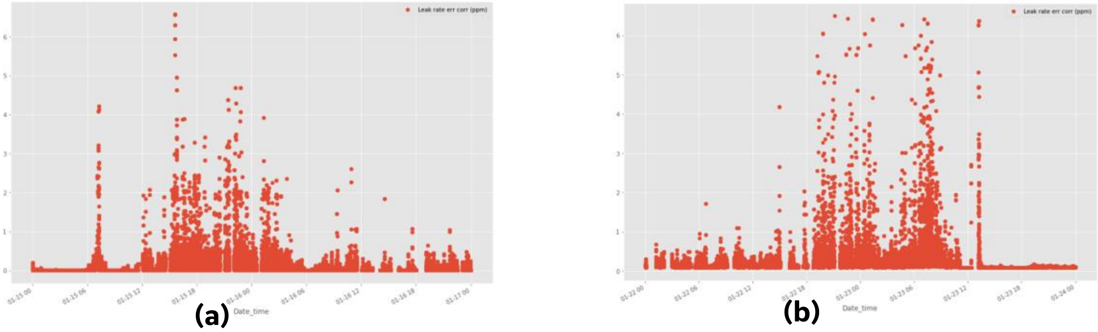

(a) (b)

Figures 9.5-11 48-hour window **(a)** Fisher L2 Compressor Level Controller - Node 45 **(b)** Norriseal Compressor Level Controller-Node 18

This is in stark contrast to the lower set of figures belonging to compressor level controllers, which show a more continuous, unimodal operation mostly in the low emission region with occasional intrusions into higher emission zones, a behavior attributed to the throttle action mode of the level controller.

6. From Operations

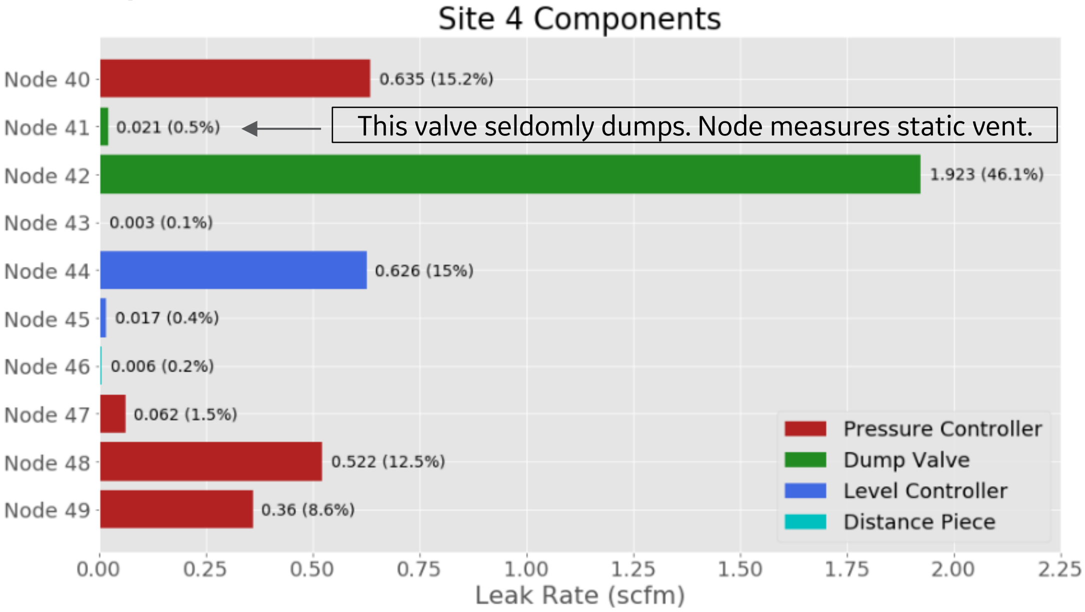

Figures 9.5-12 Site 4 Operations

After obtaining the results from each node, the team raised some questions to the operators to validate our findings with the modes of operation at different sites. Some of the main concerns include the difference in rates between two components within the same site. For example, field technicians indicated that the valve related to Node 41 is not ever actuated since the fluid is directly connected to tanks. This node measures the static vent of this valve only. As for the other dump valve, Node 42, it has a high dumping frequency since this is the valve that controls the water volumes.

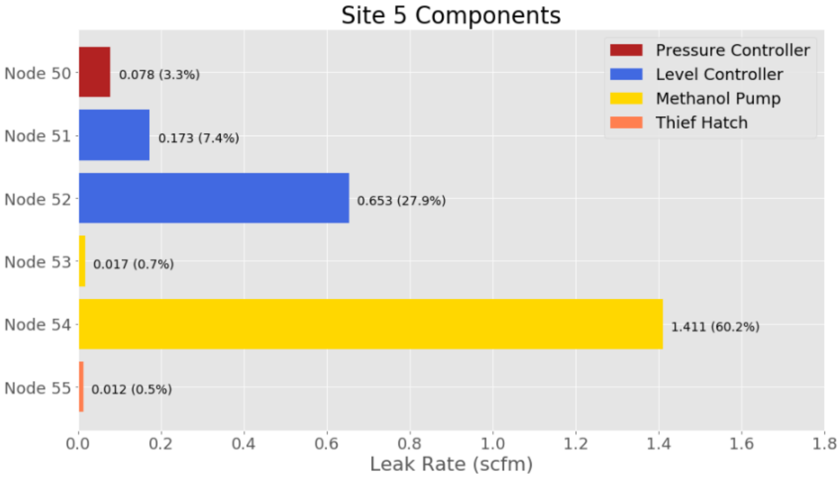

Figures 9.5-13 Site 5 Operations

Additional findings include the methanol pumps on site 5. The site manager indicated that the methanol pump related to Node 53, is not in operation, as the line is connected to sales, the venting is not necessary. The sensor will just pick up background activity. However, the methanol pump on Node 54 is running at a high rate circulating about 30 L of methanol per day, explaining the high discrepancies between the two.

10. Conclusions

Regulatory agencies provide a reference average emission rate for different components in the oil and gas industry. LUMEN is the first product of its kind to offer continuous emission monitoring for localized vents and components. Regulatory agencies, as discussed in Section 6, have different methodologies in the collection of data. Whether the emission rate is a one-time measurement, an average of reported emissions, an approximation based on models and correlations, or the result of simulations, the method LUMEN employed is unparalleled.

The application of BHGE-LUMEN (Near-Field) in this study is a differentiator in comparison with previous studies by EPA and ECCC that used Hi-Flow sampler as the basis for the development of today's widely used emission factors. It is our hope that this novel approach will lead to a new emission factor estimation strategy accompanied with significant cost reduction and higher fidelity measurements. BHGE LUMEN continuously monitored components over a 5-to-8-month period and calculated an average emission rate on a known vent tied to a component. The advantage of this method is that the resulting emission rates are unbiased by the specific time of measurement and the corresponding operating conditions snapshot. By continuously monitoring the equipment emissions, we consider different operating modes and site gas production levels, and thus represents an all-encompassing set of actual field conditions for estimating a statistically robust mean emission level for a given equipment component.

We have conducted preliminary studies to validate our findings based on limited field technician feedback. The results gave us more confidence in LUMEN's ability to track site activities and their impact on emission levels. Examples are discussed in the previous section showing how, for example, LUMEN was sensitive enough to instantaneously pick up the drastically reduced emission level upon operator switching over to low-bleed mode to higher bleed mode. In another instance, we show how updating packing more often has a significant impact on reducing emission level and hence the need for tracking service records for all components. Finally, the financial impact of component emission. The availability of this information to operators allow them to make more prudent decisions to comply with regulations and gain some financial ROI by moving to condition-based rather than scheduled maintenance. Monitoring and measuring leak rates is the first step to minimize emissions and maximize profit.

11. Next Steps

With the official LUMEN product launch later this year, BHGE is positioned to scale up these types of research programs that are directed to help customers understand their emissions footprint and governments to develop measured-based emission factors and inform regulatory agencies. By design, the scope of this study was limited to 7 sites and 10 different types of components categories (Distance Piece, Dump Valve, Level Controller, Main Flange, Methanol Pump, Pre-Lube Pump Column, Pressure Controller, Start Gas, Thief Hatch, and Vent Header). The team vision is that upon proving valuable, this work could be expanded to cover more sites with more diversified equipment components to enable ECCC to promulgate high-fidelity updated emission factors that are based on factual measurements and take into consideration parameters such as the age of equipment, rated capacity, material, volumetric throughput, geographic region, operation mode, and potentially other factors.

Expanding the Current Work to Wider Population

Current work is envisioned as a precursor for a wider study that covers more representative sample of equipment components in the Canadian Oil and Gas industry. For example, this study was limited to 10 types of equipment component categories representing a total of 54 leak sources that were carefully characterized as discussed in this report. This is probably an order of magnitude less than the sample size used by EPA to develop the current 1996 emission factors (3). The EPA inventory breaks out methane emissions for approximately 200 sources and calculates uncontrolled emissions using activity factors (e.g., equipment counts) multiplied by emission factors(3). The EPA GHG inventories largely rely on data collected in the early 1990s and may not reflect recent changes in technology, operations, and regulations. We believe that the BHGE methodology followed in this study could help industry to better understand, evaluate, and report their emission rates at the component level as explained in this study. While several studies have been conducted to determine better emission factors from various segments of the industry, the focus has been on site-level emissions rather than equipment-level emissions as discussed in this study.

Founded on the encouraging results of this study, the team proposes to expand the current work to enable better understanding of leak source characteristics over wide range of operating and environmental conditions. This will result in more representative emission factors to the leak sources in question and support ECCC mission to develop a high fidelity measured based emission factors.

Upon successful completion of this new proposal the team would be able to develop a multivariable based emission factor Formulae for each super emitter or key equipment component that is representative to key independent parameters. The coefficients of determination (r-squared values) of these parameters will be tested and a regression model will be developed to predict the emission factors based on user input. For example, if an emission rate needs to be determined for a compressor station reciprocating compressor the user would enter defined input parameters such as distance piece seal-type, age of compressor, site throughput, compressor rated capacity, and geographic region. The formula in Eq. 11.1-1 is a representative multi-variable response emission rate equation;

$$Emission\,rate\ (scfm) = a_0 + a_1x1 + a_2x2 + a_3x3 + \cdots + a_nxn \qquad \textbf{Eq. 11.1-1}$$

Where: a_1, a_2, a_3, a_4,…a_n are regression coefficients and $x1 =$ seal-type, $x2 =$ age of compressor, $x3$= throughput, $x4 =$ rated capacity, and $x4$=geographic region. Only the variables that are determined to have significant correlations to emission rate will be considered in this equation.

12. References

1. Clearstone Energy Ltd., *Overview of the GHG Emissions Inventory*, Volume 1. Prepared for Environment Canada by Clearstone Energy, Ltd. March 31, 2014.

2. Government of Canada, *Technical Backgrounder: Federal Methane Regulations for the Upstream Oil and* Gas Sector, Environment and Climate Change Canada. April 27, 2018. https://www.canada.ca/en/environment-climate-change/news/2018/04/federal-methane-regulations-for-the-upstream-oil-and-gas-sector.html

3. U.S. Environmental Protection Agency, *Methane Emissions from the Natural Gas Industry*, Volume 8: Equipment Leaks. Prepared for the Energy Information Administration by the National Risk Management Research Laboratory. June 1996.

4. Clearstone Energy Ltd., *UOG Emissions Inventory Methodology Manual*, Volume 3. Prepared for Environment Canada by Clearstone Energy, Ltd. March 31st, 2014.

5. Jörg Matthes, Lutz Gröll, and Hubert B. Keller, *Source Localization by Spatially Distributed Electronic Noses for Advection and Diffusion*, IEEE TRANSACTIONS ON SIGNAL PROCESSING, VOL. 53, NO. 5, MAY 2005.

6. A. Nehorai, B. Porat, and E. Paldi, *Detection and localization of vapor-emitting sources*, IEEE Trans. Signal Process., Volume 43, no. 1, pp. 243–253, Jan. 1995.

7. Allen Downey, *Think Stats: Probability and Statistics for Python Programmers*. O'Reilly, 2015.

8. Martinez, Wendy L., and Angel R. Martinez. *Computational Statistics Handbook with MATLAB*. CRC Press, 2016.

9. Gail M. Sullivan, Richard Feinn, *Using Effect Size—or Why the P Value Is Not Enough*. Journal of Graduate Medical Education: September 2012, Vol. 4, No. 3, pp. 279-282, 2012.